Studies on drug resistance and biofilm formation in *Candida glabrata*: focus on the implementation and optimization of CRISPR-Cas9 tools for *C. glabrata* genome editing

Inês Lopes Malpique

Thesis to obtain the Master of Science Degree in

Biotechnology

Supervisor: Prof. Dr. Miguel Nobre Parreira Cacho Teixeira

Co-supervisor: Dr. Pedro Henrique Magalhães Fernandes Pais

Examination Committee

Chairperson: Prof. Dr. Arsénio do Carmo Sales Mendes Fialho

Supervisor: Prof. Dr. Miguel Nobre Parreira Cacho Teixeira

Member of the Committee: Dr. Cláudia Sofia Pires Godinho

July 2020

Preface

The work presented in this thesis was performed at the Institute for Bioengineering and Biosciences of Instituto superior Técnico (Lisbon, Portugal), during the period October 2019 - March 2020, under the supervision of Prof. Dr. Miguel Teixeira. The thesis was co-supervised by Dr. Pedro Pais (Instituto Superior Técnico).

I declare that this document is an original work of my own authorship and that it fulfills all the requirements of the Code of Conduct and Good Practices of the Universidade de Lisboa.

Acknowledgements

First of all, I would like to express my gratitude to my supervisor Professor Miguel Teixeira, whose insight and knowledge have guided me through this research, for all the support I was given. Thank you for accepting me in your research group, the time I spent in the laboratory was very rewarding, even though my stay was shorter than I would have hoped. Also, a special appreciation for the thoughtful comments and recommendations of my co-supervisor Pedro Pais, who was always so encouraging, patient and kind to me.

I would also like to thank Professor Isabel Sá-Correia for the opportunity of joining the Biological Sciences Research Group, where the research work was developed.

To all the MCT research team, you have been so kind and helpful. Because of you, my research experience has been truly gratifying, and it is unfortunate that it ended so soon due to the current pandemics. I also want to thank my colleagues, especially those who became friends, for contributing to such a fulfilling journey that were these two years of my master's degree.

Finally, a very special thanks to my family for all the financial and emotional support. I will always be grateful for the opportunities I was given and managed to accomplish because of your encouragement. Thank you for being my safety net.

This work was supported by the Fundação para a Ciência e a Tecnologia (FCT) (contract PTDC/BII-BIO/28216/2017) as well as by the Programa Operacional Regional de Lisboa 2020 (LISBOA-01-0145-FEDER-022231, the BioData.pt Research Infrastructure). I also acknowledge funding received by the iBB from the FCT (UIDB/04565/2020) and from the Programa Operacional Regional de Lisboa 2020 (LISBOA-01-0145-FEDER-007317).

Abstract

Invasive fungal infections are estimated to kill around 1.5 million people every year. Although *C. albicans* is found to be the leading cause of invasive candidiasis, the emergence of *Candida glabrata* as a particularly antifungal resistant human pathogen attracted the attention of researchers, with concerns about health issues.

In this dissertation, the known mechanisms of *C. glabrata* pathogenicity, including drug resistance, biofilm formation and host-pathogen interactions are reviewed. Specifically, among several genes associated with the acquisition of antifungal resistance and biofilm formation in *C. glabrata*, the role of the Rpn4, Mar1, Efg1 and Tec1 transcription factors is addressed.

The first part of this work consists of a proof-of-concept, where several protocols were tested in order to implement and optimize a one vector CRISPR-Cas9 system for gene deletion in the *C. glabrata* KCHr606_Δ*ura3* strain. Following optimization, this system was successfully used to delete *RPN4* and *EFG1*, aiming their functional characterization to uncover a potential role in azole resistance and biofilm formation, respectively. Unfortunately, due to the current COVID-19 pandemics, no susceptibility and biofilm quantification assays of the mutants were accomplished, neither was the generation of CRISPR-Cas9-mediated *Cg*Δ*mar1* and *Cg*Δ*tec1* single deletion mutants and other planned multiple deletion mutants. Considering the role of Mar1, the two "GGGGAGG" motifs found in the *RSB1* promoter, which have been previously identified as potential Mar1 binding sites, were mutated through site-directed mutagenesis, and shown to influence *RSB1* gene expression in the presence of fluconazole. An upcoming Chromatin Immunoprecipitation (ChIP) analysis of the binding between Mar1 and the given motifs from *RSB1* promoter will be necessary to confirm the hypothesis of Mar1 being involved in fluconazole-induced stress responses in *C. glabrata* through the direct regulation of *RSB1*.

Overall, this work describes the implementation and optimization of CRISPR technology in *C. glabrata* and provides biological material that will prove useful in deciphering the role of new players in antifungal drug resistance and biofilm formation in this pathogen.

Keywords: CRISPR-Cas9, *Candida glabrata*, biofilm formation, antifungal drug resistance

Resumo

Estima-se que as infecções fúngicas invasivas matem cerca de 1,5 milhões de pessoas todos os anos. Embora *C. albicans* seja a principal causa de candidíase invasiva, o surgimento de *Candida glabrata* como um organismo patogénico humano particularmente resistente a antifúngicos captou a atenção de investigadores, com preocupações no que toca a questões de saúde.

Nesta dissertação, os mecanismos conhecidos de patogenicidade de *C. glabrata* são revistos, incluindo a resistência a medicamentos, a formação de biofilme e interacções entre o organismo patogénico e o hospedeiro. Especificamente, de entre vários genes associados à aquisição de resistência a antifúngicos e formação de biofilme em *C. glabrata*, é abordado o papel dos factores de transcrição Rpn4, Mar1, Efg1 e Tec1.

A primeira parte deste trabalho consiste numa "prova de conceito", onde vários protocolos foram testados para implementar e optimizar um sistema CRISPR-Cas9 de um só vetor para a eliminação de genes na estirpe KCHr606_Δ*ura3* de *C. glabrata*. Após optimização, este sistema foi usado com sucesso para eliminar os genes *RPN4* e *EFG1*, tendo como objectivo a sua caracterização funcional para descobrir um potencial papel na resistência a azóis e formação de biofilme, respectivamente. Infelizmente, devido à actual pandemia causada pelo COVID-19, os ensaios de suscetibilidade e quantificação de biofilme dos mutantes não foram realizados, nem a geração de mutantes de deleção *Cg*Δ*mar1* e *Cg*Δ*tec1*, mediada por CRISPR-Cas9, ou outros mutantes múltiplos anteriormente planeados. Considerando o papel do Mar1, os dois motivos "GGGGAGG" encontrados no promotor do gene *RSB1*, tendo sido previamente identificados como potenciais locais de ligação do Mar1, foram mutados por mutagénese dirigida, tendo sido demonstrada a sua influência na expressão do gene *RSB1* na presença de fluconazol. Uma análise futura, recorrendo a Imunoprecipitação da cromatina (ChIP), da ligação entre o Mar1 e os motivos referidos do promotor do gene *RSB1* será necessária para confirmar a hipótese de o Mar1 estar envolvido em respostas a stresse induzido por fluconazol em *C. glabrata* através da regulação directa do *RSB1*.

Globalmente, este estudo descreve a implementação e optimização da tecnologia CRISPR em *C. glabrata*, e oferece material biológico que se mostrará muito útil no estudo do papel de novos participantes na resistência a antifúngicos e formação de biofilme nesse organismo patogénico.

Palavras-chave: CRISPR-Cas9, *Candida glabrata*, formação de biofilme, resistência a drogas antifúngicas

Contents

List of figures

Acronyms

5-FC – 5-fluorocytosine

5-FU – 5-fluorouracil

ABC – ATP-binding cassette

Als – agglutinin-like sequence

ASPs - Alkali-soluble polysaccharides

BSI – Bloodstream infection

bZIP – basic leucine zipper

CASCADE – CRISPR-associated complex for antiviral defence

ChIP - Chromatin Immunoprecipitation

CRISPR – Clustered regularly interspaced short palindromic repeats

crRNA – CRISPR RNA

dCas9 – catalytically dead Cas9

DHA – Drug:H^+ antiporter

DSB – Double-strand break

dsRNA – double stranded RNA

ECM – Extracellular matrix

EPA – epithelial adhesins

GPI - glycosylphosphatidylinositol

GPI-CWP – GPI-anchored cell wall protein

HDR – Homology-directed repair

Hwp – hyphal wall protein

ICU – Intensive care unit

LTE – lipid-translocating exporter

MAP – mitogen-activated protein

MFS – Major facilitator superfamily

MGE – Mobile genetic element

NAD+ - nicotinamide adenine dinucleotide

NHEJ – Nonhomologous end-joining

PACE - proteasome-associated control element

PAM – Protospacer adjacent motif

PAMPs – pathogen-associated molecular patterns

PDRE - pleiotropic drug response element

PHS – phytosphingosine

PKA – protein kinase A

RAMP – Repeat-associated mysterious protein

RISC – RNA induced silencing complex

RNAi – interfering RNA

RNP – RNA-protein complex

ROS – Reactive oxygen species

RT-PCR – Reverse transcription polymerase chain reaction

RVD – Repeat variable di-residue

sgRNA – single guide RNA

shRNA – short hairpin RNA

siRNA – small interfering RNA

ssDNA – single-stranded DNA

TAL – Transcription activator-like

TALEN – Transcription activator-like effector nuclease

TEA/ATTS - transcriptional enhancer activators

TF – Transcription factor

tracrRNA - Trans-activating crRNA

YPS – Yapsin

YRE - Yap1 response element

ZFN – Zinc finger nuclease

1. Introduction

1.1 Thesis outline

This dissertation is organized in five chapters.

The first chapter reviews current knowledge on the mechanisms of virulence, biofilm formation and antifungal resistance in *C. glabrata*, often in comparison with the well-known pathogenic yeast *C. albicans*. Emphasis is given to the role of newly identified transcription regulators controlling some of these processes, including the azole resistance regulators Rpn4 and Mar1 and the biofilm formation regulators Efg1 and Tec1. The last section of this introductory chapter is dedicated to a description of various genome editing tools used before the development/implementation of the Clustered Regularly Interspaced Short Palindromic Repeats (CRISPR)-Cas9 system to eukaryotic cells, along with the advantages of using this more recent and effective tool for genome editing.

In the second chapter, all the materials and methods used throughout this study are listed.

The third chapter provides the results obtained during the research done in this work, starting with the optimization of a CRISPR-Cas9 system to implement in *C. glabrata*. As a proof of concept, the *ADE2* gene was selected for CRISPR-mediated gene deletion in *C. glabrata*, where several protocols and conditions were tested until a successful outcome was accomplished. This work aimed to contribute to the functional characterization of four genes with suspected important roles in *C. glabrata* azole resistance – *RPN4* and *MAR1* - and biofilm formation – *EFG1* and *TEC1* -, and this analysis started with the generation of the respective *C. glabrata* deletion mutants using the optimized CRISPR-Cas9 system. After obtaining single and multiple deletion mutants, the effect of the deletion of each group of genes and their possible genetic interactions would have been assessed with susceptibility and biofilm quantification assays, respectively. Sadly, as a consequence of the COVID-19 pandemics, the laboratory work was forced to end a lot sooner than expected, meaning only two single deletion mutants were generated (*Cg*Δ*rpn4* and *Cg*Δ*efg1*) and none of the planned assays could be done. As a complementary approach, to evaluate whether four potential Mar1 binding motifs of the *RSB1* promoter, previously identified in our lab, influenced both the basal expression of the *RSB1* gene and its expression in the presence of fluconazole, these four motifs were mutated with site-directed mutagenesis and the levels of *RSB1* gene expression were measured. Results obtained identified two of the motifs as important for the expression of *RSB1* in the presence of fluconazole.

Lastly, the overall results obtained in this work are discussed in more detail in chapter four, while future perspectives and general conclusions are also specified.

1.2 Candidiasis

The rising of human infection and disease caused by opportunistic fungal pathogens in the past few decades, especially among immunocompromised and critically ill hospitalized patients, has led to serious concerns and is therefore considered a major health problem. It is estimated that invasive fungal infections can kill around 1.5 million people every year[1]. With an increase in the number of individuals sensitive to invasive fungal infections, it is seen that the leading cause of opportunistic mycoses worldwide is *Candida* species[2,3]. These fungi are common gastrointestinal flora capable of infecting both immunocompetent and immunocompromised individuals, although there is a higher incidence of infection in immunocompromised hosts that will eventually develop Candidiasis. Thus, Candidiasis is often called the "disease of diseased"[4].

Candidiasis is a wide-ranging term that refers to cutaneous, mucosal and deep-seated organ infections. When the infection is found in the bloodstream it is called invasive candidiasis, which is harder to diagnose and is associated with organ infections with or without candidemia[5]. Candidemia is reported to be the fourth most frequent cause of bloodstream infections in the United States of America (USA), and between the sixth and tenth in Europe[5,6]. Invasive candidiasis, at its worse, can result in disseminated infections and sepsis with an associated mortality as high as 40% in the USA, a percentage that varies geographically, ranging from 29% to 76%[7–9]. The incidence of invasive candidiasis in intensive care unit (ICU) patients from 2006 to 2008 was studied in 14 European countries, with results showing a median rate of 9 candidemias per 1000 ICU admissions[10]. Additionally, the prolonged hospital stays that accompany invasive candidiasis result in increased healthcare costs.

Although 30 different species of *Candida* have been identified as human infectious agents[11], with the list still expanding, in the last decades around 95% of these infections are due to five species: *Candida albicans*, *Candida glabrata*, *Candida parapsilosis*, *Candida tropicalis* and *Candida krusei*[2,3,12]. *C. albicans* is the most studied and isolated species worldwide due to this being the leading cause of invasive candidiasis (up to two-thirds of the cases in population-based studies[5,6]). However, the extensive use of antifungal agents, especially the commonly used azole antifungals, led to increased antifungal resistance phenotypes and alterations in *Candida* species epidemiology, which resulted in a global shift in predominance favouring nonalbicans *Candida* species less susceptible to azoles, particularly *C. glabrata*[3,6,7,13,14].

Regardless the name, *C. glabrata* is actually more closely related to the model yeast *Saccharomyces cerevisiae* in phylogeny than to *C.albicans*[15]. Studies on both *C. glabrata* and *C. albicans*' genomes lead to the conclusion that these species must have followed independent evolutionary paths to pathogenesis.

1.3 Emergence of candidiasis: focus on *Candida glabrata*

Different studies have shown that *C. glabrata* is now the second or third most isolated species from patients with Invasive Candidiasis in the USA and Europe[5,14,16]. Although *C. glabrata* also colonises the oral cavity, vagina, and gut of healthy humans as innocuous commensals, it is especially recurrent in immunocompromised individuals as is the case of cancer patients, the elderly and patients receiving intensive care[5,17–19]. Moreover, it is the main species exhibiting multiazole, echinocandin and multidrug resistance[19]. This propensity for diseased host colonisation and higher drug resistance is possibly the answer to why the overall mortality seen with *C. glabrata* is so high (30-70%) when compared to other *Candida* species (15-40%)[4,17,20]. Generally, it is hard to obtain an accurate and fast

diagnosis of Candidiasis as it is usually diagnosed late and only considered after antibiotic treatments fail. Besides, there are only four main classes of antifungals being currently used - azoles, polyenes, echinocandins and pyrimidine analogs[21,22] -, a limitation that lowers the probability of the treatment being successful and even increases the probability of a fatal outcome when the pathogen displays multidrug resistance (MDR)[21].

Several risk factors have been identified for *C. glabrata* bloodstream infections, the most common being previous fluconazole use and prior exposure to a broad spectrum of antibiotics, the use of indwelling devices like urinary or venal catheters, and surgery (such as organ transplantation)[4,16,17,19,20,23,24].

Previous fluconazole use as antifungal prophylaxis, that is, as prevention of fungal infection, has played a major role in the emergence of non-susceptible *Candida* species most likely by exerting selective pressure that promotes genomic changes in the pathogen. Besides genomic alterations, like the upregulation of efflux pumps, that would improve resistance, prior fluconazole administration could also lead to changes in the patient's endogenous flora, thus promoting colonisation and infection of the organism with fluconazole-resistant *C. glabrata*[17,25,26].

Biofilms are the most prevalent type of microbial growth in nature and confer substantial protection and resistance to antifungal therapy, which results in persistent infections. *Candida* cells detached from biofilms seem to have a higher association with mortality than equivalent planktonic cells[27]. Indeed, mortality was found to be higher in patients infected by isolates that formed biofilms when compared to infections by non-biofilm-forming isolates[28,29]. It was also shown that biofilms formed by *C. glabrata* have the highest metabolic activity when compared to other *Candida*[28]. Other investigations have highlighted the protective role of biofilms to *C. glabrata* cells, revealing that biofilms need around 10 to 100 times higher concentrations of antifungal drugs to be eradicated comparatively to planktonic cells[30], a fact that had previously been reported for *C. albicans* biofilms[31].

An important factor that influences antifungal resistance in biofilms is cell density. Increased density is correlated with greater cooperation between cells through 'quorum sensing', a concept that relies on the ability to coordinate gene expression according to the population density by secretion of signaling molecules[32]. It is important to consider that the accumulation of these fungal 'quorum-sensing' molecules have influence, at a certain level, on the host cells' metabolism. For instance, farnesol, a 'quorum-sensing'-like molecule in *C. albicans*, was shown to act as an immune modulatory signalling molecule by preventing the activation of cellular immunity. This molecule can alter the differentiation of monocytes to immature dendritic cells through modulation of cell surface markers, and was shown to reduce the expression of several genes involved in cell adhesion and migration, this way impairing the ability of dendritic cells to recruit and activate T cells[33,34]. Additionally, farnesol was shown to increase resistance of *C. albicans* to reactive oxygen species (ROS) generated by the host's immune system[35], a mechanism used to induce stress and kill pathogens once inside the phagosome[36]. Still, these host-pathogen interactions remain poorly understood.

Medical devices that are particularly prone to host biofilm colonisation are catheters (central venous and urinary), which are frequently associated with *Candida* infections. Catheterization can lead to infection either by introducing organisms during the process or by allowing migration of organisms into the vessel or bladder along the surface of the catheter. Ultimately, removal of the infected device is required, often involving surgery. Even with device removal and infection treatment, the mortality rates related to these type of infections remains too high[37].

To be properly assisted and treated, cancer patients are often subjected to indwelling catheters, intravenous feeding, abdominal surgery and antibacterial drugs, making them more easily exposed to yeast colonisation and infection[24]. Cancer centres have described a shift from *C. albicans* towards *C. glabrata* as the source of fungemia, possibly due to the previous use of the antifungal fluconazole to prevent infections and the spread of disease in the patients[24,38]. The link between an increased isolation of *C. glabrata* and the use of fluconazole is strongest for cancer patients, where the percentage of *C. glabrata* colonisation is higher in patients with solid tumours when compared to patients with hematologic malignancies[17,24].

Older age has also been reported to be a risk factor for colonisation with *C. glabrata*[25,38,39]. Prior studies have noted an increased risk of *C. glabrata* fungemia, as well as higher chances of dying from the event, in older adults[38]. Anurag Malani *et al*[39] studied the relationship of *C. glabrata* colonisation of the oral cavity with age and hospital/extended care facility stay, finding that colonisation was more frequent in older residents of an extended care facility or hospital, with it being uncommon in community-dwelling persons, regardless of age. These data suggest that perhaps *C. glabrata* is acquired in the hospital or extended care facility. The use of denture also represents a risk factor for oral cavity yeast colonisation as it has been noted that individuals that wear a denture were three times more likely to harbour *C. glabrata* than those that don't[39].

Nevertheless, without external factors such as medical devices or surgery, *C. glabrata* still manages to invade and colonize host tissues, suggesting this pathogen also resorts to other invasion mechanisms yet poorly understood. The occurrence of co-infection with other microorganisms, such as *C. albicans*, is a possibility to explain *C. glabrata* invasion capacity, taking advantage of the tissue damage and consequent tissue invasion by *C. albicans*[40].

1.4 Virulence features

Interactions of microbes with plants, animals and humans comprise symbiotic, commensal and parasitic relationships, where the latter can result in disease of the host. Virulence is defined as the ability of an organism to cause disease in a given host. The host-microbe interaction is specific, and some strains may be more or less virulent than others. Hence, the degree of virulence can be altered and even become inexistent with changes occurring in either the microbe or the host. However, it should be pointed out that the capacity of causing damage is not a property of the microorganism alone. Particularly for opportunistic pathogens, virulence is only expressed under certain conditions, for example when encountering a weakened host. With this in mind, virulence could be seen as a secondary effect, perhaps as one of the possible outcomes of adapting to another selective pressure, an evolutionary accident rather than an evolutionary goal in itself. Additional microbial features, often called 'virulence factors', are needed for the host damage to be achieved[41,42].

The increasing incidence of *Candida* opportunistic pathogens is associated with a number of virulence factors, the most relevant being the ones involved in adhesion to host tissues and medical devices, biofilm formation and secretion of hydrolytic enzymes[43]. *C. glabrata* is a successful pathogen despite lacking true hyphae formation ability. Its virulence is associated to its versatility of adaptation to a variety of different environments due to high intrinsic stress resistance and its ability to form biofilms[44]. This pathogen holds several virulence factors that will be discussed in this chapter, including the ability to form biofilms and to adhere to host cells and medical devices, as well as its strategies for host immune system evasion.

1.4.1 Biofilm formation and the Efg1 and Tec1 transcription factors

Candida biofilms are composed by yeast cells immersed in a self-produced complex matrix containing extracellular biopolymers, making them much more resistant to treatments and to the host immune system than original planktonic cells. The biofilm matrix is considered a barrier to the diffusion of antimicrobials, offering additional protection to the yeast cells by limiting the access of xenobiotics to the organisms at the bottom layers of the biofilm. Under these conditions of high microbial burden and poor drug penetration, a strong selective pressure is created and, hence, resistant mutants can emerge[45]. This is why once established, biofilm infections are almost impossible to eliminate[41,44,46]. The formation of biofilms starts with the attachment and colonisation of yeast cells to a surface, followed by cell proliferation that creates a first layer of microcolonies anchored to the given surface. After cellular growth, the production of extracellular matrix begins and, depending on the *Candida* species, growth of pseudohyphae and/or true hyphae can occur[47]. When biofilm maturation is achieved, cell detachment and dispersion takes place in order to find new surfaces to colonise, this way acting as a persistent source of cells that disseminate into the bloodstream[48].

Hyphae and pseudohyphae are two filamentous forms morphologically distinguishable from each other. Pseudohyphae are wider than hyphae, consisting of chains of cells with various degrees of elongation and having constrictions at the sites of septation between adjacent cells (Figure 1, middle). True hyphae, on the other hand, form long tubes with parallel sides and no constrictions at the site of septation (Figure 1, right)[49,50].

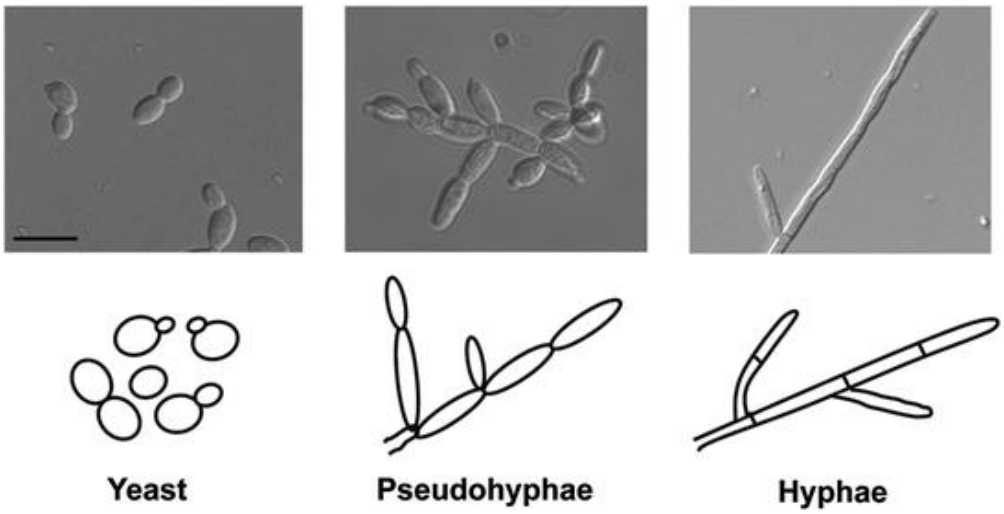

Figure 1 – Yeast, hyphae and pseudohyphae morphologies: scanning electron microscopy images of *C. albicans* different morphological stages – from Kadosh D. '*Morphogenesis in C. albicans*' (2017)[51]

The ability to form hyphae has proven to be advantageous for the microorganism, not only because these elongated filamentous structures offer increased stability to biofilms, but also because hyphal cells facilitate the bursting of macrophages in case of phagocytosis, this way helping fungal escape from the host's immune system[52,53]. Additionally, hyphal morphogenesis plays an important role in cell adhesion by regulating the expression of adhesion maintenance proteins[54]. Although *C. glabrata* does not form thick biofilms with hyphae like *C. albicans*, its biofilms are dense and compact (Figure 2) containing only blastospores - asexual fungal spores produced by budding - since this yeast is unable to generate filamentous forms[48,55]. There is still little information concerning

the composition of *C. glabrata* biofilms, however, it has been shown that this pathogen's biofilm matrix contains higher levels of both protein and carbohydrate compared with other *Candida* species[56]. This represents an interesting finding that could be related to *C. glabrata* potential virulence, as this species' infections result in the highest mortality rate[17,20] as well as high antifungal resistance[19].

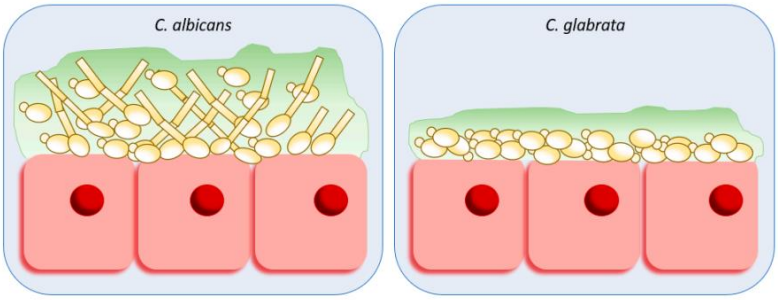

Figure 2 – Schematic depiction of biofilm formation in *C. albicans* and *C. glabrata* – from Galocha *et al 'Divergent Approaches to Virulence in* C. albicans *and* C. glabrata*: Two Sides of the Same Coin'* (2019)[40]

Because the adhesion of the microorganism to a host or medical device surface can result in biofilm formation, it is a very important step in the development of infection, and this adhesion is based on interactions between the cell wall of the pathogen and the surface it encounters. This way, it is reasonable to expect that adhesion relies on molecules present in the cell wall, as is the case of specific cell wall proteins called adhesins[48]. Most known fungal adhesins are glycosylphosphatidylinositol (GPI)-anchored cell wall proteins. In the C-terminal, there is a GPI anchor that links the adhesin to the cell wall, whereas the N-terminal contains a carbohydrate or peptide binding domain and the middle domain consists of a serine/threonine domain[57].

1.4.1.1 Transcriptional regulation of adhesion and biofilm formation in *C. albicans and C. glabrata*

In *C. albicans*, adhesion is mainly mediated by a family of eight agglutinin-like sequence (Als) proteins[48] along with the surface protein Hwp1, a member of the hyphal wall protein (Hwp) family. Both families belong to the GPI cell wall protein family[48,58]. Expression of the *ALS* and *HWP1* genes is reported to be much higher in hyphal cells than in yeast cells[58]. Specifically, among the eight members of the Als family, Als1 and Als3 were shown to be involved in biofilm surface attachment and cell adhesion to several biotic surfaces, with Als3 playing the most notorious role in biofilm formation as its deletion leads to severe biofilm defects comparing to the *wild-type* parental strain[48,59,60]. Additionally, Hwp2, Rbt1, Eap1 and Ywp1 – all members of the Hwp family of proteins – are also needed for biofilm development[61].

Regarding transcriptional regulation of biofilm formation in *C. albicans*, six major regulators have been identified: *BCR1*, *TEC1*, *EFG1*, *NDT80*, *ROB1* and *BRG1*. Nobile *et al* (2012)[47] selected these transcriptional regulators to generate six deletion mutants and test whether biofilm growth was affected *in vivo* using rat denture and catheter models, with results showing that all six regulators are required for normal biofilm formation in both *in vivo* models. The same authors studied *C. albicans* biofilm transcriptional network to uncover these transcription factors (TFs)' direct targets, ultimately pointing out that each regulator controls the expression of the other five and that most target genes are controlled by more than one master regulator. Interestingly, the overall biofilm network of *C. albicans*, containing all target genes of the six regulators, covers about 15% of the genes in the genome[47]

The adherence of *C. albicans* cells is regulated by Bcr1, a zinc finger protein that promotes biofilm formation by controlling the expression of the Als3, Als1 and Hwp1 surface adhesins, as well as the cell surface protein Ece1[62]. Bcr1 is not required for hyphal morphogenesis but it was found to stimulate hyphal adherence properties. *C. albicans bcr1*/*bcr1* mutant strains showed a defect in biofilm formation that was fully restored when the expression of Als3 was increased, but only partially rescued through increased expression of the Als1 and Hwp1 adhesins[62]. Furthermore, a deletion of the *ALS3* gene led to a biofilm formation defect similar to that of the *bcr1*/*bcr1* mutant, which implies the adhesin expression deficiency to be the major cause for the biofilm formation defect found in *bcr1*/*bcr1* mutant strains. Bcr1 acts downstream of the TF Tec1, its positive regulator[62,63].

Contrarily to other *Candida* species, like *C. albicans*, *C. glabrata* lacks the capability to form true hyphae[19,41]. Nevertheless, *C. glabrata* genome harbours several genes involved in adhesion, such as the major group of epithelial adhesins (Epa) encoded by the *EPA* genes[55,64]. The overall structure of these proteins, also belonging to the GPI protein family, is similar to that of the Als proteins in *C. albicans*[48,65], with similarities to the flocculins/lectins encoded by *FLO* genes in *S. cerevisiae* as well[66]. Nevertheless, a fundamental difference between *C. albicans* and *C. glabrata* is that *EPA* gene expression, but not *ALS* expression, is regulated by subtelomeric silencing, as most of the *EPA* genes are encoded in subtelomeric clusters[59,60,65]. This type of regulation points to a rapid genetic adaptation of *C. glabrata* to different environmental conditions during host colonization[67]. In *S. cerevisiae*, a chromatin-based transcriptional silencing has already been described, with the silencing being initiated by the binding of the telomere associated protein Rap1 to the telomeric repeats. Rap1 then recruits a complex of proteins – the Sir complex – encoded by the *SIR2*, *SIR3* and *SIR4* genes[68,69]. Sir2, a nicotinamide adenine dinucleotide (NAD^+)-dependent histone deacetylase that is thought to have the key catalytic activity of the Sir complex, deacetylates the target H3 and H4 histones, this way uncovering high affinity binding sites for Sir3 and Sir4. The binding of these two proteins is assumed to compose a repressive chromatin structure[68,69]. Additionally, Rap1 interacts with two other proteins known as Rif 1 and Rif2 (Rap1-interacting factors 1 and 2), which play a fundamental role in regulating telomere length[69]. Silencing depends indirectly on the distance of the silenced gene to the telomere, and it decreases as the silenced gene is found further away from the telomere[68,69]. In *C. glabrata*, subtelomeric silencing relies on several of the same factors as in *S. cerevisiae*, such as the Sir-complex, Rap1 and Rif1[59,68,69].

Although the family of *EPA* genes in *C. glabrata* comprises 17-23 genes, *EPA1*, *EPA6* and *EPA7* seem to be the most essential in adhesion[48,64]. Epa1 is a Ca^{2+}-dependent lectin and it has been shown that deletion of *EPA1* alone reduces *C. glabrata* adherence *in vitro* to host epithelial cells[48,55,64]. However, in murine models of systemic or vaginal candidiasis, no significant phenotypic difference was found between *EPA1* and Δ*epa1* strains of *C. glabrata*[70]. This could indicate the existence of additional adhesins that compensate *in vivo* for the absence of *EPA1*. Regarding Epa6, *C. glabrata* does not normally express *EPA6 in vitro*[55,64], yet this gene is expressed during murine urinary tract infection as a result of low nicotinic acid levels[71]. *C. glabrata* is a nicotinic acid auxotroph, so the absence of this compound – present in very low levels in the urine – leads to reduced levels of NAD^+. Consequently, this reduction could possibly inhibit the activity of the NAD^+-dependent Sir2, this way reducing the subtelomeric silencing and allowing for the expression of *EPA6*[72].

Iraqui and colleagues (2005)[59] showed that a disruption in the silencing machinery leads to the transcriptional induction of *EPA6* and *EPA7* and, consequently, to a marked increase of *in vitro* adherence and biofilm formation.

The authors also observed that the deletion of *EPA6* did not affect the number of colonies attached to the plastic surface, but the size of the colonies was significantly smaller, which implies a role of Epa6 in cell-cell adherence within the biofilm rather than in surface adherence. In another study, silencing mutant strains - Δ*rif1*, Δ*sir3* and a *rap1-21* strain with a mutation that prevents Rap1 interaction with the Sir complex – exhibited hyper-adhesion to epithelial cells and increased transcription of *EPA1* as well as induction of the usually silent *EPA6* and *EPA7* genes[69]. Together, these results indicate the existence of a complex regulatory system that controls the expression of the *EPA* genes, possibly reflecting variations in expression of different *EPA* family members in response to the particular environmental conditions encountered by *C. glabrata* cells. It has been demonstrated that *EPA1* expression is higher in lag-phased cells[73], while *EPA6* is transcribed at the highest level during the late stationary growth phase, that is, in high cell density and biofilm conditions[59].

The Yak1 kinase, together with the Sir complex (Sir2-4) and Rap1, is another protein that was demonstrated to be required for the expression of *EPA6* and *EPA7* in *C. glabrata*, acting through a subtelomeric silencing machinery. Therefore, Yak1 plays an important role in the regulation of biofilm formation in *C. glabrata*, although it remains unclear whether Yak1 is itself regulated by biofilm growth signals[59]. This kinase was previously identified in *S. cerevisiae* – showing a 58% similarity at the amino acid level to the *C. glabrata* Yak1 –, where it was described as a multifactorial protein that, among other functions, plays a role in starvation signal mediation[59]. Still related to the regulation of biofilm formation in *C. glabrata* is a protein similar to *S. cerevisiae* Cst6, a basic leucine zipper (bZIP) TF involved in chromosome stability and telomere maintenance[66,74]. To test the influence of Cst6 in *EPA6* gene expression, Riera *et al* (2012)[66] conducted a study where *C. glabrata* Δ*cst6* strains were grown in biofilm growth conditions and a more than 2-fold increase in *EPA6* expression was observed when compared to the *wild-type* parental strain, a result that points to Cst6 being a negative regulator of *EPA6* expression and, consequently, of biofilm formation. The authors also identified the Cst6 mode of action in regulating biofilm formation to be independent of the Yak1/Sir-complex signalling pathway. The Cst6 pathway for the regulation of biofilm formation in *C. glabrata* is still poorly understood, nonetheless this protein has been identified in *S. cerevisiae* as a heat-responsive TF[75]. In fact, increased levels of heat shock response proteins were observed in *C. glabrata* biofilms[76], which suggests that Cst6 could be involved in both biofilm formation and heat-shock regulation, with a possible overlap between these two pathways[66].

There is yet another signaling complex involved in the regulation of biofilm formation in *C. glabrata*: the Swi/Snf complex. It is composed by at least 11 distinct polypeptides, the most critical being Snf2 and Snf6[66], and acts in the remodelling of chromatin through the destabilization of histone-DNA interactions, this way controlling the transcription of several genes. It has been reported that Δ*snf2* and Δ*snf6* mutant strains showed reduced ability to develop biofilms and a severe decrease in *EPA6* gene expression compared to the *wild-type* strain, revealing a negative modulation of subtelomeric silencing[66]. In the same study, the authors noticed that the Swi/Snf-mediated regulation of biofilm formation was only seen when the subtelomeric silencing pathway was intact, and it was further suggested that the Swi/Snf complex modulates *EPA6* expression in a Sir4-dependent manner[66]. Regarding *EPA1* gene, the Swi/Snf complex seems to have no impact in regulating its expression, implying a Swi/Snf gene-specific regulation of the *EPA* genes in *C. glabrata*[66]. The Swi/Snf complex can also be found in *C. albicans* where it is involved in hyphal development and pathogenicity, although its direct target(s) are still unknown[77].

1.4.1.2 The importance of Tec1 and Efg1 transcription factors in *Candida* virulence

Tec1 belongs to the transcriptional enhancer activators (TEA/ATTS) family of TFs that regulates *C. albicans* virulence[78]. This TF is required for hyphal formation *in vitro*, for macrophage rapid evasion and for the expression of the secreted aspartyl proteinase genes *SAP4-6*[74,78], which have been shown to promote virulence in host systemic and mucosal candidal infections[79]. The Δ*tec1*/Δ*tec1* mutant shows severe biofilm defect and the expression of *BCR1* in this strain promotes growth on the surface substrate; however, the biofilm formed is unstable and exhibited 3-fold less biomass than the *wild-type* and complemented mutant strains, but still showed increased adherence compared to the Δ*tec1*/Δ*tec1* strain[62]. These findings establish adherence as a key property regulated by Bcr1 that promotes biofilm formation in *C. albicans*, with Als3 having the most critical role in adhesion. The defective biofilm produced by the Δ*tec1*/Δ*tec1* mutant strain was restored when the strain was complemented with an ectopic copy of the *wild-type TEC1* gene, thereby demonstrating that the *TEC1* mutation was the cause of the biofilm formation defect[63].

The biofilm TF network of *C. albicans* (comprising Bcr1, Brg1, Efg1, Ndt80, Rob1 and Tec1), disclosed by Nobile *et al* (2012)[47], was further studied, with data showing a tight connection between all the six members of the TF network, as well as the importance of each member being fully functional for normal biofilm formation[80]. Moreover, disturbances of this network at multiple TFs led to reduced *TEC1* expression, suggesting that not only *TEC1* expression is an important output of the TF network, but it is also deeply connected to the functional state of the network in general. In addition, small changes in *TEC1* expression were shown to cause significant changes in phenotype, and it was further implied that most biofilm defects observed in the TF deletion mutants of the network in question were caused by a decreased *TEC1* gene expression[80].

There is a family of proteins found exclusively in fungi, known as the APSES proteins (Asm1, Phd1, Sok2, Efg1 and StuA), that represents a group of TFs known to be crucial regulators of fungal development, along with other biological processes. All APSES proteins share a highly conserved DNA-binding domain (APSES domain), and in *C. albicans* two of these proteins have been identified: Efg1 and Efh1[81–83]. While the function of Efh1 is still uncertain, the role of Efg1 in *C. albicans* has been explored in several studies, and it was found that this TF plays an important role in promoting the filamentous growth in this yeast[84,85], acting as a regulator of yeast-to-hyphae interconversion, chlamydospore (thick-walled asexual fungal spore) formation and phenotypic switching[81–84]. Filamentation in *C. albicans* is regulated by several signaling pathways. Cph1 and Efg1 were the first identified regulators of hyphal development, acting through a Efg1-mediated cAMP/protein kinase A (PKA) pathway and a Cph1-mediated mitogen-activated protein (MAP) kinase pathway. Later on, the Cph2 protein was also found to regulate hyphal development in *C. albicans*, but in a medium-specific manner[86].

It has been demonstrated that *C. albicans* Δ*efg1* strains exhibit markedly altered biofilm phenotypes compared to wildtype strains. These mutants revealed to be less virulent and presented lower levels of infection of endothelial cells and plasma-coated catheters when comparing with *wild-type* strains[87]. As previously mentioned, Nobile *et al* (2012)[47] demonstrated that the TF Efg1 is essential for normal biofilm formation in *C. albicans*, showing the occurrence of a defect in hyphal development in Δ*efg1* strains of this yeast. Moreover, different studies identified Efg1[86] and Cph2[86,88] as regulators of *TEC1* expression, a gene that encodes a TF known to modulate hyphal development in *C. albicans* as well. In their study, Shelley Lane and colleagues (2001)[86] show two different hyphal signaling pathways, Efg1-mediated and Cph2-mediated, converging to regulate a common gene, *TEC1*, suggesting

C. albicans can respond to different medium or growth conditions - different upstream signals - with a single downstream output (Figure 3). Deletion of the *CPH2* gene in *C. albicans* was shown to generate completely smooth yeast colonies, a result consistent with the assumed role of Cph2 as a hyphal development regulator. Although the ectopic expression of *TEC1* in the *C. albicans* Δ*cph2*/Δ*cph2* mutant strain suppressed the defect, generating fine filamented colonies, the number of filaments was smaller than the number seen in the *wild-type* strain with ectopic *TEC1* expression[88]. This observation indicates other possible functions of Cph2, besides regulating *TEC1* gene expression.

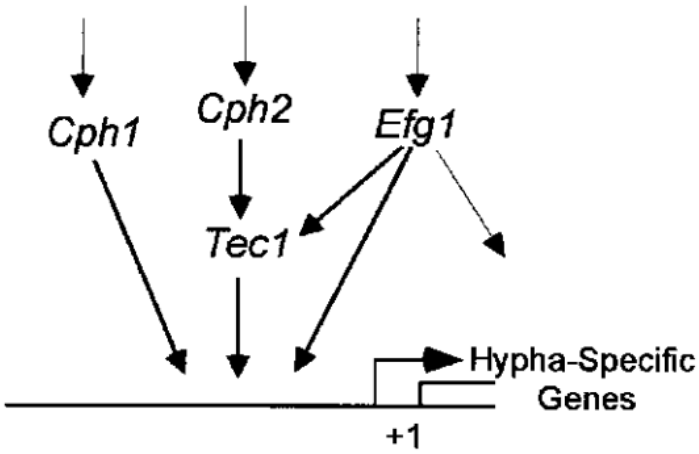

Figure 3 – Different signaling pathways in *C. albicans* converging to regulate a common set of genes in response to specific conditions – from Lane *et al* '*DNA array studies demonstrate convergent regulation of virulence factors by Cph1, Cph2, and Efg1 in* Candida albicans' (2001)[86]

C. albicans TEC1 and *EFG1* genes were also shown to be involved in regulating the production of alkali-soluble polysaccharides (ASPs), which are major components of the extracellular matrix (ECM) of *C. albicans* biofilms, with both Δ*tec1* and Δ*efg1* mutants generating defective biofilms with significantly reduced amounts of ASPs in their ECM[89].

Even though there is still little or no information about the role of the equivalent *EFG1* and *TEC1* genes in *C. glabrata*, understanding the relationship between the function of each TF and virulence in *C. albicans* and knowing that Efg1 and Tec1 are conserved in *C. glabrata* could indicate a similar involvement of Efg1 and Tec1 in virulence mechanisms of this pathogen. Among several *C. glabrata* TFs identified in our lab as biofilm regulators, *CgEFG1* and *CgTEC1* were found to have a considerable impact on biofilm formation (Cavalheiro *et al*, unpublished results). Thus, it seems relevant to further study the role of *EFG1* and *TEC1* in *C. glabrata* virulence. Considering that biofilm formation on indwelling medical devices potentiates the risk of invasive infections, these two genes represent promising targets for therapeutic purposes.

1.4.2 Surviving the host's immune system

Avoiding the mechanisms of the host's immune system is a challenge for pathogens. Once the phagocytotic cell recognizes a microbe through the PAMPs (pathogen-associated molecular patterns) exhibited on its surface, the pathogen is engulfed[90] and this triggers the phagocytic pathway inside the phagocyte, which involves phagosome maturation via fusion with endosomal vesicles followed by a switch of membrane proteins, and finally the yielding

of the phagolysosome that holds a highly hostile environment to microbes[91]. Nonetheless, it has been shown that *C. glabrata* can survive and replicate inside phagocytotic cells, such as macrophages, until these host cells finally burst and release the fungi[92,93]. Although both species have their ways to handle the host's immune system, the mechanisms of action of *C. albicans* and *C. glabrata* to do so seem to be quite different. First, *C. albicans* triggers a strong host immune response, whereas the activation of the host's immune system is weak when the pathogen is *C. glabrata* (Figure 4). Second, while *C. albicans*' escape is associated with hyphal formation that, in the case of phagocytosis, causes the macrophage to burst few hours after the yeast uptake, *C. glabrata* manages to survive and replicate intracellularly, maintaining the macrophage's viability for long periods until fungal load becomes too high, causing immune cell lysis. This suggests that *C. glabrata* has the ability to adapt to more hostile environments and evolved its own intracellular survival strategy, whilst *C. albicans* follows a quick escape strategy[91].

To further investigate *C. glabrata* response to phagocytosis, Kaur *et al* (2007)[94] analysed the interaction of *C. glabrata* cells with macrophages and found that, upon internalization by the macrophage, the transcription of a *C. glabrata*-specific cluster of eight genes that encode a family of putative GPI-linked aspartyl proteases is induced. These genes are closely related to the *YPS* (Yapsin) genes of *S. cerevisiae*, and, in this yeast, they are induced during cell wall remodelling, with their deletion leading to an increase in cell's sensitivity to cell wall disrupting agents[94]. The transcriptional response of *C. glabrata* when exposed to macrophages consists of the remodelling of carbon metabolism, which includes the induction of genes encoding enzymes involved in β-oxidation, glyoxylate cycle and gluconeogenesis. But what is the role of macrophage-induced *YPS* genes? Kaur and colleagues proposed that Yps proteases could be involved in cell surface remodelling by removal of certain GPI-anchored cell wall proteins (GPI-CWPs) according to different host environments. In *C. glabrata*, these GPI-CWPs include a family of adhesins encoded by the *EPA* genes. Interestingly, *yps* mutants of *C. glabrata* present a serious defect in the processing of Epa1 from the cell surface, a GPI-linked adhesin known to play an important role in *C. glabrata* adherence to host cells[94]. This implies a role of the Yps proteins in *C. glabrata* virulence. Additionally, Yps proteases may confer protection against immune recognition through removal of GPI-CWPs targeted by the host's immune system.

Following phagocytosis, one of the phagocytic cell's response to create an intracellular stress environment for the engulfed pathogen is the production of reactive nitrogen species (RNS), such as nitric oxide (NO), that helps killing the pathogen[95]. When infected with *wild-type S. cerevisiae*, macrophages are activated in order to increase the production of NO, however, infection of macrophages with *wild-type C. glabrata* results in no such activation. On the other hand, *yps* mutant *C. glabrata* cells were shown to strongly stimulate NO production by infected macrophages, an outcome that suggests *YPS*-mediated cell wall remodelling may play a role in modifying or even supressing the activation of macrophages[94].

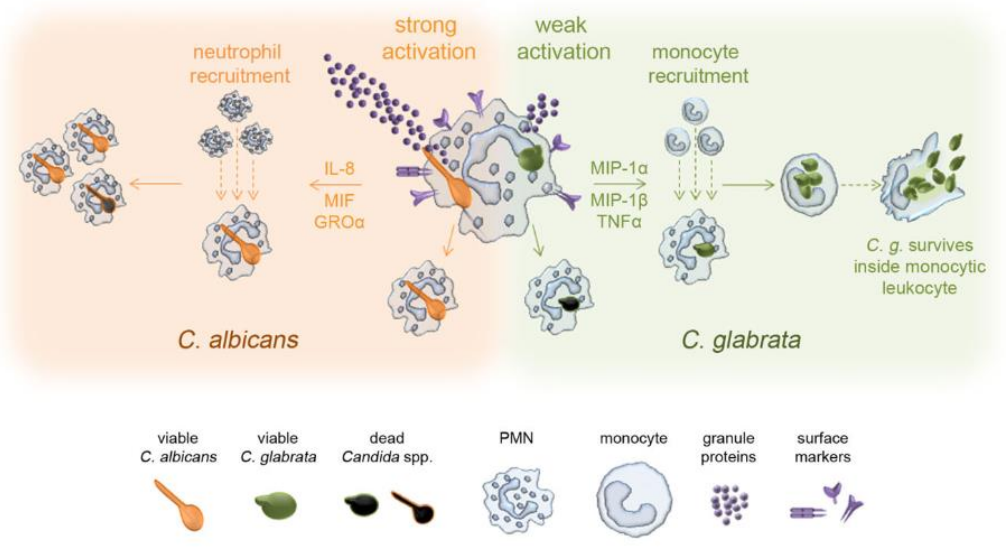

Figure 4 – Different responses of host immune system to *C. albicans* and *C. glabrata* – from Duggan *et al 'Neutrophil activation by* Candida glabrata *but not* Candida albicans *promotes fungal uptake by monocytes'* (2015)[96]

The survival of *C. glabrata* inside a phagocytotic cell seems to be related to the interference with the normal phagosomal maturation, inhibiting the formation of the phagolysosome and, consequently, inhibiting phagosome acidification[32,91]. Other challenges *C. glabrata* cells face after phagocytosis are increased oxidative stress and nutrient deprivation, but this yeast has shown to be capable of detoxifying or even inhibit the production of ROS induced by the macrophage. Different studies have established a set of genes found to influence *C. glabrata* viability in macrophages, including genes involved in the modulation of ROS production[97]. Also, to overcome starvation, *C. glabrata* goes through autophagic processes to recycle internal resources and sustain its viability inside the phagocytotic cell[32,91,93]. Hence, it has been proposed that *C. glabrata* induces endocytosis by host cells in order to penetrate host tissues[97,98]. All these mechanisms of action for intracellular survival could potentially aim for *C. glabrata*'s diffusion and establishment of infection in the host organism.

In order to survive within different host niches, *C. glabrata* is forced to adapt its metabolism according to nutrient availability, sometimes facing glucose-limited environments, as is the case of the intestine where the assimilation of lactate, an alternative carbon source, is required for the pathogen to survive[30]. It has been shown that the carbon source available in the microenvironment influences the efficiency of pathogen phagocytosis by the host's immune system cells. For example, *C. albicans* cells are reported to escape from macrophages, avoiding phagocytosis, more efficiently when grown in the presence of lactic acid rather than glucose, according to the work of Ene *et al* (2013)[99]. The same authors concluded that the carbon source modulates stress and antifungal resistance in *C. albicans* through alterations in the cell wall of the pathogen, although the exact mechanisms behind it are still unclear[100,101]. With the carbon source having such a considerable impact on the cell surface of *C. albicans*, it is possible to assume that the changes in phagocytosis efficiency could be related to cell wall modifications, where PAMPs are present. Previous studies on the interaction of macrophages and *C. glabrata* cells grown with acetic acid as the carbon source revealed that these cells are better phagocytosed and more easily killed by macrophages after infection than cells grown in glucose[30].

1.5 Antifungal drug resistance: emphasis on azoles and the transcription factors Rpn4 and Mar1

The impact of fungal pathogens on human health has become a public health problem, especially since the effectiveness of most antifungals used is affected by the pathogen's ability to develop resistance. In addition, host toxicity and undesirable side effects are also a concern when using antifungals, limiting their use in medical practice[102,103]. According to their effects on pathogens, antifungals can be classified as fungicides – being able to kill fungi – or fungistatic agents – inhibiting fungal growth and reproduction without killing the fungi[104].

Currently, there are four main classes of antifungals used in the treatment of systemic mycoses, each class with a specific mechanism of action (Figure 5): echinocandins, that inhibit fungal cell wall biosynthesis; polyenes, that bind to ergosterol in the cell membrane, leading to cell lysis; pyrimidine analogs, that block the DNA synthesis; and azoles, that target ergosterol biosynthesis[102,103,105]. There is also a fifth class that includes allylamines, although compounds of this class are generally used for treating superficial dermatophyte fungal infections[103,106].

Echinocandins inhibit the 1,3-β-D-glucan synthase, an enzyme - encoded by *FKS1* in *C. albicans* (*FKS2* in *C. glabrata*) - necessary for β-glucan synthesis, a major component of the fungal cell wall[102]. In yeast cells (such as *Candida* spp), β-glucan account for 30% to 60% of the cell wall, whereas in filamentous fungi (like *Aspergillus* spp) they are found in the hyphae. Thus, the use of echinocandins in yeast cells results in cell wall disruption and triggering of cell lysis, achieving a fungicidal effect. On the other hand, in filamentous fungi, echinocandins inhibit hyphae growth, causing a fungistatic effect. These antifungals are well tolerated by the human organism since there is no β-glucan or β-glucan synthase found in humans[105]. Although echinocandin resistance is a rare event, it has been reported in *Candida*, and it is mainly associated to amino acid substitutions within highly conserved regions of the Fks subunits of glucan synthase[102,106]. In *C. glabrata*, mutations in *FKS2* were shown to be responsible for echinocandin resistance[107]. Nevertheless, because *FKS2* expression is dependent of the protein calcineurin, resistance caused by *FKS2* could be reversed through calcineurin inhibitor administration[102].

Polyenes are amphipathic – with both polar (hydrophilic) and nonpolar (lipophilic) regions - natural molecules known as macrolides, most of them being produced by *Streptomyces* bacteria[108]. This class of antifungals targets ergosterol of fungal cell membranes, forming pores in the membrane that increase cell permeability and lead to the loss of ionic balance, resulting in cell death[109]. Amphotericin B is the most widely used polyene and it is mostly effective in systemic invasive fungal infections. Polyene resistance is not very common in clinical isolates of fungal pathogens, however, polyenes in general have several side effects in humans, making them very toxic. This toxicity could be associated with the low, yet not indifferent affinity of polyenes to cholesterol, the human equivalent of ergosterol[108].

Flucytosine, also known as 5-fluorocytosine (5-FC), is a pyrimidine analog with fungistatic activity that is converted to 5-fluorouracil (5-FU) by a cytosine deaminase present in susceptible fungi. The uptake of 5-FC occurs through a cytosine permease, yet this compound does not have antifungal activity by itself. This activity is achieved through the conversion of 5-FC into 5-FU, that is then integrated into DNA and RNA where it can block protein synthesis or inhibit DNA replication, this way interfering with cellular functioning of fungi[106,109]. As there is little or no cytosine deaminase activity found in mammalian cells, toxicity of 5-FC is selective to fungi[97]. Nonetheless, significant side effects have been reported, such as bone marrow suppression and hepatotoxicity[110,111], and the

development of 5-FC resistance in fungi has become a very common phenomenon. For this reason, the use of 5-FC as monotherapy has been disregarded, being generally preferred in combination therapy[106,108–111]. Two mechanisms of resistance with the use of 5-FC can be distinguished: specific mutations that result in activity deficiencies in enzymes required for the uptake, cellular transport and metabolism of 5-FC; or an increase in pyrimidine biosynthesis, which will compete with the antimetabolites of 5-FC and reduce its antimycotic activity[112].

Allylamines, such as terbinafine, have fungicidal activity against many fungi by interfering with ergosterol synthesis through the inhibition of squalene epoxidase. As a result of this inhibition, treated fungi rapidly accumulate the intermediate squalene and become deficient in the final product of the pathway, ergosterol, an essential component of fungal cell membranes[110,113]. Contrarily to other inhibitors of ergosterol biosynthesis, reports on terbinafine resistance in pathogenic fungi are uncommon, but Klobučníková *et al* (2003)[114] have identified a single-base substitution in the *ERG1* gene encoding the enzyme squalene epoxidase as the main cause for terbinafine resistance. The same authors found that even minor changes in fungal squalene epoxidase activity may lead to significant resistance of cell growth to terbinafine, indicating a probable emergence of resistant isolates with a more extensive use of terbinafine for the treatment of fungal infections[114].

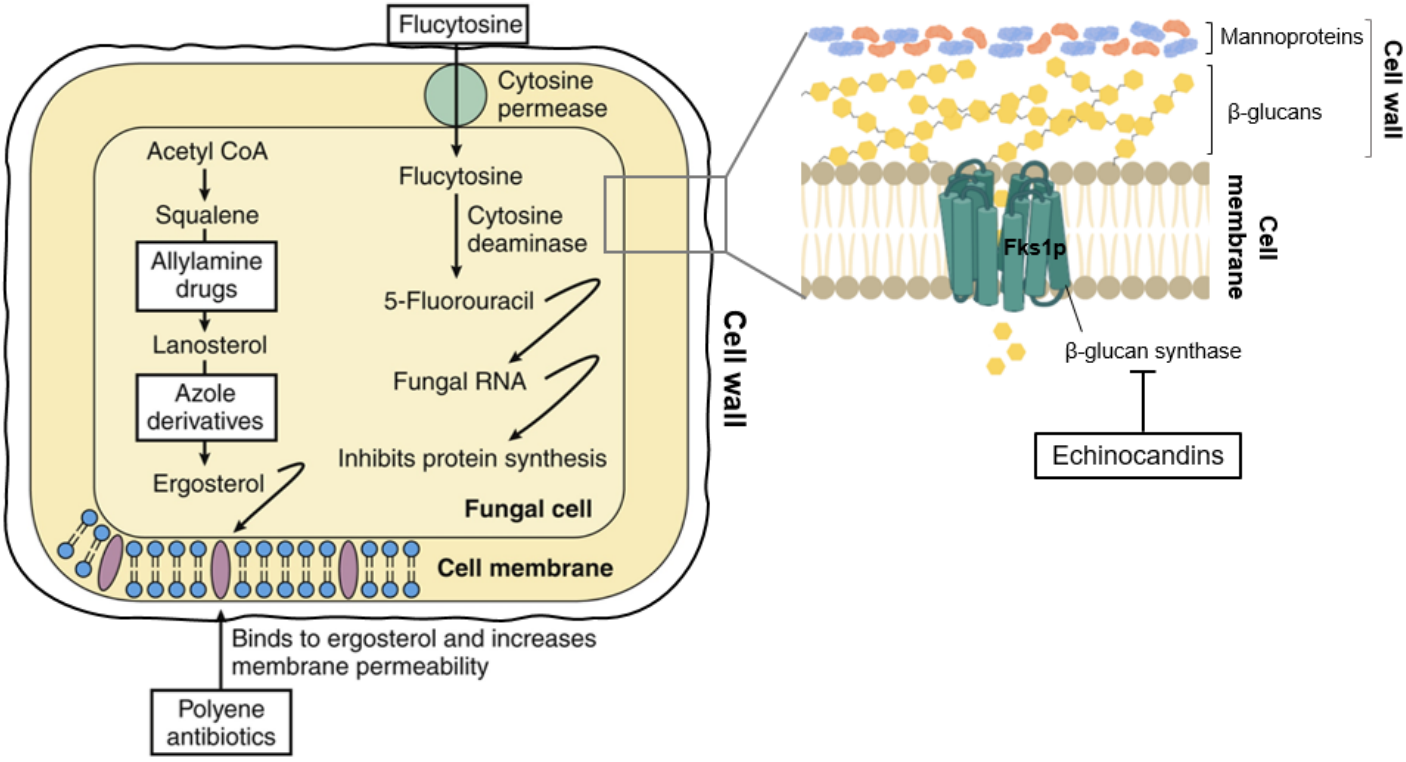

Figure 5 – The mechanisms of action of antifungal agents – from Brenner *et al* '*Pharmacology*' (2012)[115] (adapted)

C. glabrata is known to have a naturally low susceptibility to azoles and has been frequently observed to develop rapid antifungal resistance in patients treated with antifungal agents. The fact that azoles are fungistatic - inhibit the growth of fungi without killing them - instead of fungicidal could be a limitation for the efficacy of this class

of compounds in long-term treatment regimes, possibly facilitating the emergence of drug resistant strains by providing a selective environment[116]. Azoles and their derivatives are a class of antifungal drugs widely used in clinical practice to treat fungal infections in humans, from less severe injuries, for example in the skin and vaginal tract, to more dangerous infections in immunocompromised patients. Depending on the number of nitrogen atoms in an azole ring, azoles can be categorized into two subclasses: the first class comprises imidazoles which have two nitrogen atoms in a ring, and the second class consists of triazoles, that is, azoles with three nitrogen atoms in a ring, as is the case of fluconazole[106,117]. The mode of action of fungistatic azoles is to inhibit C14α-lanosterol demethylase encoded by *ERG11* gene, a cytochrome P450 enzyme involved in the conversion of lanosterol to ergosterol (Figure 6). This disruption of ergosterol biosynthesis, the major membrane sterol in fungi, as well as the accumulation of C14α-methylated sterols (*e.g.* lanosterol), alters the normal permeability and fluidity of the membrane and results in a plasma membrane with modified structure and function, which ultimately leads to blocking of fungal growth and proliferation[106,117–119].

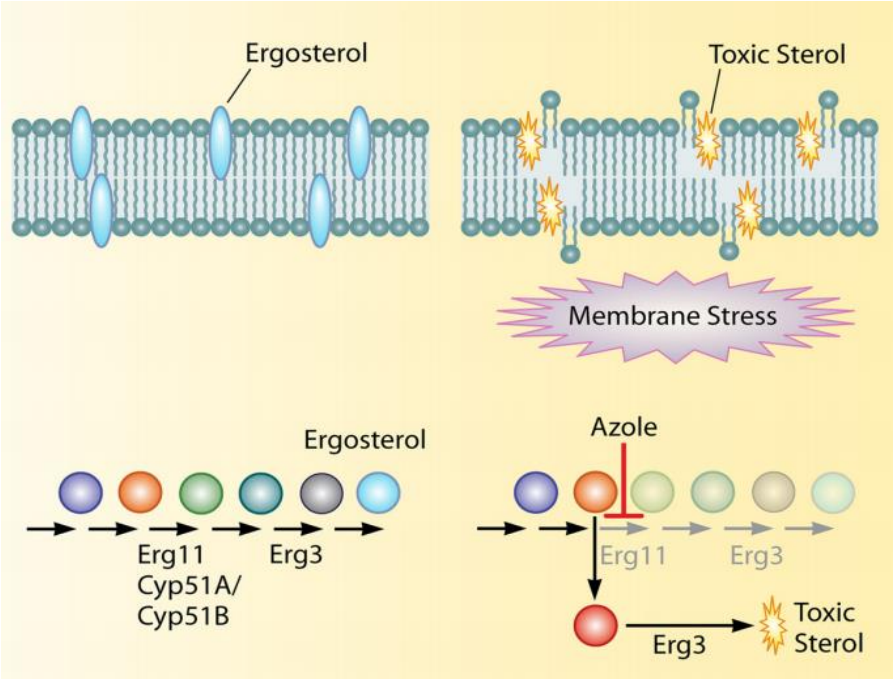

Figure 6 – The mechanism of action of azole antifungal agents in ergosterol biosynthesis – from Shapiro *et al* '*Regulatory Circuitry Governing Fungal Development, Drug Resistance, and Disease*' (2011)[120]

The acquisition of azole resistance in *C. glabrata* has been associated with mutations in the *PDR1* TF, leading to changes in the expression of downstream targets[21,121,122]. Alterations such as single point mutations in functional domains of *PDR1* have been described as the main mechanism for the enhancement of azole resistance in *C. glabrata*, and this TF was shown to bind directly to fluconazole, resulting in the transcriptional upregulation of genes encoding drug efflux pumps from the ATP-binding cassette (ABC) superfamily such as the *C. glabrata CDR1* (*CgCDR1*), *CgPDH1*/*CgCDR2* and *SNQ2*[21,121,123,124]. In support of this, Tsai *et al* (2006)[125] acknowledged that one single amino acid substitution in the TF CgPdr1 could lead to its hyperactivation and azole resistance, and Caudle *et al* (2011)[121] also showed increased transcription of *CgCDR1*, *CgPDH1* and *CgSNQ2* as well as higher azole resistance in *C. glabrata* strains with single point mutations in the putative functional domains of *CgPDR1*. These gain-of-function mutations in *PDR1*, that ultimately result in an increased efflux of azoles, play an essential role in mediating *C. glabrata* azole resistance. Another mechanism of *C. glabrata* for azole resistance involves

major facilitator superfamily (MFS) transporters. Catarina Costa and colleagues explored the determinant role of several multidrug resistance transporters from the MFS in *C. glabrata*'s resistance to different antifungal drugs, highlighting the importance of the Drug:H+ Antiporter (DHA) family transporters CgAqr1[126], CgQdr2[123] and CgTpo3[127] in flucytosine, imidazole and both imidaloze and triazole resistance, respectively. The major regulator of multidrug resistance in *C. glabrata*, CgPdr1, was found to directly control the gene expression of CgQdr2 and CgTpo3 encoding genes[123,127,128].

A connexion between high frequency of acquired azole resistance in *C. glabrata* and the loss of mitochondria has already been shown in several studies[21,116,122,125,129], however, the exact molecular mechanism underlying azole resistance and dysfunctional mitochondria in *C. glabrata* is not clear. A possible process is the overexpression of the major drug resistance transcriptional factor *PDR1*, which in turn induces the transcription of genes encoding ABC transporters, more specifically of the *CgCDR1* and *CgCDR2* genes[21,122,125,129]. Hence, when exposed to fluconazole, *C. glabrata* is able to acquire ABC transporter mediated resistance through the loss of mitochondrial functions. Kaur *et al* (2004)[116] proposed that this loss of mitochondria function in *C. glabrata* is reversible, making it possible for this pathogen to switch between competence (azole-susceptible) and incompetence (azole-resistant) mitochondrial stages in response to azole exposure.

It has been shown that *C. glabrata* can display high mutation rates when in contact with antifungal agents. Being an haploid organism, a single DNA mutation in *C. glabrata* is enough to generate an associated phenotype. The occurrence of mutations can be prompted by the so-called hyper-mutator phenotype. Healey *et al*.[130] hypothesized a decreased activity of the DNA repair machinery in *C. glabrata* clinical isolates that can explain this quick emergence of genetic changes accountable for drug resistance[130]. Later, a deficient DNA mismatch repair machinery was correlated to a *MSH2* defect[131]. Resistance to the class of echinocandin drugs, unlike azoles, remains relatively low, at < 3% with most *Candida* species[132]. However, with the broadening of azole resistance, in the past decade there has been an extensive echinocandin use, providing substantial selective pressure for the development of multidrug resistance[133]. Consequently, *C. glabrata* is reported to have increased echinocandin resistance and oftentimes shows cross-resistance between azoles and echinocandins, yielding multidrug-resistant strains[45,133,134]. Even so, there is a great variation in *C. glabrata* resistance rates between health centres around the world, making it essential to have previous knowledge about the local *Candida* species distribution and antifungal resistance rates to guide initial therapy, especially in high-risk patients colonised by *Candida* and in those previously exposed to or currently receiving antifungal treatment[133]. As a result of intrinsic and easily acquired drug resistance, treatment failure and high mortality rate, *C. glabrata* is revealing to be the next threat to implementing effective treatment of patients at risk for Candida bloodstream infections, considerably gaining the attention of investigators and clinicians in the past decade.

The molecular mechanisms underlying *C. glabrata* infectivity are far from being completely understood, making it necessary to find new approaches to study the virulence factors of this pathogen. Recent advances in technology and the development of more efficient genetic engineering techniques should promote research into *C. glabrata*'s virulence mechanisms, host–pathogen relationship and reveal novel putative drug targets.

1.5.1 The Rpn4 transcription factor and azole resistance

In *S. cerevisiae*, the Rpn4 TF is responsible for the resistance to several stress factors such as heat-shock, oxidative stress and DNA damage-associated stress[135]. The Rpn4 TF has also been described to be part of the regulating system of proteasomal genes[135–137]. The ubiquitin-proteasome system is responsible for the majority of intracellular proteolysis, including damaged and misfolded proteins, therefore being an important regulatory mechanism in many cellular processes and against cellular damage caused by xenobiotics[135,137]. Regulation of the expression of yeast proteasome subunits occurs through the binding of the Rpn4 TF to a proteasome-associated control element (PACE), a particular motif found in the promoters of almost all proteasome subunit genes[135–137]. A *RPN4* deletion in *S. cerevisiae* generates strains with insufficient proteasomal activity, resulting in yeast cells hypersensitive to various stress factors and a significant decrease in cell survival under stress conditions[135,138,139]. Interestingly, Rpn4 regulates the expression of the *PDR1* gene, while, in turn, Pdr1 acts as a transactivator of *RPN4*, suggesting a link between this TF and multidrug resistance. Another target of Rpn4 is *YAP1*, a gene that encodes a TF whose function is both being an oxidative stress sensor and an expression regulator of genes involved in cellular responses to this type of stress[135,137,138]. The Yap1 TF was found to bind a Yap1 response element (YRE) present in the *RPN4* promoter under oxidative stress conditions, suggesting a positive feedback between Rpn4 and Yap1[137,138]. A fascinating network of TFs including Rpn4, Yap1 and the drug resistance TFs Pdr3 and Yrr1 was found to control the adaptive response of *S. cerevisiae* to the fungicide mancozeb[140,141]. It is important to highlight that the Rpn4-mediated regulation of the mentioned target genes occurs markedly under stress conditions but it is almost negligible in normal conditions[138].

A *S. cerevisiae RPN4* ortholog has been found in *C. glabrata*, yet less is known about its role in this pathogen. Nonetheless, *CgRPN4* has been described as a putative TF for proteasome genes and Vermistky *et al*. (2006)[142] demonstrated that *CgRPN4* was upregulated in fluconazole-resistant *C. glabrata* Pdr1 gain-of-function mutants. Recent research involving the cloning and subsequent expression of *CgRPN4* in a *S. cerevisiae* Δ*rpn4* mutant strain revealed that *CgRPN4* restored the resistance to oxidative, proteotoxic and DNA damage-associated stress[135]. In this study it was also shown that CgRpn4 is able to bind to the promoters of ScRpn4 target genes. The authors demonstrated that CgRpn4 is capable of functionally replacing ScRpn4, thus proposing that this TF could strongly contribute to oxidative stress resistance in *C. glabrata*[135].

A possible link between the *RPN4* gene and azole resistance in *C. glabrata* was recently uncovered in our lab[143], and further studies are ongoing to understand the mechanisms underlying Rpn4-dependent antifungal resistance of this pathogen.

1.5.2 The Mar1 transcription factor and azole resistance

The Mar1 TF, encoded by ORF *CAGL0B03421g*, has remained fully uncharacterized. Nevertheless, this gene shares some similarities with the also uncharacterized TF encoded by *CgHAP1* (*CAGL0K05841g*). Until now, no unequivocal *CgMAR1* orthologs have been found in other species. The closest similarities were found in the *HAP1* gene from *S. cerevisiae*, although recent work is pointing to distinct functions between these two genes. *ScHAP1* encodes a zinc finger TF involved in the regulation of gene expression in response to levels of heme and oxygen[144]. On the other hand, Klimova and colleagues observed that when deleted the zinc cluster gene *CgZCF4*, to which *CAGL0B03421g* belongs, *C. glabrata* generated colonies sensitive to ketonazole and slightly sensitive to

fluconazole[145]. Additionally, very recently Mar1 was found to confer azole drug resistance in our lab (Pais *et al*, unpublished results). RNA-sequencing was used to study its role in fluconazole stress response, leading to the identification of the Mar1 regulon in this context. Among its target genes, *RSB1* appears to be particularly promising in the context of azole resistance.

S. cerevisiae RSB1 encodes a seven-transmembrane segment plasma membrane protein, member of the lipid-translocating exporter (LTE) family of fungi[146]. Loss of the integral membrane protein ScRsb1 leads to hypersensitivity to several compounds, such as PHS (phytosphingosine), suggesting a role of this protein in influencing the cell's tolerance to the compounds tested[147]. A *RSB1* homolog can be found in *C. albicans* as *RTA2*, a gene that encodes a sphingolipid flippase shown in recent studies to be involved in azole resistance[148,149]. *C. glabrata RSB1* is predicted to encode, similarly to its *S. cerevisiae* and *C. albicans* homologs, a sphingolipid flippase with seven-transmembrane domains[142,150,151]. It is, therefore, possible that Rsb1 provides a similar contribution to azole resistance in *C. glabrata*. A comparison of the data obtained in a wide genome analysis of both azole-resistance and azole-sensitive *C. glabrata* clinical isolates can provide a general idea of the set of the genes involved in drug resistance acquisition. It is known that *C. glabrata*'s intrinsic low susceptibility to azoles is related to the increased expression of genes controlled by CgPdr1, and this modulation of gene expression is obtained through binding of the Pdr1 TF to pleiotropic drug response elements (PDREs) present in a given gene's promoter[122]. The promoter region of *CgRSB1* was found to possess a PDRE[149], and this gene was in fact shown to be upregulated in azole-resistant isolates[142,149–151]. However, a different study revealed an increased response of *CgRSB1* to mitochondrial dysfunction but a lack of response to fluconazole induction, which suggests the existence of TFs, other than CgPdr1, that control *CgRSB1* expression[146].

When analysing the binding sites enriched in a set of promoters of genes activated by the TF Mar1, it was found that these sequences are present in the *RSB1* promoter, thus representing possible Mar1 binding sites. To validate this idea, an experimental approach, consisting of evaluating the *RSB1* activation when the assumed Mar1 binding sites of its promoter are mutated, is being pursued.

1.6 Genome Editing Tools

1.6.1 What was used before CRISPR-Cas came along

The first genome editing technologies were developed around the 1960s, after the discovery of the double helix structure of DNA (1953 – Watson & Crick) and the achievement of synthesizing DNA *in vitro* for the first time (1958 - Arthur Kornberg)[152]. Using Genome Engineering tools, one is able to efficiently and precisely perform a genetic modification by introducing a double-strand break (DSB) in a specific target sequence of the genome and, subsequently, generate desired alterations during the following DNA break repair[153]. Targeted genome engineering is widely applied in biomedical research, medicine and agriculture.

Before the discovery of Clustered Regularly Interspaced Short Palindromic Repeats (CRISPR) genome engineering tool, several techniques were used to edit the genome of microorganisms. A very common approach to elucidate the functions of specific genes is their inactivation to further analyse the phenotypic consequences in the cell or organism. This can be achieved with either gene knockout or gene knockdown. When a gene is knocked

out, there is no expression of functional protein in the cell, whereas the knocking down of a gene results in a reduction of gene expression without completely silencing it[154]. An example of molecules used to target genes in order to supress gene expression - gene knockdown - are interfering RNAs (RNAi). In response to double stranded RNA (dsRNA), cells trigger a reaction that relies on the activity of two proteins, the first one being a ribonuclease (RNase) III called DICER that processes long dsRNA – complementary to the target transcript - into small interfering RNAs (siRNAs), which are then loaded on Argonaute, the second protein, thereby forming the RNA induced silencing complex (RISC). This complex will bind and cleave the target mRNA, i.e. the transcript of the gene of interest, by base-pair interaction, leading to gene knockdown. If the binding is not fully base-paired, mRNA translation will only be inhibited[92,154–156]. The RNAi pathway is found in a wide range of organisms like animals, plants and fungi, providing evolutionary advantages by protecting these organisms against viruses[92]. When using the RNAi system for genetic engineering (Figure 7), short RNAs can be introduced in the cell as either siRNAs or shRNAs (short hairpin RNAs), the latter being double stranded RNAs with a loop structure that are processed into siRNAs by DICER. Both siRNAs and shRNAs are ~ 21 bp long and are designed with a sequence complementary to the target mRNA[154].

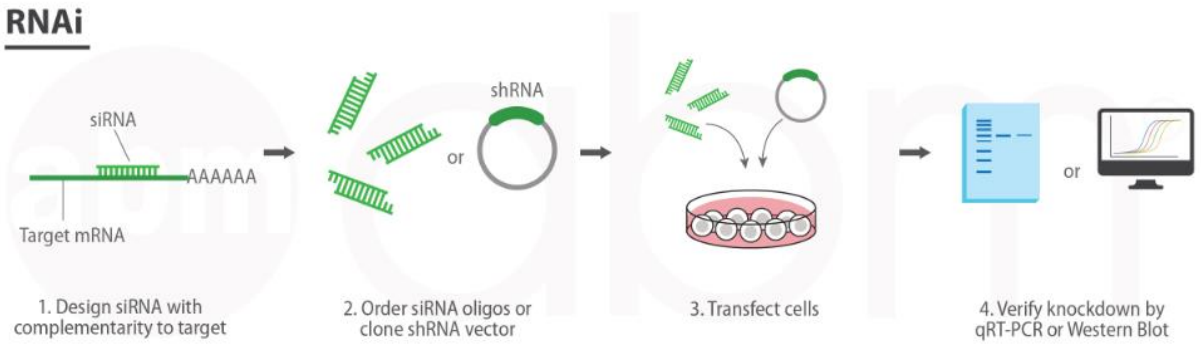

Figure 7 – Workflow for gene silencing with RNAi – from abm Inc. '*CRISPR vs. TALENs vs. RNAi: Which system is best for your gene silencing project?*' (2019)[154]

When it comes to ease of design and experimental set-up, siRNA as a tool for genome editing is very advantageous and can be designed to target almost any mRNA at any locus, achieving detectable gene knockdown in only 24h. However, off-target effects when using RNAi are quite common since the binding of siRNA to mRNA doesn't require strict sequence complementarity, and this cross-hybridization with off-target transcripts may cause phenotypes that reflect silencing of unintended transcripts besides the target gene[154,157]. Moreover, some targets seem to be either easier or harder to silence, depending on their accessibility to the RNAi machinery[156].

The discovery of Zinc Finger Nucleases (ZFNs), a highly targeted genome engineering technique, also revealed to be very effective for gene modifications. ZFNs are hybrid restriction enzymes comprised of two functional domains. The first domain is a designed chain of zinc finger protein modules that recognize and bind to a target DNA sequence with very high specificity. Typically, ZFNs have 3 to 6 zinc finger modules, with each individual zinc finger module recognizing a specific set of nucleotide triplets. The second domain of ZFNs is composed by the DNA nuclease domain of the protein FokI, which confers the DNA cleaving functionality. Because the FokI enzyme functions as a dimer, DNA cleavage by ZFNs requires nuclease dimerization around the target DNA,

hence the need for designing two different ZFNs to bind upstream and downstream of the targeted cleaving site (Figure 8).

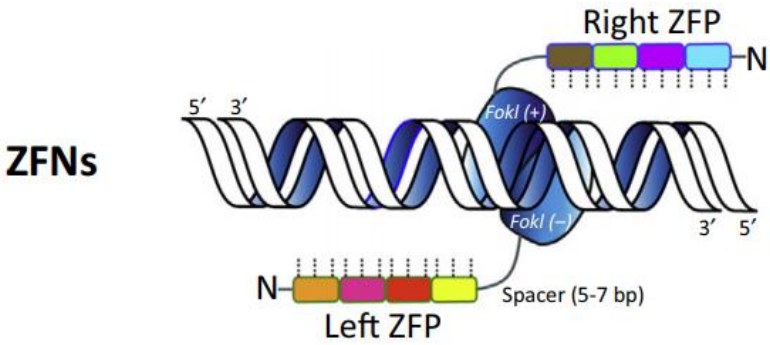

Figure 8 – ZFNs' mode of action for genome engineering - from Kanchiswamy *et al* '*Fine-Tuning Next-Generation Genome Editing Tools*' (2016)[158]

After binding and dimerization around the target DNA, ZFNs introduce a DSB, leading to initiation of one of two cellular DNA repair processes: the nonhomologous end-joining (NHEJ) or the homology-directed repair (HDR). For gene deletion applications, in the absence of a supplied DNA repair template, the preferred process for DNA repair is NHEJ, which can perform random insertions or deletions in the DNA that typically result in disruption of gene function. On the other hand, if an exogenous repair template is also supplied with the ZFN pair, homologous recombination via the HDR mechanism will induce the incorporation of exogenous DNA at the break site. However, designing ZFNs that recognize specific sites in a reliable fashion has proven to be slow and more dubious than it seemed, causing some concerns about the off-target cleavage associated with these hybrid enzymes[152,159–161].

A better solution emerged after the discovery of a class of transcription activator-like (TAL) proteins, which lead to the development of Transcription Activator-Like Effector Nucleases, or TALENs, used for gene knockout (Figure 9). TALENs work on a similar principle as ZFNs. These nucleases are artificial restriction enzymes that consist of a TAL protein with a DNA-binding domain (derived from the plant pathogen *Xanthomonas sp.*) fused to the FokI enzyme's DNA nuclease domain, also used to design ZFNs. The TAL effector DNA-binding domain binds to the DNA to recognize individual nucleotides instead of triplets, and contains 33-35 amino acid repeats that can differ from each other by two amino acids at positions 12 and 13 – known as repeat variable di-residue (RVD) -, which will determine which nucleotide each repeat will bind to. A combination of 12 to 31 of these TAL DNA binding repeats allows the TALEN to target a specific DNA sequence in the genome. Two different TALENs, one for each target DNA strand, must dimerize in order for the FokI nuclease domain to cut the DNA and create a double-stranded break (DSB). The generated DSB will then be repaired by error-prone NHEJ to yield small insertions and deletions (indels) at the break sites. Afterwards, it is necessary select and isolate the cells containing the frameshift mutation that leads to gene knockout[154,158,162,163].

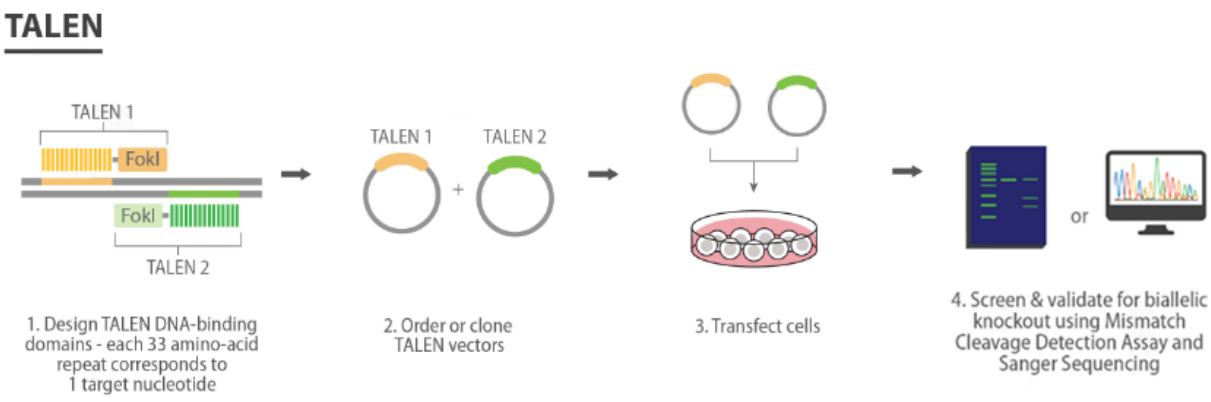

Figure 9 – Workflow for gene silencing with TALENs – from abm Inc. '*CRISPR vs. TALENs vs. RNAi: Which system is best for your gene silencing project?*' (2019)[154]

TALENs can be designed to target almost any given 30 to 40 bp DNA sequence, and, since TAL effector modules are able to recognize single bases, TALENs can mutate small DNA sequences (such as enhancers or miRNA-coding sequences) that may lack targetable sites for other types of nucleases. Furthermore, this technique also has the advantage of having low off-target editing effects[154,158,162]. But using TALENs also have its disadvantages: they are difficult to clone due to their large repetitive sequences, and the construction of TALENs encoding plasmids is laborious and time-consuming, since they must be used in pairs and that requires double cloning work[154,158]. It seemed that there was a need to keep looking out for a better approach, until CRISPR-Cas came along.

1.6.2 Clustered Regularly Interspaced Short Palindromic Repeats (CRISPR)

The discovery of this technique started when Francisco Mojica found in several archeal microbes a structure, with multiple copies of a palindromic repeat sequence of 30 bases separated by spacers of approximately 36 bases, with no similarities when compared the known microbe families of repeats. He connected this finding with a previous published paper by a Japanese group in 1987[164] that mentioned similar structures in eubacteria, which motivated him to pursue further investigations on this structure's function in prokaryotes since it was found in such distant microbes. Later on, these structures were given the name of Clustered Regularly Interspaced Short Palindromic Repeats (CRISPR) and, by 2005, Mojica and colleagues revealed that these sequences in fact contained DNA from bacteriophages[165]. In parallel, Ruud Jansen *et al*[166] discovered the presence of four specific CRISPR-associated (*cas*) genes regularly present in the immediate vicinity of the CRISPR regions.

The following years of research showed evidence that CRISPR technology was adapted from the natural defence mechanisms present in many bacteria and most of the characterized Archaea (the domain of single-celled microorganisms). Bacteriophages are viruses that infect bacteria, taking advantage of their genetic machinery to replicate. In response to this kind of invader, bacteria developed an adaptive defence mechanism known as CRISPR. Although the sequences and lengths of CRISPR arrays vary, they all have a characteristic pattern of alternating repeat and spacer sequences. Previous investigations also lead to the finding of a specific set of CRISPR-associated (*cas*) genes close to CRISPR sites, which encode for the Cas proteins[167,168].

The CRISPR locus consists of short repetitive elements (repeats) - with a palindromic pattern and usually ranging from 28 to 37 base pairs - with unique variable sequences (spacers) of similar length alternating with these repeated sequences. When infected by a virus, the spacers derived from the foreign genetic material are incorporated into the CRISPR array, allowing host's recognition of the virus and, consequently, the fighting against future attacks. This way, spacers function as storage of immunological memory[167,169]. Unlike microbes, mammalian cells have different intracellular environments and organization with a significantly larger genome coiled in an elaborate chromatin structure. Knowing this, the question was whether CRISPR system could be re-engineered to become a functional system for editing human genome remained unclear[170,171]. Finally, Feng Zhang, who had previously worked on other genome editing systems like ZNFs and TALENs, and his colleagues were the first to successfully adapt CRISPR-Cas9 for genome editing in eukaryotic cells[172].

1.6.2.1 CRISPR-Cas molecular mechanisms: adaptation, maturation, interference

The CRISPR-Cas system acts in a sequence-specific manner by recognizing and cleaving foreign mobile genetic elements – MGEs – such as bacteriophages, transposons or plasmids. The defence mechanism can be divided into three stages, the first one being adaptation or spacer acquisition, followed by CRISPR RNA (crRNA) biogenesis and, finally, target interference or silencing (Figure 10).

During adaptation, the Cas proteins recognize a distinct sequence of the invading MGE, called a protospacer, and incorporate it into the host CRISPR locus, yielding a new spacer. This enables the host organism to memorize the intruder's genetic material and displays the adaptive nature of this immune system. Thus, spacers are the key elements to the specificity of CRISPR's defence mechanisms[173,174]. Following this event, the CRISPR array with the acquired spacers is transcribed into pre-crRNA, which is subsequently cleaved and processed by Cas proteins and host factors into short mature crRNAs. The crRNA, sometimes referred to as guide RNA, comprises a conserved repeat fragment as well as a spacer that complements a sequence from the invading genetic element. This way, Cas proteins can recognize crRNAs and form an effector complex that targets the foreign nucleic acid by hybridization between the crRNA spacer and the foreign protospacer, inducing sequence-specific cleavage of the crRNA–foreign nucleic acid complex and, thus, protecting the host against a second infection[175,176]. Importantly, Cas-mediated target recognition requires the presence of a short protospacer adjacent motif (PAM) flanking the target sequence on the invading DNA, being a requirement for strand separation and formation of crRNA-target DNA heteroduplex[177–179]. In the absence of the PAM, the Cas9 protein will not recognize even target sequences fully complementary to the guide RNA sequence[180]. However, mismatches between the spacer and target DNA may occur, as well as mutations in the PAM. If this happens, the Cas-crRNA effector complex will not target and cleave the foreign DNA, meaning the host will not become immune to a next attack. To operate as a defence system, all three stages of the CRISPR system must be functional, but it is important to note that each of these processes can work independently[181].

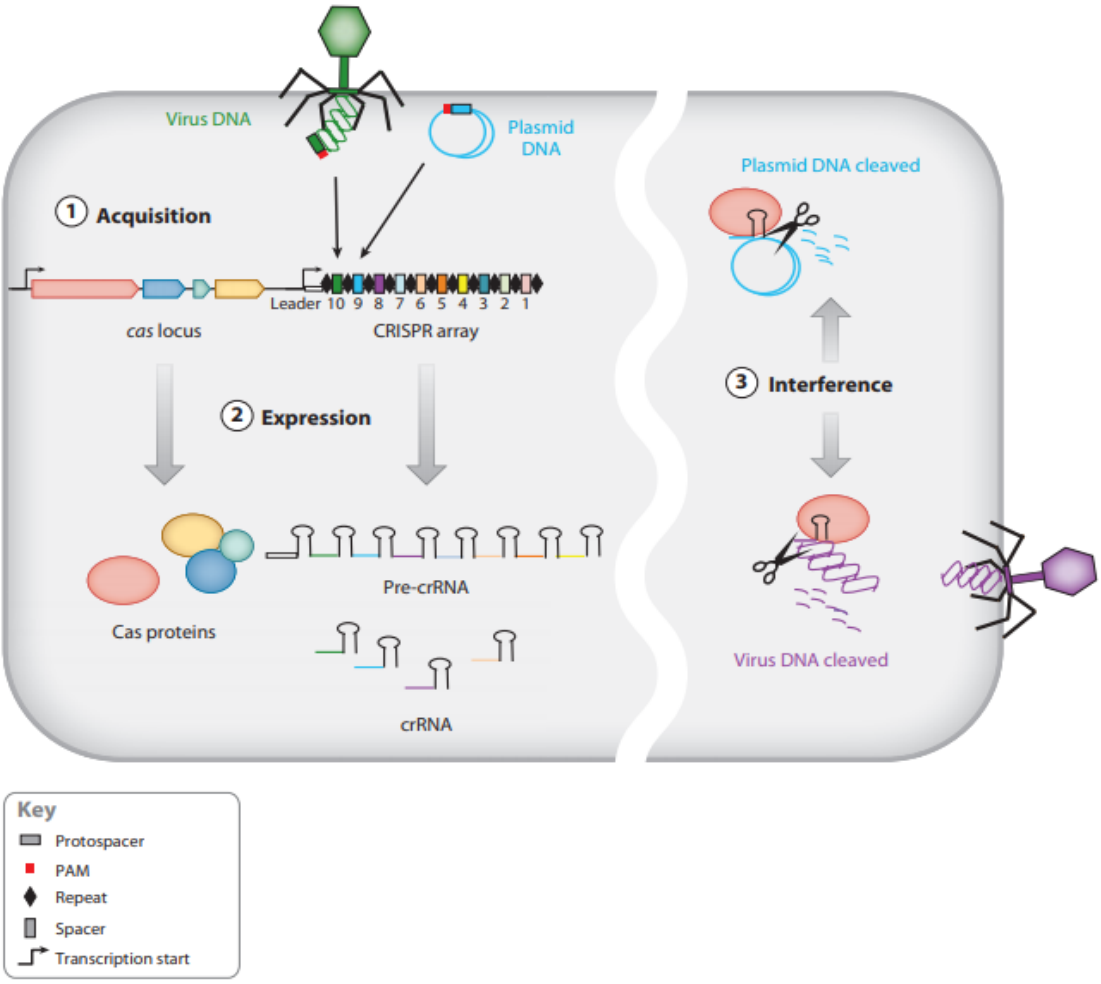

Figure 10 – The stages of CRISPR-Cas adaptive immune system – from Bhaya *et al* '*CRISPR-Cas Systems in Bacteria and Archea: Versatile Small RNAs for Adaptative Defense and Regulation*' (2011)[181]

1.6.2.2 Classification of CRISPR-Cas systems

The CRISPR-Cas system can be divided into two partially independent subsystems (Class 1 and Class 2), according to the composition of the effector genes. Within these two classes, the CRISPR-Cas systems are also classified in three main types - types I, II and III -, which are further divided into at least ten subtypes[182] (Figure 11). The first subsystem - class 1 - comprises multiprotein effector complexes and requires the core proteins (present in all CRISPR-Cas systems) Cas1 and Cas2, which are involved in new spacer acquisition during the adaptation step. The second subsystem - class 2 - entails a single multifunctional effector protein for processing of primary CRISPR transcripts (crRNA) and recognition and degradation of invading foreign nucleic acid[181,183].

The three CRISPR-Cas system types use distinct molecular mechanisms to achieve nucleic acid recognition and cleavage, and were defined according to the presence of signature proteins: Cas3 for type I, Cas9 for type II and Cas10 for type III. Typical type I loci, a subclassification of class 1 subsystems, contain the Cas3 gene, which encodes the Cas3 helicase/nuclease, a large multidomain protein with separate helicase and DNase activities. In addition, there are multiple Cas proteins that form CASCADE-like complexes (CASCADE meaning CRISPR-associated complex for antiviral defence) that are involved in the interference step. Type II system is characterized

by the Cas9 protein, a large multifunctional protein that seems to be sufficient for generating crRNA, as well as targeting foreign DNA for degradation. This is the simplest of the three CRISPR-Cas types, with only four genes that compose the operon. Type III system has the signature RAMP (repeat-associated mysterious protein), Cas10, which is likely involved in the processing of crRNA and possibly also in target DNA cleavage, being to some extent functionally analogous to the Type I CASCADE [165,181,184].

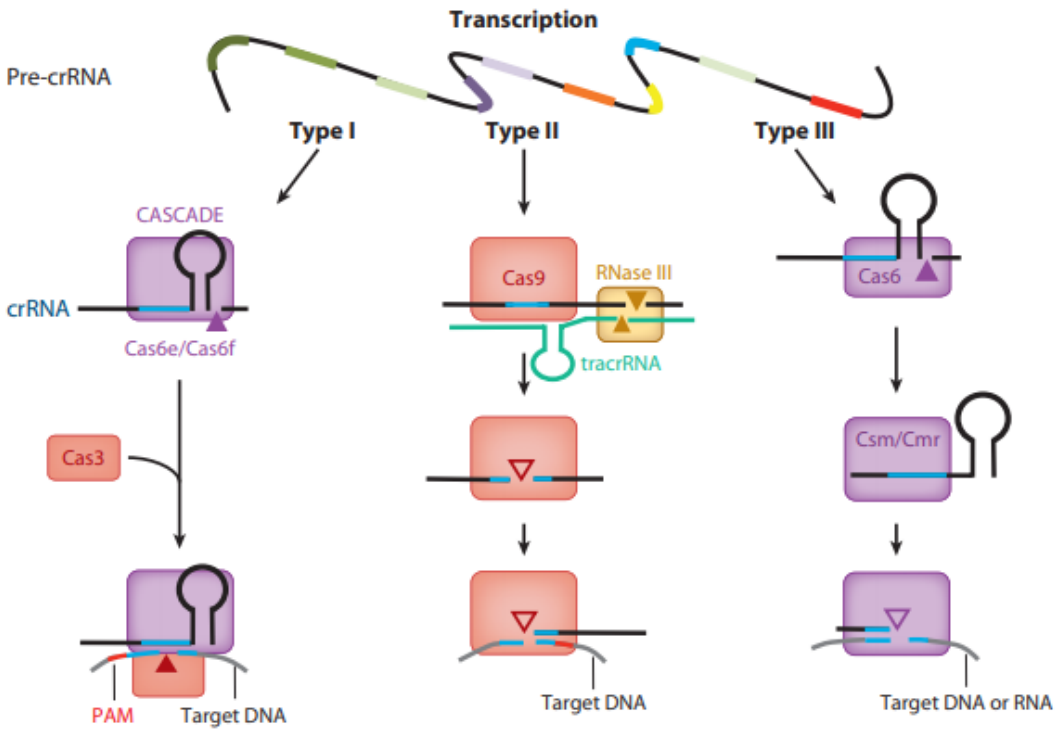

Figure 11 – Mechanisms of action of Types I, II and III in CRISPR-Cas technology - from Bhaya *et al* *'CRISPR-Cas Systems in Bacteria and Archea: Versatile Small RNAs for Adaptative Defense and Regulation'* (2011)[181]

In the process of maturation of pre-crRNA and interference with invading sequences, types I and III have features in common, with Cas proteins and crRNAs as the lone components required for expression and interference. On the other hand, type II systems process pre-crRNA by means of a distinct mechanism, requiring a small non-coding RNA - tracrRNA (trans-activating crRNA) –, complementary to the repeat sequences in pre-crRNA, encoded in the CRISPR array along with the repeat-spacer and Cas genes. This tracrRNA acts as a scaffold, linking the crRNA to Cas9. The tracrRNA:pre-crRNA repeat duplexes formed will trigger processing by the double-stranded RNA-specific endoribonuclease RNase III, in the presence of Cas9. The mature hybridized duplex crRNA:tracrRNA binds with the protein Cas9 to form a ternary silencing complex. The tracrRNA molecule is thus essential for triggering pre-crRNA processing as well as activation of crRNA-guided DNA cleavage by Cas9[185–187].

1.6.2.3 CRISPR-Cas9

Given de fact that the type II system only requires a single protein for RNA-guided DNA recognition and cleavage, it represents a system with high specificity and ease of use, which proved to be very useful for genome engineering applications. Cas9 is a peculiar endonuclease that can be programmed by the crRNA:tracrRNA duplex to cleave

in a site-specific manner target DNA, allowing elucidation of gene functions, gene activation/inactivation and correction of disease-causing mutations[186,188].

The type II CRISPR system has been adapted from different bacteria, like *Streptococcus pyogenes*, for targeted genome editing in the past years. In 2012, Martin Jinek *et al*[185] showed that the protein Cas9 can be programmed with a single chimeric guide RNA (sgRNA), where they engineered a single transcript - a result from the fusion of the crRNA to the tracrRNA – which recruits the Cas9 to specific target regions for desired dsDNA cleavage[185,189] (Figure 12).

The protospacer portion of the crRNA consists of twenty nucleotides at the 5' end of the gRNA complementary to the target DNA For Cas9 to cleave the DNA, it is essential that the target locus is located immediately after the 5' of a PAM sequence containing a 5'-NGG-3' (the canonical PAM sequence, where "N" is any nucleotide) in the non-target strand, but not in its target-strand complement[179,190].

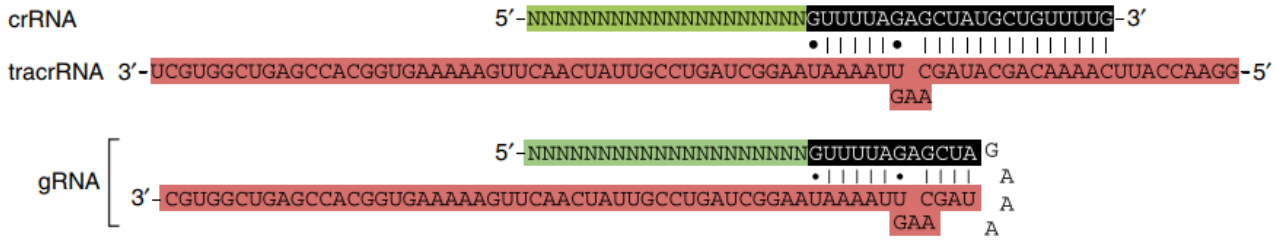

Figure 12 – An example of a crRNA-tracrRNA hybrid and a gRNA for CRISPR-Cas systems – from D. Sanders *et al* '*CRISPR-Cas systems for editing, regulating and targeting genomes*' (2014)[190]

In the guide sequence, all positions of the bases contribute to global specificity. Nevertheless, mismatches in bases of the guide RNA located more distantly from the PAM are less significant for Cas9 specificity to the targeted locus[191]. When applying CRISPR-Cas9 in genome editing, the protein Cas9 cuts the DNA and originates precise double-strand breaks at the targeted gene (Figure 13).

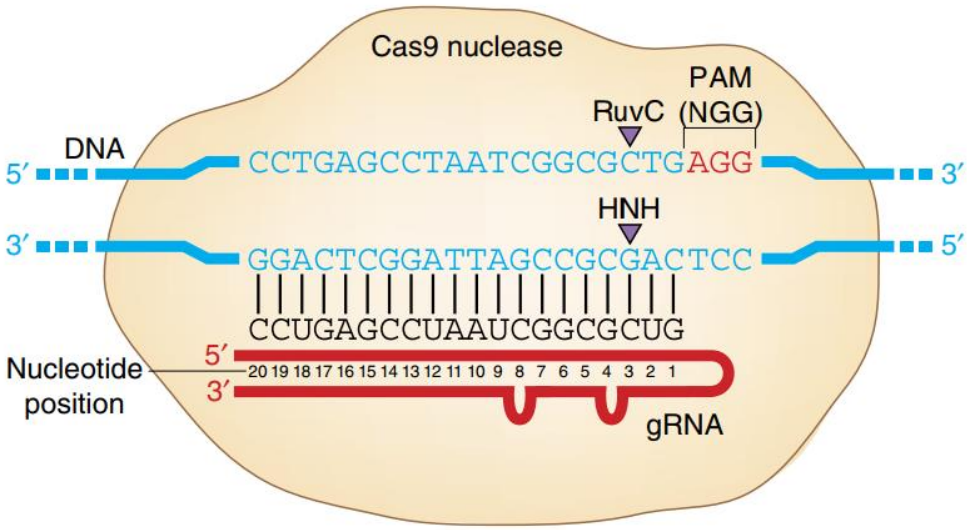

Figure 13 – Cas9 nuclease and gRNA to target and cleave DNA. Cas9 contains RuvC and HNH nuclease domains (arrowheads) – from D. Sanders *et al* '*CRISPR-Cas systems for editing, regulating and targeting genomes*' (2014)[190]

After cleavage, the targeted DNA can undergo one of two endogenous DNA repair pathways: the nonhomologous end joining (NHEJ) pathway, which is error-prone, or the homology-directed repair (HDR) pathway, a method with high fidelity. In the absence of a repair template, DSBs result in random insertions or deletions (indels) at the site of cleavage through NHEJ, this being the most common outcome. These indel mutations can originate gene knockouts by disrupting a coding exon, possibly causing frameshifts and premature stop codons, or even disrupting binding-sites of promoters and enhancers. On the other hand, in the existence of a repair template, the HDR pathway takes place. The repair template can either be single stranded DNA oligonucleotides or double stranded DNA with "homology arms" (sequences identical to the cut ends of the chromosome) flanking the insertion sequence, and it will be inserted where the DSB occurred by HDR to correct the break. HDR pathway is the desired method when the goal is to introduce specific and precise point mutations or sequences of interest through recombination of the target locus with the exogenous DNA repair template[190,192–194].

Previous studies have demonstrated the possibility of implementing the CRISPR-Cas9 system in eukaryotes, namely yeasts, providing details about this genome engineering tool for site-specific mutations.

1.6.2.4 CRISPR-Cas system versatility

The CRISPR-Cas9 system has become very popular as it is simple to design, inexpensive and extremely versatile for a variety of biological applications and cell types/organisms. CRISPR-Cas technology is not limited to genome engineering applications such as cutting and nicking DNA – the latter generating a single-stranded DNA (ssDNA) break instead of a DSB – as well as using base editors to precisely edit DNA without creating DSB. This system can also be applied in transcriptional regulation, acting either as a transcriptional activator or repressor, or even performing targeted epigenetic modifications[195]. The discovery of other types of CRISPR systems, for example the type VI that uses the protein Cas13, allowed the targeting and editing of RNA rather than DNA, which can be used in mammalian cells to attenuate RNA levels[196]. In a more complex approach, it is now possible to use CRISPR as a tool for genetic screening experiments by using CRISPR pooled libraries consisting of thousands of plasmids, each containing multiple gRNAs for each target gene. With this method, a population of mutant cells is created and then screened for a phenotype of interest[197]. There are a few other applications for CRISPR-Cas systems, for instance using these systems to purify and visualize genomic loci or adapt the systems to tag proteins[195]. Together, these examples reveal the impressive versatility of the CRISPR-Cas systems and how it has made it a powerful tool to improve the knowledge about biological systems, with so much potential in the field of disease research[198,199].

1.6.2.5 Application of CRISPR-Cas9 in yeasts

As a model yeast, the application of CRISPR has been more extensively studied in *S. cerevisiae*. There are several systems available (some of them mentioned above), including commercial options designed for distinct purposes. The traditional system used is focused on cleaving DNA, but there is also the possibility of using nickases – Cas9 with one nuclease domain mutated to simply cut one strand of DNA – along with two gRNAs that target opposite strands of the gene of interest. This double nicking strategy is favourable since it reduces unwanted off-target effects[200]. One can also introduce mutations in yeast cells by fusing a catalytically dead Cas9 (dCas9) to a cytidine deaminase protein, creating a specific cytosine base editor that can alter DNA bases without cleaving the target DNA. Moreover, the option to use CRISPR-Cas systems in yeasts for activating or interfering with transcription

is also available, this time fusing a dCas9 to a transcriptional activator or repressor peptide, respectively. dCas9 can even be used in yeasts to purify a region of genomic DNA and its associated proteins and nucleic acids[201].

Given the pathogenic nature of *Candida* species, it became an asset to be able to apply CRISPR-Cas systems to these yeasts. In order to create a CRISPR system for *Candida*, there are certain technical challenges that need to be overcome. For example, it required recoding of the *CAS9* gene since the CUG codon in the *Candida* clade is decoded *in vivo* as serine and not leucine. It also needs to be considered the absence of autonomously replicating plasmids in *Candida* as well as the lack of expression systems for small RNAs[202]. For instance, in the case of *C. albicans*, because episomal plasmids are not stable in this yeast, the construct (Cas9 and gRNA encoding DNA fragments) must be linearized to enable integration. Initially, different groups of investigators reported to have developed CRISPR-mediated genome editing systems for use in *C. albicans*. One of the systems, developed by Vyas *et al*[202], required the expression of Cas9 and gRNA from a linear DNA fragment that is integrated in the genome at the *ENO1* locus, and also the integration at the target locus of unmarked donor DNA, that is, the repair template, via HDR. Afterwards, Min *et al*[203] detected a potential limiting step in the Vyas *et al* system, saying "the desired genome editing frequency may have been limited to the integration frequency of the Cas9-gRNA expression construct". Thus, with the premise that the mentioned construct does not require genomic integration for functional activity, they developed another system (later revised by Huang *et al*[204]). This time, independent DNA fragments containing the coding sequences of Cas9 and gRNA were introduced into cells transiently and without direct selection, also with integration of selectable markers via HDR at the target locus[205].

Several groups continued on optimizing CRISPR systems for *C. albicans*, for example Nguyen *et al* in 2017[205], and soon this gene editing tool began to be applied in multiple other *Candida* species, such as *C. glabrata*[206], *C. parapsilosis*[207] and *C. orthopsilosis*[208]. Although efficient mutagenesis in *C. albicans* and *S. cerevisiae* requires the addition of a repair template, *C. glabrata* only requires *CAS9* and a guide RNA, suggesting that HDR is the predominant repair pathway in *C. albicans* and *S. cerevisiae*, while the NHEJ pathway prevails in *C. glabrata*[209]. Thus, to use CRISPR mutagenesis in *C. albicans*, providing a repair template is necessary for efficient mutagenesis, hence the need for a co-transformation with both the plasmid (with the *CAS9* and the gRNA) and the repair template. This co-transformation represents a limitation to CRISPR mutagenesis[209].

Considering *C. glabrata*, Enkler *et al* (2016)[206] established an efficient CRISPR-Cas9 system to be used in this yeast that generates loss-of-function mutations via the NHEJ repair pathway. To do so, they designed two plasmids, one for expressing the Cas9 protein and the other for the sgRNA. They first tested how *C. glabrata* fitness was affected when using either a vector where *CAS9* expression was under the *S. cerevisiae TEF1* promoter (plasmid p414-*CAS9*(*TEF1*)) - developed by DiCarlo and colleagues[210] – or a vector with the *C. glabrata* promoter *CYC1* (pRS314-*CAS9*(*CYC1*)), concluding that in both cases *CAS9* expression hampers *C. glabrata* fitness, delaying its average generation time. To avoid this problem, transformations with the *CAS9* expressing plasmid were carried out in *C. glabrata* strains already expressing sgRNA under the control of either *S. cerevisiae* (*pSNR52*) or *C. glabrata* (*pRNAH1*) promoters **(**Figure 14**)**. The results obtained suggest that for efficient gene disruption by NHEJ repair in *C. glabrata*, *CAS9* should be expressed under the (*C. glabrata*) promoter *pCYC1* in combination with sgRNAs expression under the (*C. glabrata*) *pRNAH1* promoter[206].

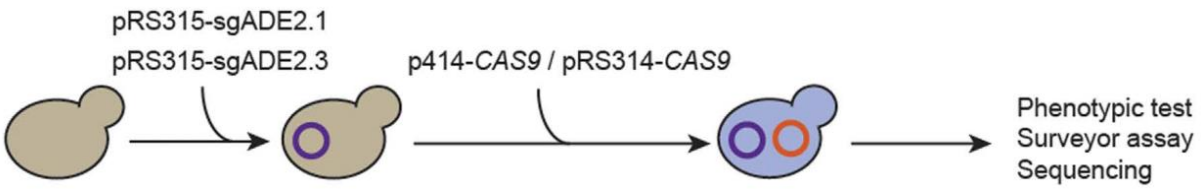

Figure 14 – *C. glabrata* sequential transformations with sgRNA and *CAS9* expression plasmids and following experiments – from Enkler *et al* '*Genome engineering in the yeast pathogen* Candida glabrata *using the CRISPR-Cas9 system*' (2016)[206]

Later, in 2017, Grahl *et al*[211] explored a different approach where, instead of using a *CAS9* and sgRNA expressing plasmids, they carried out the transformations on *C. glabrata* (among other fungal pathogens) using CRISPR RNA-Cas9 protein complexes (RNPs) along with a repair template containing the desired gene modification. The purpose was to learn if RNPs could be used to make genetic alterations in *C. glabrata* without the need for defined promoters for heterologous gene expression. The CRISPR machinery used in this study consisted of purified Cas9 protein and two RNAs - crRNA and tracrRNA - that, together, compose the gRNA. To assemble the components, crRNA and tracrRNA are co-incubated and then added to the purified Cas9 protein in order for the RNA-protein complex to form prior to transformation via electroporation. This approach has the advantage of using commercially available Cas9 protein and custom-synthesized RNAs, requiring only the synthesis of the deletion construct. Moreover, to design the RNAs and the deletion construct, little information about the organism's biology is needed[211].

Still in 2017, Cen and colleagues[212] developed a CRISPR-Cas9 system for mutagenesis in *C. glabrata*. Here, two consecutive transformations were done, the first being the introduction of the *CAS9* expressing plasmid, followed by the co-transformation of the gRNA plasmid with the repair DNA template in the Cas9 expressing *C. glabrata* strain. In comparison with results obtained in Cen *et al* (2015)[213] by homologous recombination (*C. glabrata* transformed via electroporation with DNA cassette containing a marker), their results show that the CRISPR-Cas9 system is more efficient in deleting target genes. However, the efficiencies of each technique are nonetheless low, with 0.4% of correct transformants using the homologous recombination approach and 1.1% of correct transformants using the CRISPR-Cas9 system[212].

Finally, in 2018, Vyas *et al*[209] reported a more efficient CRISPR system to apply in several yeasts, *C. albicans* and *C. glabrata* included, using a Unified Solo vector that incorporates *CAS9*, gRNA and repair template into a single vector instead of two, as was used in previous published *C. glabrata* systems. This new vector will either integrate the genome or maintain itself as an episome, depending on the organism transformed, and allows the comparison of CRISPR mutagenesis results between several different fungal species using a single system based on the same design[209].

2. Materials and Methods

Strains and culture media

C. glabrata single deletion mutant KCHr606_Δ*ura3* strain was used in all the experiments involved in CRISPR-Cas9-mediated gene deletion. The *C. glabrata* L5U1 strain was also used. Yeast cells were cultured in Yeast-Pentose-Dextrose (YPD) medium (Yeast Extract: 20g/L; Peptone: 10g/L; Glucose: 20g/L), Minimal Medium Broth (MMB) medium (Glucose: 20g/L; Ammonium Sulfate: 2,7g/L; Yeast Nitrogen Base without amino acids and ammonium sulfate: 1,7g/L) or MMB medium supplemented with adenine (3mg/L or 20mg/L), when required. DH5α *E. coli* cells were grown in Luria-Bertani (LB) medium or LB medium supplemented with ampicillin (150mg/L), when required. Liquid cultures were grown with orbital agitation (250rpm) at 30ºC (yeast) or 37º (*E. coli*). Solid media were achieved by adding 20g/L agar to each respective medium.

Plasmids, sgRNA design and cloning

The plasmid used throughout the CRISPR-Cas9 system experiments was the *S. cerevisiae* and *C. glabrata* Solo CRISPR vector pV1382 developed by Vyas *et al*[209]. For site-directed mutagenesis of the *RSB1* promoter, the plasmid used was pYEP354_*CgRSB1*prom_*lacZ*, an expression fusion plasmid where the *RSB1* promoter region was fused with a *lacZ*-coding sequence at the pYEP354 basal vector. A list of *C. glabrata* genes and correspondent guide sequences with "no off-targets" (off-target scores at other locations lower than 0.2) was obtained from Vyas *et al*[209] (http://osf.io/ARDTX/). With the off-target effects practically excluded, the gRNAs were chosen based on the on-target score (on-target activity calculated with the Rule Set 2 from Doench J. *et all*[214]), with higher scores being more favourable. Following the criteria of Vyas *et al*[209], the gRNA sequences – forward (Fw) and reverse (Rv) - for three different target genes (*ADE2*, *RPN4*, *EFG1*, *MAR1* and *TEC1*) were designed (Table 1).

Table 1 – sgRNA sequences for each target gene deletion

		Genome	gRNA	
		Strand of the target gene	**Strand of the gRNA**	**Sequence (20 nt)**
GENE	***CgADE2* (*CAGL0K10340g*)**	Rv	Rv	ACAACACAAGGCCAAATTAA
	***CgRPN4* (*CAGL0K01727g*)**	Rv	Rv	AGGATGAGCTGTACAATATG
	***CgEFG1* (*CAGL0M07634g*)**	Fw	Fw	ACACATACTTACCCCCACCA
	***CgMAR1* (*CAGL0B03421g*)**	Rv	Rv	AGAGCGATGAGTAACCCTGT
	***CgTEC1* (*CAGL0M01716g*)**	Rv	Rv	AAAGTACCCATGTCTAACAC

Because the gRNAs will be inserted in the pV1382 between the promoter *SNR52* and the gRNA scaffold sequence, the restriction enzyme chosen for plasmid digestion was BsmBI. To clone the sgRNA into the BsmBI-digested

expression vector, two oligonucleotides (forward and reverse) were synthesized with 4 nucleotides in the 5' end and one nucleotide in the 3' end that are compatible with the ends of the BsmBI-digested vector. Considering this, the complete sgRNA sequences, with the plasmid nucleotides (italic) flanking the 20 nucleotide guide sequences (bold), are the following:

Guide_*CgADE2*_TOP – Fw: 5'-*GATCG***ACAACACAAGGCCAAATTAA***G*-3'

Guide_*CgADE2*_BOT – Rv (reverse complemented): 5'-*AAAAC***TTAATTTGGCCTTGTGTTGT***C*-3'

Guide_*CgRPN4*_TOP – Fw: 5'-*GATCG***AGGATGAGCTGTACAATATG***G*-3'

Guide_*CgRPN4*_BOT – Rv (reverse complemented): 5'-*AAAAC***CATATTGTACAGCTCATCCT***C*-3'

Guide_*CgEFG1*_TOP – Fw: 5'-*GATCG***ACACATACTTACCCCCACCA***G*-3'

Guide_*CgEFG1*_BOT – Rv (reverse complemented): 5'-*AAAAC***TGGTGGGGGTAAGTATGTGT***C*-3'

Guide_*CgMAR1*_TOP – Fw: 5'-*GATCG***AGAGCGATGAGTAACCCTGT***G*-3'

Guide_*CgMAR1*_BOT – Rv (reverse complemented): 5'-*AAAAC***ACAGGGTTACTCATCGCTCT***C*-3'

Guide_*CgTEC1*_TOP – Fw: 5'-*GATCG***AAAGTACCCATGTCTAACAC***G*-3'

Guide_*CgTEC1*_BOT – Rv (reverse complemented): 5'-*AAAAC***GTGTTAGACATGGGTACTTT***C*-3'

Although the guiding sequences for CRISPR-mediated deletion of the *MAR1* and *TEC1* genes were designed, further steps (cloning into the plasmid and so on) were not achieved.

The protocol used for cloning the sgRNA into pV1382 was the following: Plasmid digestion: 2µg of plasmid DNA were digested with 1µL of BsmBI (10U) in a total volume of 50µL (10x 3.1 Buffer 5µL + H_2O). Anneal of sgRNA oligos: The sgRNA primers (100µM) were annealed by adding 1µL of each oligo (Fw and Rv) to 5µL of T4 Ligase buffer (10x) and 43µL of H_2O, followed by incubation (PCR program "GRNAANN" described in Table 2). In this step, a negative control was prepared with 2µL of H_2O instead of the oligos. Ligation of sgRNA into plasmid: With the sgRNA oligos annealed, the following step was sgRNA ligation into the vector by assembling in a tube 2µL of T4 Ligase buffer (10x), 0,5µL of T4 Ligase, 40ng of the digested vector, 1µL of the annealed sgRNA and H_2O up to 20µL. For the negative control it was added 1µL of the negative control mix prepared in the annealing step. The ligation occurred under 16ºC of incubation overnight. DH5α cells transformation: Finally, transformation of *E. coli* chemically competent DH5α cells with the pV1382 + sgRNA was performed by heat shock (42ºC for 3 minutes) after adding 20µL of the sample plasmid/control to 150µL of cells kept on ice. Following the heat-shock step, the cells were again kept on ice for 5 minutes, 800µL of LB medium were added and then the cells were incubated with shaking at 37ºC for 1h. Selection was made on LB medium plates with ampicillin (150mg/L).

The primer for confirmation of a successful sgRNA cloning on pV1382 consists of a 20 nucleotides sequence present in the *SNR52* promoter a few nucleotides upstream the BsmBI restriction site: 5'-GCTGTAGAAGTGAAAGTTGG-3' (9908-9927 of pV1382).

Table 2 – PCR program for sgRNA annealing

PCR program - **"GRNAANN"**	
Temperature (ºC)	**Time**
95º	5 min
16º	1 min
12º	forever

Repair template design and construction

To create the repair template cassette, two primers were designed with a 20 nucleotide TAG sequence identified in bold (primer *ScADE2* deletion in Vyas *et al*[209]) and 40 nucleotides upstream (primer forward) and downstream (primer reverse) the target gene, identified in italic, known as the homology arms:

RT_*CgADE2*deletion_TOP – Fw:

5'-*TGTTACCAACGATACAGGTTTATTTTGCTTACGAATAATA***GAGGGGGACATATATAAGTT**-3'

RT_*CgADE2*deletion_BOT – Rv (reverse complemented):

5'-*GAATTTCAAGCAAAGACTAACTGGTTTTATAGATGGTGCT***AACTTATATATGTCCCCCTC**-3'

RT_*CgRPN4*deletion_TOP – Fw:

5'-*CAATTCTATTAAAACTTTCCTCTCGAGAGCGGTAACGAGG***GAGGGGGACATATATAAGTT**-3'

RT_*CgRPN4*deletion_BOT – Rv (reverse complemented):

5'-*TCCGAAATTTTAAAAGAAATTTGAATGATGTTGGGGGTAT***AACTTATATATGTCCCCCTC**-3'

RT_*CgEFG1*deletion_TOP – Fw:

5'-*GGTTAATGAGCGTAGACTTGAACTGAAAAGAAAATGTGCG***GAGGGGGACATATATAAGTT**-3'

RT_*CgEFG1*deletion_BOT – Rv (reverse complemented):

5'-*GTTATACAATGGTACATAGCGATTCATTACGAATATTAAG***AACTTATATATGTCCCCCTC**-3'

RT_*CgMAR1*deletion_TOP – Fw:

5'-*TTAAGTATTCCGCTATACTCACTGTACCCTAAAGACGACA***GAGGGGGACATATATAAGTT**-3'

RT_*CgMAR1*deletion_BOT – Rv (reverse complemented):

5'-*CTGTGGAAAAATTAAATACACAAACATAACAAATGCACAC***AACTTATATATGTCCCCCTC**-3'

RT_*CgTEC1*deletion_TOP – Fw:

5'-*ATCGTACTCCCCCCCACAAATAACGCCCTCAATCTATATT***GAGGGGGACATATATAAGTT**-3'

RT_*CgTEC1*deletion_BOT – Rv (reverse complemented):

5'-*TCTGCAGAAAAAATAAAAATGTAGCATTCCTACATCTCTC***AACTTATATATGTCCCCCTC**-3'

To generate the repair template, 1.5µL of each designed oligo sequence (forward and reverse) was added to a mixture (5µL of reaction buffer (10x), 2.5µL Mg^{2+}, 0.8µL dNTPs, 0.5µL Taq polymerase and H_2O up to 50µL) to perform a PCR reaction (PCR program "RTEXTENS" described in Table 3). With 40 nucleotides of both upstream and downstream primers plus 20 nucleotides of TAG sequence, the size of the generated repair template cassette is 100bp. To confirm the existence of the repair template in the samples after PCR, 4µL of each sample were ran into a 0.8% agarose gel (100V, 400mAmp) with GreenSafe. The repair template was purified from the PCR reaction samples using the NZYGelPure kit.

The repair template cassettes designed for *MAR1* and *TEC1* gene deletion were not generated.

Table 3 – PCR program for repair template extension

PCR program - "RTEXTENS"		
Temperature (ºC)	**Time**	**Cycles**
94º	5 min	
94º	30 sec	35X
46º	45 sec	
72º	30 sec	
72º	10 min	

Yeast cells transformation and screening for genetic modification

Yeast cells were cultured in YPD medium. Transformation with pV1382_guide*ADE2* and repair template was tested with two different protocols, the Lithium Acetate method (kit MP biomedicals) and the Transformation of Expression Vectors into Yeast protocol from Gietz and Woods. Transformation with pV1382_guide*RPN4* and pV1382_guide*EFG1* with corresponding repair templates was carried out following the Lithium Acetate method (kit MP biomedicals). Cells where then plated in appropriate selection medium (MMB without uracil for *RPN4* and *EFG1* deletion mutants and MMB without adenine and uracil for *ADE2* deletion mutants) and incubated at 30ºC for 5-8 days (as needed) until colony growth. The detection of colonies genetically modified in *C. glabrata ADE2* deletion mutant plates was possible through visual confirmation since these colonies displayed a red pigmentation. For *C. glabrata RPN4* and *EFG1* deletion confirmation, a screening assay was needed. The DNA of candidate colonies was extracted as described below, followed by PCR amplification of the modified target *locus*. The primer forward used to confirm a successful gene deletion corresponds to the TAG sequence, which is expected to be inserted in the *locus* of the gene targeted for deletion: 5'-GAGGGGGACATATATAAGTT-3'. The primer reverse corresponds to a selected region downstream of the gene targeted for deletion, in this case *CgRPN4* and *CgEFG1*:

***CgRPN4*_deletion_conf_Rv**: 5'-CTGAGCTTGCTAAGATCAAT-3';

***CgEFG1*_deletion_conf_Rv**: 5'-CATGCCAAATCCCTATACTA-3'

The PCR program used for amplification of the gene deletion sequence using the two primers mentioned above is described in Table 4. For this, 0.4µL of each designed oligo sequence (forward and reverse) was added to a mixture (2.5µL of reaction buffer (10x), 1.5µL Mg^{2+}, 0.4µL dNTPs, 0.1µL Taq polymerase and H_2O up to 25µL).

Table 4 – PCR program for gene deletion confirmation

PCR program - "CONF"		
Temperature (ºC)	**Time**	**Cycles**
95º	3 min	
95º	15 sec	30X
46º	30 sec	
72º	30 sec	
72º	7 min	

DNA extraction

All experiments considering plasmid extractions from *E. coli* were carried out using the NZYMiniprep kit. For DNA extraction from *C. glabrata*, a different procedure was followed: biomass from the grown colonies was collected and added to 200 µL of lysing buffer (for 12mL: 0,6mL Tris-HCl 50mM + 1,2mL EDTA 50mM pH 8.0 + 0,175g NaCl 250mM + 360µL SDS 0,3% + water until total volume is 12mL) with 0.5 mm glass beads, followed by vortex and then incubated for 1h at 65ºC. After resting in ice for 2 minutes, a 15-minute 13 000 rpm centrifugation at 4ºC followed, and the supernatant was transferred to a tube containing 1/10 of the supernatant volume of Sodium Acetate (3M, pH 4.8) and 2 volumes of absolute ethanol. This mixture was stored at -20ºC for 30 minutes and then centrifuged for 20 minutes, 13000rpm at 4ºC. The DNA pellet was washed with 500µL 70%

ethanol, followed by an 8-minute 13000rpm centrifugation at 4ºC and ethanol evaporation through speed vacuum. The DNA was resuspended in water.

Cloning of the *CgRBS1* promoter and site-directed mutagenesis

The pYPE354 plasmid was used as described before to clone and express the *lacZ* reporter gene. pYEP354 contains the yeast selectable marker *URA3* and the bacterial selectable marker *AmpR* genes. *CgRSB1* promoter DNA was generated by PCR, using genomic DNA extracted from the sequenced CBS138 *C. glabrata* strain, and primers present in Table 5. The first primer contains a region with homology within the beginning of the *CgRSB1* promoter and a recognition site for the EcoRI restriction enzyme, flanked by additional bases. The second primer contains a region with homology within the end of the *CgRSB1* promoter and the beginning of the *CgRSB1* coding sequence and a recognition site for the PstI restriction enzyme, flanked by additional bases. The amplified fragment was ligated into the pYEP354 vector (T4 Ligase, New England Biolabs), previously cut with the same restriction enzymes, to obtain the pYEP354_*CgRSB1*prom_*lacZ* plasmid. The putative CgRsb1 consensus in the *CgRSB1* promoter was mutated by site-directed mutagenesis using the primers in Table 5. The designed primers contain two mutations within each four of the potential consensus, resulting in the production of each the mutated consensus by PCR amplification (Table 6) to obtain the pYEP354_mut_*CgRSB1*prom_*lacZ* plasmids. For this, 1µL of each primer (forward and reverse) were added to 2µL of the plasmid DNA (30ng/µL), 10µL of HF buffer (5x), 2µL of Mg^{2+}, 0,5µL of Phusion polymerase, 1µL of dNTPs, 1,5µL of DMSO and H_2O up to a total amount of 50µL per reaction. The original template was then degraded by DpnI digestion (add 0,8µL DpnI to 40µL of each sample; incubation at 37ºC for 1h. The remaining 10µL of each sample were used as control - undigested).

Table 5 – Primers used for cloning the *RSB1* promoter into the pYEP354 plasmid, for site-directed mutagenesis of *RSB1* promoter motifs 1 to 4, and for RT-PCR evaluation of lacZ gene expression, under the control of the *RSB1* promoters.

		Primers	Sequence
Cloning of *RSB1* promoter		Fw	5’-CCGGAATTCCGTACACAAGCAGCTAGGTAAT-3’
		Rv	5’-AACTGCAGCTCATCCATCATTAGTTATT-3’
Site-directed mutagenesis	Motif 1	Fw	5'-GACCCGAGGTGTTTCCAAAATCGGTCCCACGCTTC-3'
		Rv	5'-GAAGCGTGGGACCGATTTTGGAAACACCTCGGGTC-3'
	Motif 2	Fw	5'-CTCAGAAATTGGGGTTGGGGGGGAGGGATG-3'
		Rv	5'-CATCCCTCCCCCCCAACCCCAATTTCTGAG-3'
	Motif 3	Fw	5'-GAAATTGGGGGAGGGGGGTTGGGATGAGGTGGAAGTG-3'
		Rv	5'-CACTTCCACCTCATCCCAACCCCCCTCCCCCAATTTC-3'
	Motif 4	Fw	5'-CATCGCAAGGAATAATAACCGGGATGTAGTACAATAGTGGTTC-3'
		Rv	5'-GAACCACTATTGTACTACATCCCGGTTATTATTCCTTGCGATG-3'
RT-PCR	*LacZ* expression	Fw	5’-TGGCTGGAGTGCGATCTTC-3’
		Rv	5’-CGTGCATCTGCCAGTTTGAC-3’
	RDN25 expression	Fw	5’-AACAACTCACCGGCCGAAT-3’
		Rv	5’-CAAGCGTGTTACCTATACTCCGCCGTCA-3’

The PCR program used is described in Table 6:

Table 6 – PCR program for site-directed mutagenesis of 4 motifs in the *RSB1* promoter

PCR program - "PHUSION"		
Temperature (ºC)	**Time**	**Cycles**
95º	1 min	
95º	50 sec	20X
***63º**	50 sec	
72º	9 min	
72º	7 min	

*****The temperature of annealing depends on the primers used:

Primers for motif 1: $T_{annealing}$ = 63ºC

Primers for motifs 2 and 3: $T_{annealing}$ = 62ºC

Primers for motif 4: $T_{annealing}$ = 58ºC

E. coli competent cells (DH5α) were then transformed with the four pYEP354_mut_*CgRSB1*prom_*lacZ* plasmids (10µL sample/control + 150µL cells + 50µL TCM were kept on ice for 15 min; heat shock at 42ºC for 3 min then kept on ice for 5 min; 800µL LB medium was added to each transformation tube followed by a 37ºC incubation with shaking for 1h and, finally, samples were plated in LB + ampicillin selective medium).

RT-PCR gene expression measurement

The transcript levels of the *CgRSB1* or the *lacZ* reporter gene encoding for β-galactosidase were determined by quantitative real-time PCR (RT-PCR). L5U1 cells transformed with the pYEP354_*CgRSB1*prom_*lacZ* or each pYEP354_mut_*CgRSB1*prom_*lacZ* plasmids were grown in BM supplemented with leucine until mid-exponential phase. Fluconazole exposure, cell harvesting and storage were performed as mentioned above. For total RNA extraction, the hot phenol method was applied[215]. Synthesis of cDNA for real time RT-PCR experiments, from total RNA samples, was performed using the Multiscribe™ reverse transcriptase kit (Applied Biosystems) and the 7500 RT-PCR Thermal Cycler Block (Applied Biosystems), following the manufacturer's instructions. The quantity of cDNA for the following reactions was kept around 10 ng. The subsequent RT-PCR step was carried out using SYBR® Green (NZYTech) reagents with default parameters established by the manufacturer and the primers in Table 5. The *CgRDN25* gene transcript levels were used as an internal reference.

3. Results

3.1 CRISPR-Cas9 system implementation and optimization in *C. glabrata*

The functional characterization of a gene to understand the mechanisms underlying its mode of action becomes possible with the use of advanced genetic manipulation tools, where the CRISPR-Cas9-based editing system has emerged as a particularly powerful tool successfully applied in a variety of organisms, from microorganisms to human cells.

The CRISPR-Cas9 system operates with the endonuclease protein Cas9 for RNA-guided DNA recognition and cleavage, representing a system with high specificity very used for genome engineering applications[188]. By modifying a 20-nucleotide sequence at the 5' end of sgRNA, it is, in principle, possible to target any desired gene. However, when selecting the target sequence of a gene, there are a few things that need to be considered. The first consists in the presence of a PAM sequence immediately downstream of the target sequence, which could be a limitation when editing the genome of AT-rich organisms. Another concern is minimising off-target effects that trigger unintended mutations within the genome, and to do so, the target sequence must be unique throughout the genome. Also, to achieve effective gene knock-out, it is recommended that the target sequence be within the first half of the gene since the targeting of 3' exons could fail to obtain complete inhibition of gene function[216]. Nonetheless, appropriate target recognition by sgRNA in the CRISPR-Cas9 system is rather specific, with decreases in Cas9 cleavage activity when a single nucleotide mismatch occurs in the sgRNA sequence[216].

The initial goal of this work consisted in the implementation and optimization of a CRISPR-Cas9 system for gene deletion via homology-directed repair (HDR) in *C. glabrata*, and it was based on the work of Vyas *et al*[209]. Here, a single-plasmid CRISPR system was used, providing also a repair template cassette to increase the efficiency of homologous recombination in *C. glabrata*, since the dominant DNA repair pathway of this yeast is NHEJ[209]. The main advantage of this system over the previous ones developed for *C. glabrata* is the use of a solo vector (pV1382 - Figure 15) expressing both *CAS9* and sgRNA. The several selection markers found in this solo vector are also advantageous to use in a wider range of strains: a *URA3* marker that can be used for counterselection in *ura3* auxotrophs, the dominant-selectable *NAT1* gene, which confers resistance to the drug nourseothricin (NAT^R) and the ampicillin resistance gene (*ampR*) that is used for selection of transformed *E. coli*[209].

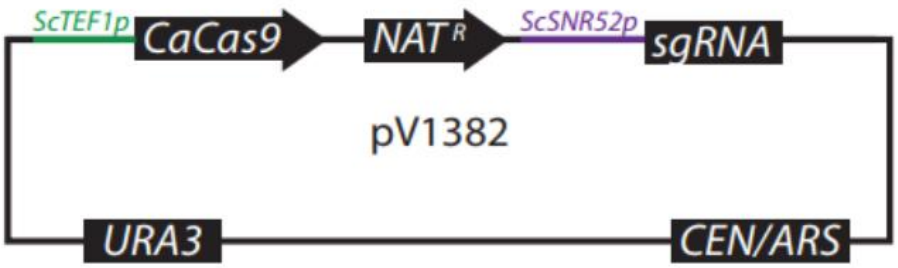

Figure 15 - Vector pV1382 used for CRISPR-Cas9 mutagenesis in *C. glabrata* - from Vyas *et al* '*New CRISPR Mutagenesis Strategies Reveal Variation in Repair Mechanisms among Fungi*' (2018)[209]

The first step of a CRISPR project (Figure 16) begins with the design of sgRNA, a short synthetic RNA composed of a scaffold sequence responsible for Cas9 binding, and a targeting sequence consisting of a ~20 nucleotides spacer that guides the Cas9 and binds to the target DNA *locus*[217]. For Cas9 to cleave the DNA, it is essential that the target *locus* is located immediately after the 5' of a short protospacer adjacent motif (PAM) sequence containing a 5'-NGG-3' (the canonical PAM sequence, where "N" is any nucleotide) in the non-target strand, but not in its target-strand complement[179,190]. However, this PAM sequence should not be included as a part of the sgRNA. The sgRNA sequences used were chosen from the guide compilation tables designed by Vyas *et al*[209] that included the guide sequences corresponding to each annotated gene in the genome of *C. glabrata*, with exception of target sequences that had 6 instances of T in the 20 nucleotides before the NGG as it would lead to premature termination from polymerase (Pol) III promoters (such as *SNR52*)[218].

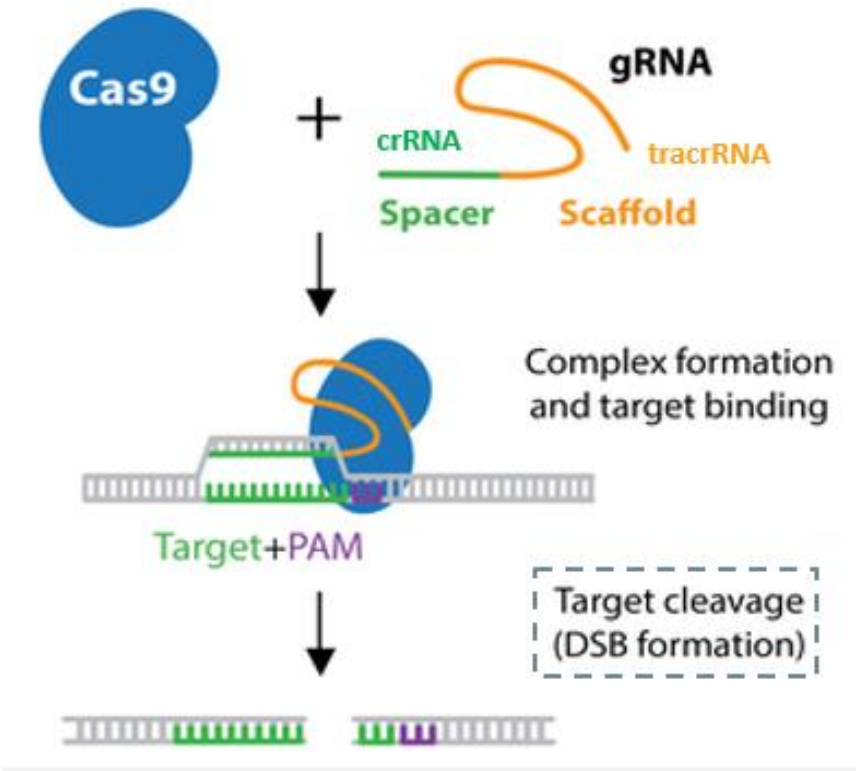

Figure 16 - The components and mode of action of a CRISPR-Cas9 system - from Addgene '*CRISPR Guide*' (https://www.addgene.org/guides/crispr/) (adapted)[219]

3.1.1 Optimization of sgRNA cloning (*CgADE2*) into pV1382 in *E. coli* DH5α cells

The *ADE2* gene was chosen as a proof-of-concept platform to optimize a CRISPR-Cas9 system for gene deletions in *C. glabrata* (Figure 17), since the disruption of *ADE2* in this yeast results in the accumulation of a red-pigmented intermediate due to blocking of adenine biosynthesis, allowing visual identification of the *C. glabrata* Δ*ade2* colonies[220].

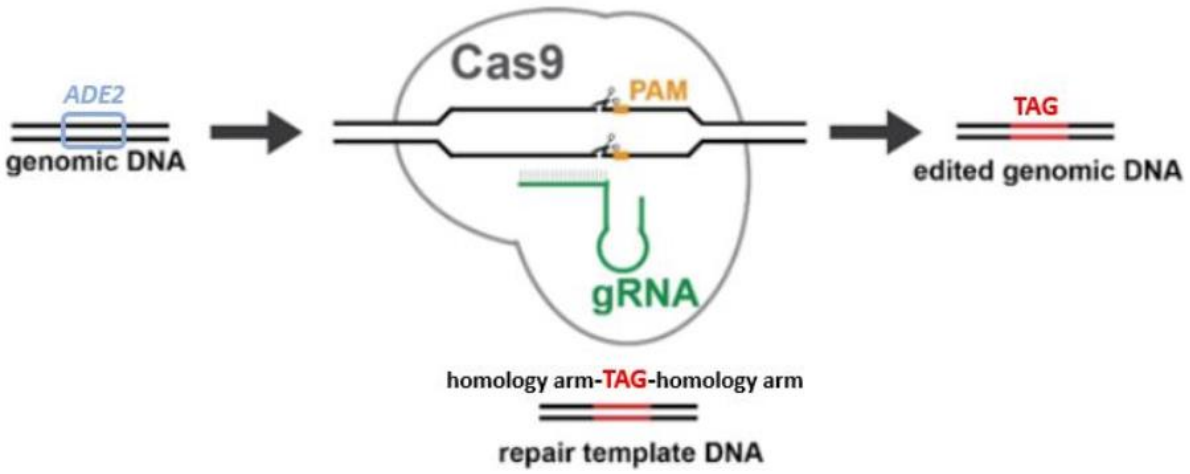

Figure 17 - Schematic representation of the implementation of a CRISPR-Cas9 system in *ADE2* deletion - adapted from Vyas *et al* '*An Introduction to CRISPR-Mediated Genome Editing in Fungi*' (2019)[221]

The protocol of cloning a sgRNA into pV1382 started with the plasmid digestion with the restriction enzyme BsmBI (Figure 18). Here, three different conditions were tested as it is represented in Table 7. The oligos used to produce the sgRNA sequence were annealed and ligated into the linearized pV1382 plasmid, giving rise to pV1382_guide*ADE2*. During the ligation of sgRNA into the vector, a negative control was prepared where no sgRNA oligos were added to the vector ligation mixture. When the plasmid is digested and opened, it is no longer active. Since the restriction enzyme used for digestion (BsmBI) does not create complementary sticky ends in the plasmid, it cannot re-circularize on its own. For the re-circularization to occur, it would either be due to the presence of the initial fragment or with a guide sequence added, but in the negative control there is no addition of sgRNA oligos. Therefore, in these plates the chance of plasmid re-circularization and, therefore, re-activation is lower, meaning the number of colonies grown is expected to be lower than in the sample plates.

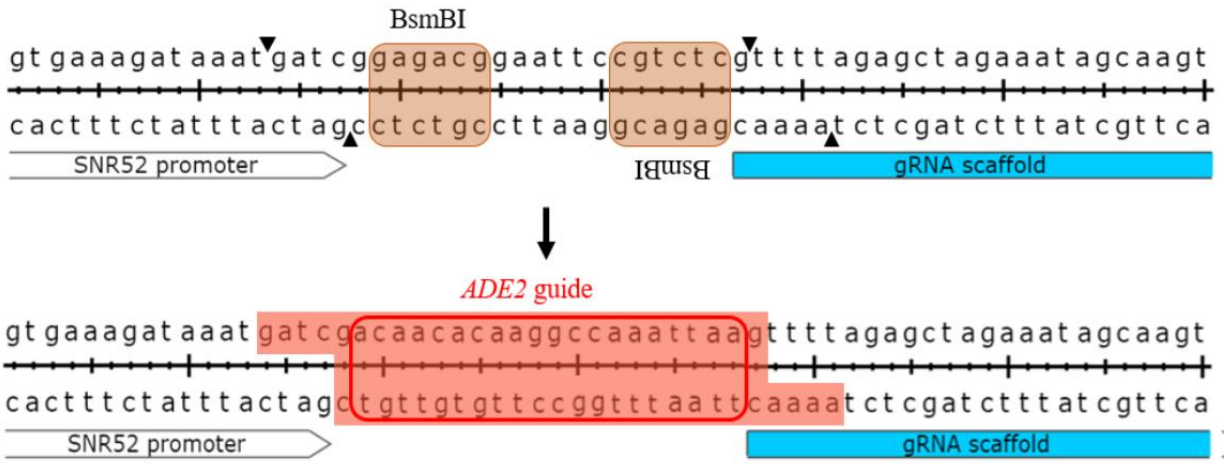

Figure 18 - Cloning of *ADE2* guide sequence into pV1382: plasmid digestion with BsmBI (sequences of recognition shaded in brown) is followed by ligation of annealed oligos (red shaded sequences) with desired guide sequence

Following transformation of *E. coli* cells with pV1382_guide*ADE2*, selection of transformants was achieved by plating the cells in LB medium with ampicillin. The number of colonies grown in each plate is shown in Table 7:

Table 7 - Different plasmid digestion conditions with corresponding number of colonies grown in each plate.

pV1382_guide*ADE2*		**Plasmid digestion with BsmBI**		**Transformation of DH5α (nº CFUs)**	
		Incubation temperature (ºC)	Incubation time (min)	Sample	Negative control
	1.	55º	10	18	19
	2.	55º	60	26	7
	3.	37º	30	35	70

Comparing the number of colonies between the samples and the respective negative controls, it is seen that the results of both digestion conditions number 1 (55ºC, 10min) and 3 (37ºC, 30min) are invalid, since it was expected that the number of colonies in the sample plates would be significantly higher than the number of colonies in the negative control. This is the case of the plates in condition 2., so this protocol was selected for further work, as is proved to be the most suitable for the BsmBI restriction activity. The NZYMiniprep kit was used for plasmid extraction from candidate colonies (sample plate 2.) and the successful sgRNA cloning was confirmed by sequencing. Sequencing results revealed the cloning of the sgRNA into pV1382 was successful, which permitted the use of pV1382_guide*ADE2* in CRISPR-Cas9 mediated gene deletions.

3.1.2 Using a CRISPR-Cas9 system for *CgADE2* disruption

For CRISPR-Cas9 mediated *ADE2* gene deletion in a URA$^-$ strain (KCHr606_Δ*ura3*), two different yeast transformation protocols were tried out. In the first three assays, the Alkali-Cation Yeast Transformation kit protocol from MP Biomedicals was used. In the fourth assay, the Transformation of Expression Vectors into Yeast protocol (Gietz and Woods, 2000) was followed. Distinct cell concentrations were tested in the transformation reactions, with best results being achieved with cultures grown to OD 0.6-0.8. To determine the range of DNA that leads to higher transformation efficiency, the transformation assays were performed with different amounts of DNA, as it is represented in Table 8. Two different concentrations of adenine in MMB medium were also tested, and the results show that cells grew only when transformed with amounts of pV1382_guide*ADE2* above 1µg and plated in a medium with 20mg/L of adenine instead of 3mg/L. The presence of adenine is required so that the successfully edited strains (ADE-) are able to grow in the transformation plate. The absence of uracil in the MMB medium allows for the selection of transformed cells, since the strain of *C. glabrata* used is Δ*ura3*. Different amounts of repair template aimed at *CgADE2* deletion for the generation of knockout strains were also tested. It seems that 3µg is enough to achieve its purpose. The presence of red/pink colonies (Figure 19), which corresponds to the Δ*ade2* phenotype, revealed the CRISPR-Cas9 *ADE2* deletion was successful in numerous colonies. Both transformation protocols displayed a successful outcome, although the number of colonies obtained using the MP Biomedicals transformation kit was significantly higher (Table 8). To confirm the Δ*ade2* phenotype, several

colonies were collected and plated in MMB medium, this time without adenine. The absence of colonies grown in this plate supported the idea that *ADE2* was successfully deleted.

Table 8 - Results of different transformation protocols of *C. glabrata* cells using a CRISPR-Cas9 system for *ADE2* deletion

	pV1382_ guideADE2 (µg)	Repair template (µg)	Transformation Plates Medium	Colonies	Red colonies	Total nº colonies	% genetically engineered colonies	Transformation Protocol
1st assay	0,3	5	MMB + Adenine (3mg/L)	No	-	-	-	Alkali-Cation Yeast Transformation kit (MP Biomedicals)
	0,5	5	MMB + Adenine (3mg/L)	No	-	-	-	
2nd assay	0,5	5	MMB + Adenine (3mg/L)	No	-	-	-	
	0,7	5	MMB + Adenine (3mg/L)	No	-	-	-	
3rd assay	1	3	MMB + Adenine (3mg/L)	No	-	-	-	
	2	3	MMB + Adenine (3mg/L)	No	-	-	-	
	3	3	MMB + Adenine (3mg/L)	No	-	-	-	
	1	3	MMB + Adenine (20mg/L)	Yes	42	217	19,35%	
	2	3	MMB + Adenine (20mg/L)	Yes	54	314	17,20%	
	3	3	MMB + Adenine (20mg/L)	Yes	27	179	15,10%	
4th assay	1	3	MMB + Adenine (20mg/L)	Yes	3	16	18,7%	Transformation of Expression Vectors into Yeast (Gietz and Woods, 2000)
	2	3	MMB + Adenine (20mg/L)	Yes	10	40	25%	
	3	3	MMB + Adenine (20mg/L)	Yes	9	24	37,5%	

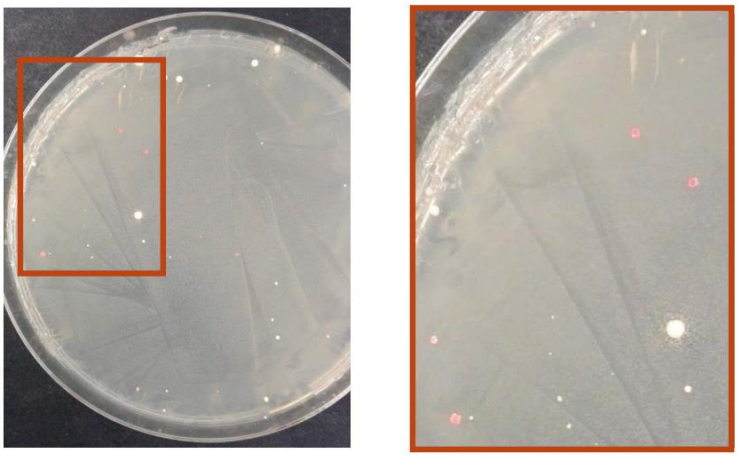

Figure 19 - *C. glabrata* KCHr606_Δ*ura3* strain transformed with pV1382_guide*ADE2* and repair template for CRISPR-Cas9 mediated *ADE2* gene deletion. The brown box presents a magnified view of red/pink colonies from the left figure.

3.2 Application of a CRISPR-Cas9 system to *C. glabrata* gene characterization

A CRISPR-Cas9 system, previously optimized and implemented in *C. glabrata* for *ADE2* gene deletion, was used in the attempt to generate several deletion mutants in a *C. glabrata* URA$^-$ strain (KCHr606_Δ*ura3*) in order to further investigate and functionally characterize the deleted genes.

For this work, *EFG1* and *TEC1* were selected, aiming the analysis of their role in biofilm formation, whereas *RPN4* and *MAR1* were chosen for being potentially involved in azole antifungal resistance in *C. glabrata*. gRNAs and repair templates were designed for the deletion of the above mentioned four genes, however, the CRISPR-Cas9 system and further steps could only be applied to *EFG1* and *RPN4*, as a consequence of the COVID-19 pandemics that forced the laboratory work to end sooner than expected.

3.2.1 CRISPR-Cas9 mediated *EFG1* gene deletion

The cloning of the corresponding sgRNA into pV1382 was performed as previously described for the deletion of *CgADE2* (Figure 20), as was the construction of the repair template designed for gene deletion.

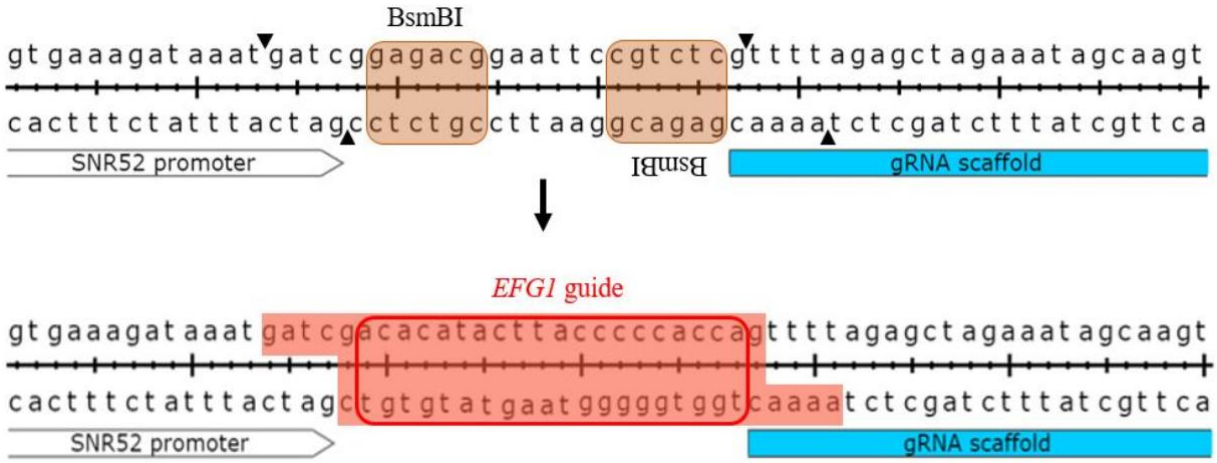

Figure 20 - Cloning of *EFG1* guide sequence into pV1382: plasmid digestion with BsmBI (sequences of recognition shaded in brown) is followed by ligation of annealed oligos (red shaded sequences) with desired guide sequence.

Transformation of *C. glabrata* cells (using the Alkali-Cation Yeast Transformation kit protocol) with the plasmid and the repair template was carried out and colonies were obtained. The DNA from the colonies corresponding to potential CRISPR-Cas9-generated *C. glabrata* Δ*efg1* deletion mutant strains was extracted and sequenced, revealing that the intended genome editing was achieved.

With the generated Δ*efg1* mutant strain, it is now possible to carry out biofilm quantification assays to test whether *C. glabrata*'s ability to form biofilm is affected in the absence of *EFG1*. Unfortunately, this step could not be accomplished as a result of a sudden loss of access to the laboratory to continue investigations, caused by the COVID-19 pandemics. A biofilm quantification assay would allow for a possible confirmation of an involvement of *EFG1* in the mechanisms underlying biofilm formation, as it is expected a biofilm reduction in the Δ*efg1* mutant strain compared to *wild-type*. Furthermore, to verify if the outcome of this assay is directly related to the *EFG1* gene or if it represents an indirect result, a phenotypic complementation would be carried out by introducing an *EFG1* expression plasmid in the *C. glabrata* Δ*efg1* mutant strain and comparing biofilm phenotypic results between the complemented and mutant strains.

3.2.2 CRISPR-Cas9 mediated *RPN4* gene deletion

Following the protocols formerly applied, a CRISPR-Cas9 system was implemented in *C. glabrata* to generate Δ*rpn4* strains, providing a repair template to be inserted at the DNA break site (Figure 21).

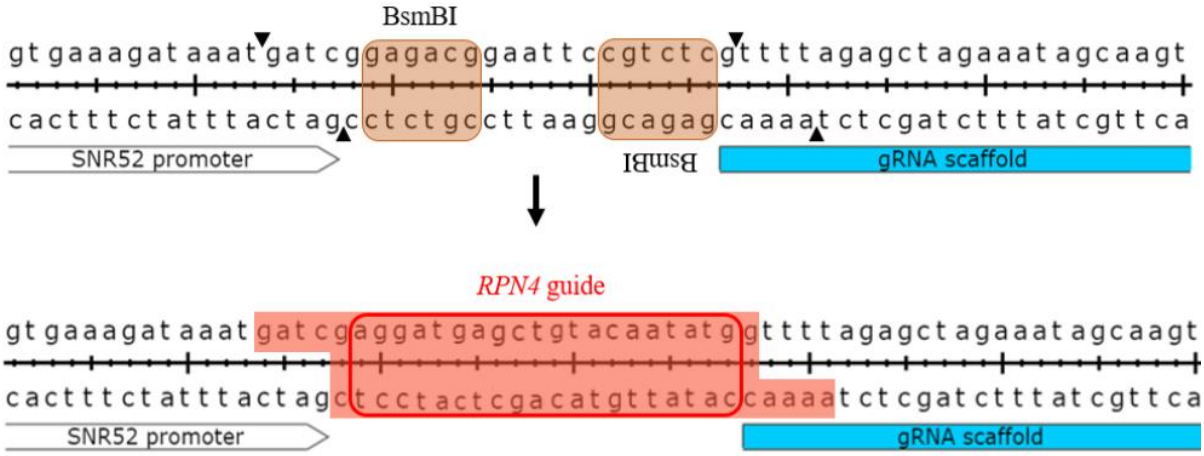

Figure 21 - Cloning of *RPN4* guide sequence into pV1382: plasmid digestion with BsmBI (sequences of recognition shaded in brown) is followed by ligation of annealed oligos (red shaded sequences) with desired guide sequence.

Confirmation of the intended gene deletion was achieved by PCR, carried out over DNA extracted from potential *C. glabrata* Δ*rpn4* colonies, followed by an electrophoresis that shows several colonies with a PCR product consistent with what would be expected for a positive gene deletion. However, confirmation by DNA sequencing was not yet obtained as a result of a sudden loss of access to the laboratory to continue investigations, caused by the COVID-19 pandemics.

Once the Δ*rpn4* mutant strain is confirmed, the next step would be to engage in antifungal susceptibility assays. As it was mentioned above, this step of the experimental work could not be done, although it would be of great interest to carry on investigations about the role of *CgRPN4* in antifungal resistance. Though it has been shown that the deletion of *RPN4* generated *C. glabrata* mutants with increased susceptibility to azoles[222], what was planned was the generation of multiple deletion mutants of genes presumed to be involved in antifungal resistance - Δ*rpn4* Δ*mar1* Δ*pdr1*. This approach of combining mutations would help perceiving the interactions between these specific genes when compared to individual mutations.

3.3 Site-directed mutagenesis of possible Mar1 binding sites in the *RSB1* promoter

To assess whether the predicted *RSB1* promoter response elements for the TF Mar1 where indeed correct, specific mutations were introduced in each one of these four potential recognition motifs through site-directed mutagenesis (Figure 22).

***RSB1* promoter:**

ATCATTCGTACACAAGCAGCTAGGTAATATACAACTACACGTAAAACATGTGATCTCCAT
AAAAAAAAGCGTTCCACGGATCCGCATTGTCTCTGCGAGTGGTTTGTACAGTATGGACGC
AGCAGTGCTTCTCACAACGTTTTGTACGCGTTTTCTCTACCACACTTAGGGGTTTTTCCG
TGGAAATACTCCTTATTTGAAAGTTAAAGCGTCGCAGAAAGCCAAGAGTAATTCCGCGGT
GTTTTTTTCTCTCTCGTCGTTTTGCAGTGTAGTTCCACTCGCTTTTCCCCCCTTACTGTA
CTGTGCGGTTGATAGGAGTGCCAAGAGAATGGCGCACAACGCACTTTCACTCTTCCTTCT
GTAAGCTTTTCCACTTATTAAGGTTATGGGCCAAAAACCACAGTCGTGTCTAAGGAAGTC
CGTGCAAAGCACAAGACCCGAGGTGTTTCCTCGATCGGTCCCACGCTTCTTTCAGTGACC
AGCACGACGAGGGAATTAAAATAGCGCAAGCAGAAAGGGCATTGATGAGATCTGGAGAAA
CCTGCGCAGAGAGGCGGCACATCTCCTTTTTTTTTGTAATTACTTATCCGTTTTAGGAAA
TCAAGGGCTAAATTGCATTATTGCCTCAGAAATTGGGGGAGGGGGGGAGGGATGAGGTGG
AAGTGTAGAAAGGATTGCGTAATCCCTTCTCTACAGTTGTAATACTCTTGACTAAGGGTT
GTGTCAAGGAAGCAAGCCAGACTAACTTGAACTTGATAGTGGCCTCATCGCAAGGAATAA
TAACCTCTATGTAGTACAATAGTGGTTCAAGGGAAGAGAAAAATTTTTTATAGGAGTTAA
CGCATATTGAAAGAAACAAGGGTCCTGAACTGTGGACTCATTTAAATAAAATAGTAATAA
AAATCATTGTATTTATTCAAGGACCATGTAGAAATAAAGAAATAATCTTTATTCTTGATC
AAAAGGCAAAGACAATACAATACTAATAAAAAAATAACTA

↓ Site-directed mutagenesis

ATCATTCGTACACAAGCAGCTAGGTAATATACAACTACACGTAAAACATGTGATCTCCAT
AAAAAAAAGCGTTCCACGGATCCGCATTGTCTCTGCGAGTGGTTTGTACAGTATGGACGC
AGCAGTGCTTCTCACAACGTTTTGTACGCGTTTTCTCTACCACACTTAGGGGTTTTTCCG
TGGAAATACTCCTTATTTGAAAGTTAAAGCGTCGCAGAAAGCCAAGAGTAATTCCGCGGT
GTTTTTTTCTCTCTCGTCGTTTTGCAGTGTAGTTCCACTCGCTTTTCCCCCCTTACTGTA
CTGTGCGGTTGATAGGAGTGCCAAGAGAATGGCGCACAACGCACTTTCACTCTTCCTTCT
GTAAGCTTTTCCACTTATTAAGGTTATGGG**mut 1**AAACCACAGTCGTGTCTAAGGAAGTC
CGTGCAAAGCACAAGACCCGAGGTGTTTCCAAAATCGGTCCCACGCTTCTTTCAGTGACC
AGCACGACGAGGGAATTAAAATAGCGCAAGCAGAAAGGGCATTGATGAGATCTGGAGAAA
CCTGCGCAGAGAGGCGGCACATCTCCTTTTTTTTTGT**mut 2**ACTT**mut 3**GTTTTAGGAAA
TCAAGGGCTAAATTGCATTATTGCCTCAGAAATTGGGTTGG GGGTTGGGATGAGGTGG
AAGTGTAGAAAGGATTGCGTAATCCCTTCTCTACAGTTGTAATACTCTTGACTAAGGGTT
GTGTCA**mut 4**AGCAAGCCAGACTAACTTGAACTTGATAGTGGCCTCATCGCAAGGAATAA
TAACCGGGATGTAGTACAATAGTGGTTCAAGGGAAGAGAAAAATTTTTTATAGGAGTTAA
CGCATATTGAAAGAAACAAGGGTCCTGAACTGTGGACTCATTTAAATAAAATAGTAATAA
AAATCATTGTATTTATTCAAGGACCATGTAGAAATAAAGAAATAATCTTTATTCTTGATC
AAAAGGCAAAGACAATACAATACTAATAAAAAAATAACTA

Figure 22 – *RSB1* promoter with four potential Mar1-binding motifs highlighted: motif 1 in orange, motifs 2 and 3 in blue and motif 4 in green. *Wild-type* promoter (top) and promoter with mutations in each motif: mut 1, mut 2, mut 3 and mut 4 (bottom)

Following this procedure, activation of the *RSB1* promoter - cloned in the plasmid pYEP354 immediately before the reporter gene *lacZ* - was measured by quantifying the expression of *lacZ* with RT-PCR.

Furthermore, the *RSB1* promoter activation was measured in the presence and absence (control) of fluconazole, as Mar1 is suspected to play a role in gene regulation in response to azole-induced stress. The results obtained are represented in Figure 23.

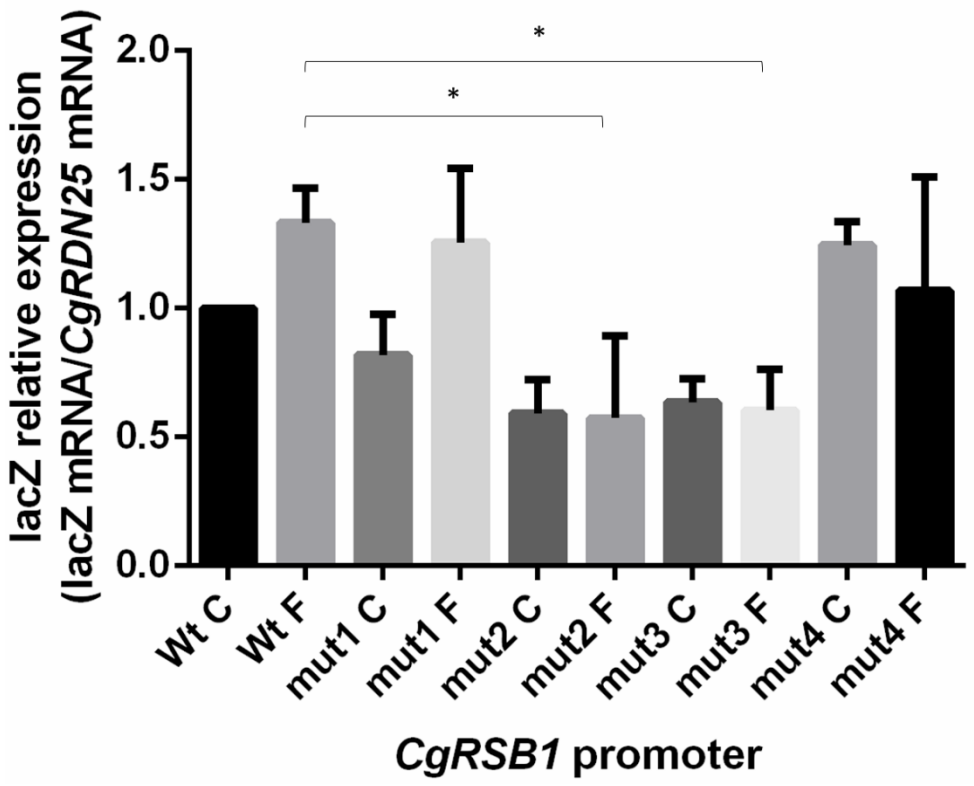

Figure 23 – Comparison of *CgRSB1* promoter activation, in the presence (F) and absence (C) of fluconazole, between cells containing the *wilt-type* (Wt) promoter and the promoter mutated in motifs 1-4 (mut1-mut4). Activation was measured through the relative expression of the reporter gene *lacZ*.

To understand if the *RSB1* promoter motifs affect the basal expression of the gene, it is necessary to compare the expression of *lacZ* between the *wild-type* promoter and the mutated motifs in control conditions. Statistical analysis did not show a significant difference in the activation levels of the control mutated promoters compared to the control *wild-type*, hence, it is possible to assume that the four selected *RSB1* promoter motifs do not affect the basal expression of *RSB1*. On the other hand, in the presence of fluconazole it is possible to detect considerable variations in the promoter activation. When analysing the data from Figure 23, it is seen that mutations in motifs 2 and 3 (mut2 and mut3) of the *RSB1* promoter reduce its activation in the presence of fluconazole when comparing with the *wild-type* promoter (highlighted in Figure 23 with *). These results suggest that motifs 2 and 3, both sharing the same sequence – GGGGAGG -, of the *RSB1* promoter are potentially involved in the expression of *RBS1* when fluconazole is present in the medium.

A further evaluation of this regulation mechanism can be achieved with the use of Chromatin Immunoprecipitation (ChIP), a method that will confirm whether the TF Mar1 actually binds to these two motifs of the *RSB1* promoter in order to activate *RSB1*.

4. Discussion and Future Perspectives

This study describes how an innovative genome editing technology like the CRISPR-Cas9 system can be used as a valuable tool for the functional characterization of numerous *C. glabrata* genes presumed to be involved in this pathogen's virulence and antifungal drug resistance mechanisms.

The CRISPR-Cas system is considered to be one of the major breakthrough discoveries of genetics, currently being explored for genome edition of a great deal of organisms. A CRISPR-Cas based approach has several advantages compared to the already existing genome engineering techniques. For instance, while being robust, this technology is very user-friendly since it only requires the construction of a recombinant plasmid containing the sequences coding for the Cas9 protein and the gRNA, a target-specific small guide sequence. As a consequence, this approach is less time-consuming, which is a very valuable asset. The design of the gRNA allows for the targeting of a vast number of genes, provided they are located next to a PAM sequence. This requirement is, however, a restriction for the targetable genomic loci. There are already quite a few studies developing approaches to expand the targeting range of CRISPR-Cas9, for example through protein engineering of Cas9 to alter PAM recognition[178].

The first part of this work consisted of the implementation and optimization of a CRISPR-Cas9 system, previously developed by Vyas *et al*[209], to implement in the *C. glabrata* KCHr606_Δ*ura3* strain for gene deletions. This system was chosen mainly because of the advantages of using a solo vector that encodes both Cas9 and the gRNA, this way facilitating cell transformation. One important aspect to minimize the off-target effects by the CRISPR-Cas9 system is the off-target prediction. Here, adequate gRNA design was carried out according to a list of *C. glabrata* genes and guiding sequences, provided by Vyas and colleagues, with the predicted off-target sites.

A series of optimization steps were carried out (Figure 24), starting with the testing of different incubation conditions for plasmid digestion to achieve a suitable outcome of gRNA cloning into the plasmid. Once the solo vector containing the designed gRNA and Cas9 coding sequences was obtained, the optimization of the CRISPR-Cas9 system itself began. During the transformation of *C. glabrata* cells with the solo vector, a repair template was also supplied in order to increase the odds of the HDR pathway to act upon the CRISPR-Cas9-generated DSB. Two different transformation protocols were tried out and optimized for CRISPR-Cas9 mediated *ADE2* gene deletion in *C. glabrata* until the desired outcome, which in this case was obtaining red colonies (Δ*ade2* phenotype), was achieved. It has been demonstrated that the NHEJ pathway is the dominant repair pathway following a DSB in *C. glabrata*[209], however, supplying a repair template was shown to, at a certain level, circumvent this tendency and favour the action of the HDR pathway. Even though the percentages of efficiency obtained for gene deletion using this CRISPR-Cas9 system were not as high as expected, the results were satisfactory enough to carry on with CRISPR-mediated deletions of a number of *C. glabrata* genes of interest to be further studied. The higher percentage of genome editing efficiency obtained in the study of Vyas and colleagues[209], from which the CRISPR-Cas9 system used in this work was based on, could be partially related to the yeast transformation protocol they followed, consisting of a combination of a lithium acetate and electroporation protocol. Here, the transformation of *C. glabrata* did not include the electroporation step, but the use of lithium acetate followed by heat-shock treatment (among other steps described in the protocols referred in the 'Materials and Methods' section).

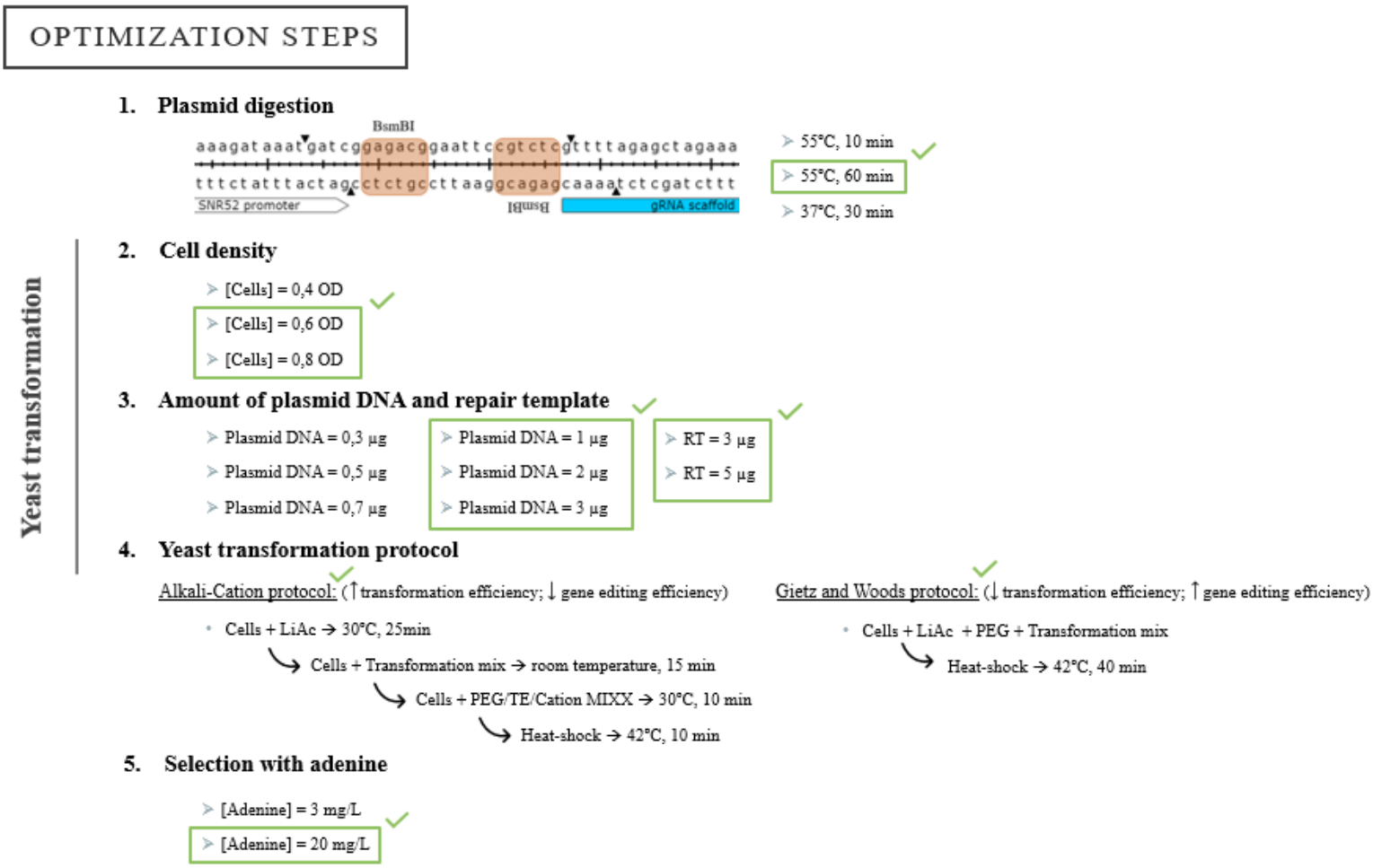

Figure 24 – Overall optimization steps tested throughout this work to achieve an efficient protocol for CRISPR-Cas9-mediated gene deletions in *C. glabrata*

With countless studies recognising *C. glabrata* as an emerging human pathogen[5,14,16], understanding its virulence mechanisms became an important concern for public health. *C. glabrata* was shown to have an intrinsically low susceptibility to azole antifungal drugs[3,6,7,13,14], also being the main *Candida* species exhibiting multidrug resistance[19]. The fast azole resistance acquisition seen in *C. glabrata* has been associated with gain-of-function mutations in *PDR1*[21,121,122], and results such as the upregulation of *CgRPN4* seen in fluconazole-resistant Pdr1 gain-of-function mutants of *C. glabrata*[142], among other, led to the idea of a possible link between *CgRPN4* and azole resistance in this pathogen. Therefore, *CgRPN4* was chosen to be further studied in this work, that began with its deletion using the previously optimized CRISPR-Cas9 system. From the colonies obtained, several were considered potential *C. glabrata* Δ*rpn4* mutants according to the confirmation PCR and electrophoresis. It was not possible, however, to confirm a successful CRISPR-Cas9-mediated *RPN4* deletion through DNA sequencing due to unexpected loss of laboratory access as a consequence of the COVID-19 pandemics. Assuming the intended gene deletion was achieved, the next phase planned for this part of the work would be to create, again using the CRISPR-Cas9 system, a *C. glabrata* Δ*rpn4* Δ*mar1* Δ*pdr1* multiple deletion mutant and, later on, carry out azole susceptibility assays, as all three genes are presumed or known to play a role in antifungal resistance.

Another known virulence feature of *C. glabrata* is its ability to form biofilms, in which the *EFG1* and *TEC1* genes are presumed to play a role[47]. For further characterization, both genes were planned to be deleted in *C. glabrata* using the CRISPR-Cas9 system, yet only the Δ*efg1* deletion mutant was obtained, as the COVID-19 pandemics prevented the *TEC1* gene studies to go beyond the design of its repair template and gRNA. The next phase planned for this part of the work would be to create, again using the CRISPR-Cas9 system, a *C. glabrata* Δ*efg1* Δ*tec1* double deletion mutant and, later on, carry out biofilm formation assays, as both genes are presumed to play a role in this process.

The multiple deletion mutant method would help elucidate the genetic interactions between the deleted genes, more specifically the extent to which the function of one gene depends on the presence of a second or third genes. The existence of such genetic interactions can be inferred when the loss of the group of genes has a stronger phenotypic effect than the loss of any of the genes alone[223], thus facilitating the identification and characterization of gene functions and cellular pathways[224]. Additionally, since the single and multiple deletion strains were being built in a *URA3*- background, it would further be possible to confirm gene functions through gene expression complementation.

The recently discovered potential link between the uncharacterized CgMar1 TF and fluconazole stress responses, uncovered through previous unpublished work from our team, encouraged a deeper analysis of this protein's functions, which led to the hypothesis of Mar1 being a transcriptional regulator of *RSB1*, binding to its promoter in response to fluconazole-induced stress. The results from the RT-PCR analysis of the *RSB1* promoter activation, where a comparison is made between the *wild-type* promoter and four mutated possible Mar1-binding motifs, showed that in control conditions these motifs are not relevant for the basal expression of *RSB1*. However, two of the motifs, specifically motifs 2 and 3 (both with the GGGGAGG sequence) were shown to influence *RSB1* gene expression when fluconazole was added to the medium. This outcome supports the theory of Mar1 being involved in fluconazole stress responses mediated, at least partially, by *RSB1*. However, confirmation of whether or not Mar1 binds to the two *RSB1* promoter motifs recognized as relevant for this matter is still needed. This confirmation would be achieved with ChIP, a method that includes the crosslink between the Mar1 protein and its DNA binding sites, followed by chromatin shearing into short fragments and isolation of the DNA-interacting protein (crosslinked to DNA) by immunoprecipitation[225]. The protein binding sites, after protein release, are amplified with PCR and sequenced. Again, due to the COVID-19 pandemics, this step could not be accomplished. Even though the closest Mar1 ortholog found is the *S. cerevisiae* Hap1 TF, the GGGGAGG motif is not included in the list of known Hap1 consensus binding sites[226], supporting the idea of these proteins having different functions. Interestingly, the GGGGAGG sequence is found in the promoter regions of *CgSNQ2*, a drug efflux pump from the ABC superfamily, and *CgQDR2*, a MFS transporter, both known to be involved in azole resistance mechanisms in *C. glabrata*. This finding could, perhaps, point towards the involvement of Mar1 in *SNQ2* and *QDR2* regulation, in the presence of fluconazole, through the binding to the mentioned motif, although previous RNA-seq analysis done in our lab (Pais *et al*, unpublished results) did not seem to support this idea. Additionally, the GGGGAGG motif is also present in the *C. albicans RTA2* promoter region, a *CgRSB1* ortholog that encodes a protein known to mediate azole resistance responses[227]. Having seen how the GGGGAGG motif affects *CgRSB1* gene expression in the presence of fluconazole, it is possible that this motif has a similar effect in the expression of *RTA2* in *C. albicans* under such conditions, and if so, it would be interesting to find the TF - possibly a Mar1

ortholog - responsible for the regulation of *RTA2* by binding to the said motif. All of these theories require further *in silico* investigations as well as RNA-seq and ChIP assays to confirm possible influences in gene expression and possible TF binding sites.

Altogether, this study provided optimized valuable tools to be applied in the genetic manipulation of *C. glabrata*. Additionally, two putative Mar1 binding sites in the *RSB1* promoter region were uncovered, while two new deletion mutants were obtained, that will contribute to leverage ongoing studies on the mechanisms of biofilm formation and azole resistance in this pathogen.

References

1. Brown, G. D. *et al.* Hidden killers: Human fungal infections. *Sci. Transl. Med.* **4**, (2012).

2. Pfaller, M. A. & Diekema, D. J. Epidemiology of invasive candidiasis: A persistent public health problem. *Clin. Microbiol. Rev.* **20**, 133–163 (2007).

3. Yapar, N. Epidemiology and risk factors for invasive candidiasis. *Ther. Clin. Risk Manag.* **10**, 95–105 (2014).

4. Sandhu, R., Dahiya, S., Sayal, P. & Budhani, D. Increased role of nonalbicans Candida, potential risk factors, and attributable mortality in hospitalized patients. *J. Heal. Res. Rev.* **4**, 78 (2017).

5. Antinori, S., Milazzo, L., Sollima, S., Galli, M. & Corbellino, M. Candidemia and invasive candidiasis in adults: A narrative review. *Eur. J. Intern. Med.* **34**, 21–28 (2016).

6. Méan, M., Marchetti, O. & Calandra, T. Bench-to-bedside review: Candida infections in the intensive care unit. *Crit. Care* **12**, 1–9 (2008).

7. Kullberg, B. J. & Arendrup, M. C. Invasive candidiasis. *N. Engl. J. Med.* **373**, 1445–1456 (2015).

8. Bitar, D. *et al.* Population-based Analysis of Invasive Fungal Infections. **20**, 1149–1155 (2014).

9. Strollo, S., Lionakis, M. S., Adjemian, J., Steiner, C. A. & Prevots, D. R. Epidemiology of hospitalizations associated with invasive candidiasis, United States, 2002-2012. *Emerg. Infect. Dis.* **23**, 7–13 (2017).

10. Klingspor, L. *et al.* Invasive Candida infections in surgical patients in intensive care units: A prospective, multicentre survey initiated by the European Confederation of Medical Mycology (ECMM) (2006-2008). *Clin. Microbiol. Infect.* **21**, 87.e1-87.e10 (2015).

11. Gabaldón, T., Naranjo, M. A. & Marcet-Houben, M. Evolutionary genomics of yeast pathogens in the Saccharomycotina. 1–10 (2016).

12. Clancy, C. J. & Nguyen, M. H. Diagnosing invasive candidiasis. *J. Clin. Microbiol.* **56**, 1–9 (2018).

13. Bassetti, M., Righi, E., Montravers, P. & Cornely, O. A. What has changed in the treatment of invasive candidiasis? A look at the past 10 years and ahead. *J. Antimicrob. Chemother.* **73**, i14–i25 (2018).

14. Diekema, D., Arbefeville, S., Boyken, L., Kroeger, J. & Pfaller, M. The changing epidemiology of healthcare-associated candidemia over three decades. *Diagn. Microbiol. Infect. Dis.* **73**, 45–48 (2012).

15. Dujon, B. *et al.* Genome evolution in yeasts. *Nature* **430**, 35–44 (2004).

16. Carreté, L. *et al.* Genome comparisons of Candida glabrata serial clinical isolates reveal patterns of genetic variation in infecting clonal populations. *Front. Microbiol.* **10**, 1–13 (2019).

17. Krcmery, V. & Barnes, A. J. Non-albicans Candida spp. causing fungaemia: Pathogenicity and antifungal resistance. *J. Hosp. Infect.* **50**, 243–260 (2002).

18. Pfaller, M. A., Diekema, D. J., Fungal, I. & Participant, S. Twelve years of fluconazole in clinical practice : global trends in species distribution and fluconazole susceptibility of bloodstream isolates of Candida. *Clin. Microbiol. Infect. Dis.* **10**, 11–23 (2004).

19. Deorukhkar, S. Virulence Markers and Antifungal Susceptibility Profile of Candida glabrata: An Emerging Pathogen. *Br. Microbiol. Res. J.* **4**, 39–49 (2014).

20. Gupta, A., Gupta, A. & Varma, A. Candida glabrata candidemia: An emerging threat in critically ill patients. *Indian J. Crit. Care Med.* **19**, 151–154 (2015).

21. Ksiezopolska, E. & Gabaldón, T. Evolutionary emergence of drug resistance in candida opportunistic pathogens. *Genes (Basel).* **9**, (2018).

22. Odds, F. C., Brown, A. J. P. & Gow, N. A. R. Antifungal agents: Mechanisms of action. *Trends Microbiol.* **11**, 272–279 (2003).

23. Deorukhkar, S. C., Roushani, S. & Bhalerao, D. Candidemia due to Non-Albicans Candida Species : Risk Factors , Species Distribution and Antifungal Susceptibility Profile Journal of Microbial Pathogenesis. *J. Microb. Pathog.* **1**, 1–6 (2017).

24. Farmakiotis, D., Tarrand, J. J. & Kontoyiannis, D. P. Drug-Resistant Candida glabrata Infection in Cancer Patients. *Emerg. Infect. Dis.* **20**, 1833–1840 (2014).

25. Vallabhaneni, S. *et al.* Epidemiology and Risk Factors for Echinocandin Nonsusceptible Candida glabrata Bloodstream Infections: Data From a Large Multisite Population-Based Candidemia Surveillance Program, 2008–2014. *Open Forum Infect. Dis.* 1–7 (2015). doi:10.1093/o

26. Lee, I., O. Fishman, N., E. Zaoutis, T. & Al, E. Risk Factors for Fluconazole - Resistant Candida glabrata Bloodstream Infections. *Arch. Intern. Med.* **169**, 379–383 (2009).

27. Uppuluri, P. *et al.* Dispersion as an important step in the Candida albicans biofilm developmental cycle. *PLoS Pathog.* **6**, (2010).

28. Treviño-Rangel, R. de J., Peña-López, C. D., Hernández-Rodríguez, P. A., Beltrán-Santiago, D. & González, G. M. Association between Candida biofilm-forming bloodstream isolates and the clinical evolution in patients with candidemia: An observational nine-year single center study in Mexico. *Rev. Iberoam. Micol.* **35**, 11–16 (2018).

29. Tumbarello, M. *et al.* Risk factors and outcomes of candidemia caused by biofilm-forming isolates in a tertiary care hospital. *PLoS One* **7**, 1–9 (2012).

30. Mota, S. *et al.* Candida glabrata susceptibility to antifungals and phagocytosis is modulated by acetate. **6**, 1–12 (2015).

31. Ramage, G., Walle, K. V. A., Wickes, B. L. & Lo, L. Standardized Method for In Vitro Antifungal Susceptibility Testing of Candida albicans Biofilms. **45**, 2475–2479 (2001).

32. Rodrigues, C. F., Silva, S. & Henriques, M. Candida glabrata: A review of its features and resistance. *Eur. J. Clin. Microbiol. Infect. Dis.* **33**, 673–688 (2014).

33. Leonhardt, I. *et al.* The fungal quorum-sensing molecule farnesol activates innate immune cells but suppresses cellular adaptive immunity. *MBio* **6**, 1–14 (2015).

34. Dixon, E. F. & Hall, R. A. Noisy neighbourhoods: Quorum sensing in fungal-polymicrobial infections. *Cell. Microbiol.* **17**, 1431–1441 (2015).

35. Westwater, C. *et al.* Candida albicans-Conditioned Medium Protects Yeast Cells from Oxidative Stress: a Possible Link between Quorum Sensing and Oxidative Stress Resistance. *Microbiology* **4**, 1654–1661 (2005).

36. Flannagan, R. S., Cosío, G. & Grinstein, S. Antimicrobial mechanisms of phagocytes and bacterial evasion strategies. *Nat. Rev. Microbiol.* **7**, 355–366 (2009).

37. Ramage, G., Martínez, J. P. & López-Ribot, J. L. Candida biofilms on implanted biomaterials: A clinically significant problem. *FEMS Yeast Res.* **6**, 979–986 (2006).

38. Malani, A. *et al.* Candida glabrata Fungemia: Experience in a Tertiary Care Center. *Clin. Infect. Dis.* **41**, 975–981 (2005).

39. Malani, A. N., Psarros, G., Malani, P. N. & Kauffman, C. A. Is age a risk factor for Candida glabrata colonisation? *Mycoses* **54**, 531–537 (2011).

40. Galocha, M. *et al.* Divergent approaches to virulence in C. Albicans and C. Glabrata: Two sides of the same coin. *Int. J. Mol. Sci.* **20**, (2019).

41. Gabaldón, T. & Carreté, L. The birth of a deadly yeast: Tracing the evolutionary emergence of virulence traits in Candida glabrata. *FEMS Yeast Res.* **16**, 1–9 (2016).

42. Brunke, S., Mogavero, S., Kasper, L. & Hube, B. Virulence factors in fungal pathogens of man. *Curr. Opin. Microbiol.* **32**, 89–95 (2016).

43. Sardi, J. C. O., Scorzoni, L., Bernardi, T., Fusco-Almeida, A. M. & Giannini, M. J. S. M. Candida species: current epidemiology, pathogenicity, biofilm formation, natural antifungal products and new therapeutic options. *J. Med. Microbiol.* **62**, 10–24 (2013).

44. Rodrigues, C. F., Silva, S., Azeredo, J. & Henriques, M. Candida glabrata's recurrent infections: biofilm

formation during Amphotericin B treatment. *Lett. Appl. Microbiol.* **63**, 77–81 (2016).

45. Perlin, D. S. Echinocandin Resistance in Candida. *Clin. Infect. Dis.* **61**, S612–S617 (2015).

46. Zarnowski, R. *et al.* Novel entries in a fungal biofilm matrix encyclopedia. *MBio* **5**, 1–13 (2014).

47. Nobile, C. J. *et al.* A Recently Evolved Transcriptional Network Controls Biofilm Development in Candida albicans. *NHI* **148**, 126–138 (2012).

48. Araújo, D., Henriques, M. & Silva, S. Portrait of Candida Species Biofilm Regulatory Network Genes. *Trends Microbiol.* **25**, 62–75 (2017).

49. Sudbery, P. E. The germ tubes of Candida albicans hyphae and pseudohyphae show different patterns of septin ring localization. *Mol. Microbiol.* **41**, 19–31 (2001).

50. Sudbery, P. E. Growth of Candida albicans hyphae. *Nat. Rev. Microbiol.* **9**, 737–748 (2011).

51. Kadosh, D. Morphogenesis in C. albicans. in *Candida albicans: Cellular and Molecular Biology* 41–62 (Springer International Publishing, 2017). doi:https://doi.org/10.1007/978-3-319-50409-4_4

52. Gulati, M. & Nobile, C. J. Candida albicans biofilms: development, regulation, and molecular mechanisms. *HHS Public Access* **18**, 310–321 (2016).

53. Chen, H., Zhou, X., Ren, B. & Cheng, L. The regulation of hyphae growth in Candida albicans. *Virulence* **11**, 337–348 (2020).

54. Mccall, A. D., Pathirana, R. U., Prabhakar, A., Cullen, P. J. & Edgerton, M. Candida albicans biofilm development is governed by cooperative attachment and adhesion maintenance proteins. *npj Biofilms Microbiomes* (2019). doi:10.1038/s41522-019-0094-5

55. Negri, M., Henriques, M., Williams, D. W. & Azeredo, J. Adherence and biofilm formation of non-Candida albicans Candida species. **19**, 241–247 (2011).

56. Silva, S. *et al.* Biofilms of non-Candida albicans Candida species: quantification, structure and matrix composition. 681–689 (2009). doi:10.3109/13693780802549594

57. Verstrepen, K. J. & Klis, F. M. Flocculation, adhesion and biofilm formation in yeasts. *Mol. Microbiol.* **60**, 5–15 (2006).

58. Desai, J. V. & Mitchell, A. P. Candida albicans biofilm development and its genetic control. *Microbiol Spectr.* **3**, 1–19 (2015).

59. Iraqui, I. *et al.* The Yak1p kinase controls expression of adhesins and biofilm formation in Candida glabrata in a Sir4p-dependent pathway. *Mol. Microbiol.* **55**, 1259–1271 (2005).

60. Cavalheiro, M. & Teixeira, M. C. Candida Biofilms: Threats, challenges, and promising strategies. *Front. Med.* **5**, 1–15 (2018).

61. de Groot, P. W. J., Bader, O., de Boer, A. D., Weig, M. & Chauhan, N. Adhesins in human fungal pathogens: Glue with plenty of stick. *Eukaryot. Cell* **12**, 470–481 (2013).

62. Nobile, C. J. *et al.* Critical role of Bcr1-dependent adhesins in C. albicans biofilm formation in vitro and in vivo. *PLoS Pathog.* **2**, 0636–0649 (2006).

63. Nobile, C. J. & Mitchell, A. P. Regulation of cell-surface genes and biofilm formation by the C. albicans transcription factor Bcr1p. *Curr. Biol.* **15**, 1150–1155 (2005).

64. Rodrigues, C. F., Rodrigues, M. E., Silva, S. & Henriques, M. Candida glabrata biofilms: How far have we come? *J. Fungi* **3**, (2017).

65. D'Enfert, C. & Janbon, G. Biofilm formation in Candida glabrata: What have we learnt from functional genomics approaches? *FEMS Yeast Res.* **16**, 1–13 (2015).

66. Riera, M., Mogensen, E., d'Enfert, C. & Janbon, G. New regulators of biofilm development in Candida glabrata. *Res. Microbiol.* **163**, 297–307 (2012).

67. Maestre-Reyna, M. *et al.* Structural basis for promiscuity and specificity during Candida glabrata invasion of host epithelia. *Proc. Natl. Acad. Sci. U. S. A.* **109**, 16864–16869 (2012).

68. Kaur, R., Domergue, R., Zupancic, M. L. & Cormack, B. P. A yeast by any other name: Candida glabrata and its interaction with the host. *Curr. Opin. Microbiol.* **8**, 378–384 (2005).

69. Castaño, I. *et al.* Telomere length control and transcriptional regulation of subtelomeric adhesins in Candida glabrata. *Mol. Microbiol.* **55**, 1246–1258 (2005).

70. Cormack, B. P. *et al.* An Adhesin of the Yeast Pathogen Candida glabrata Mediating Adherence to Human Epithelial Cells Published by : American Association for the Advancement of Science Stable URL : http://www.jstor.org/stable/2898737 An Adhesin of the Yeast Pathogen Candida gl. **285**, 578–582 (2016).

71. Domergue, R. *et al.* Nicotinic Acid Limitation Regulates Silencing of Candida Adhseins During UTI. *Science (80-.).* **308**, 866–870 (2005).

72. Filler, S. G. Candida-host cell receptor-ligand interactions. *Curr. Opin. Microbiol.* **9**, 333–339 (2006).

73. De Las Peñas, A. *et al.* Virulence-related surface glycoproteins in the yeast pathogen Candida glabrata are encoded in subtelomeric clusters and subject to RAP1- and SIR-dependent transcriptional silencing. *Genes Dev.* **17**, 2245–2258 (2003).

74. Pais, P., Costa, C., Cavalheiro, M., Romão, D. & Teixeira, M. C. Transcriptional control of drug resistance, virulence and immune system evasion in pathogenic fungi: A cross-species comparison. *Front. Cell. Infect. Microbiol.* **6**, (2016).

75. Wu, W. S. & Li, W. H. Identifying gene regulatory modules of heat shock response in yeast. *BMC Genomics* **9**, 1–15 (2008).

76. Jayampath Seneviratne, C., Wang, Y., Jin, L., Abiko, Y. & Samaranayake, L. P. Proteomics of drug resistance in candida glabrata biofilms. *Proteomics* **10**, 1444–1454 (2010).

77. Mao, X., Cao, F., Nie, X., Liu, H. & Chen, J. The Swi/Snf chromatin remodeling complex is essential for

hyphal development in Candida albicans. *FEBS Lett.* **580**, 2615–2622 (2006).

78. Schweizer, A., Rupp, S., Taylor, B. N., Röllinghoff, M. & Schröppel, K. The TEA/ATTS transcription factor CaTec1p regulates hyphal development and virulence in Candida albicans. *Mol. Microbiol.* **38**, 435–445 (2000).

79. Schaller, M. *et al.* Secreted aspartic proteinase (Sap) activity contributes to tissue damage in a model of human oral candidosis. **34**, (1999).

80. Glazier, V. E. *et al.* Genetic analysis of the Candida albicans biofilm transcription factor network using simple and complex haploinsufficiency. *PLoS Genet.* **13**, 1–25 (2017).

81. Zhao, Y. *et al.* The APSES family proteins in fungi: characterizations, evolution and functions. *Fungal Genet. Biol.* **81**, 271–280 (2014).

82. Noffz, C. S., Liedschulte, V., Lengeler, K. & Ernst, J. F. Functional mapping of the Candida albicans Efg1 regulator. *Eukaryot. Cell* **7**, 881–893 (2008).

83. Ramírez-Zavala, B. & Domínguez, Á. Evolution and phylogenetic relationships of APSES proteins from Hemiascomycetes. **8**, 511–519 (2008).

84. Bockmüh, D. P. & Ernst, J. F. A potential phosphorylation site for an A-Type kinase in the Efgl regulator protein contributes to hyphal morphogenesis of Candida albicans. *Genetics* **157**, 1523–1530 (2001).

85. Sonneborn, A., Tebarth, B. & Ernst, J. F. Control of white-opaque phenotypic switching in Candida albicans by the Efg1p morphogenetic regulator. *Infect. Immun.* **67**, 4655–4660 (1999).

86. Lane, S., Birse, C., Zhou, S., Matson, R. & Liu, H. DNA Array Studies Demonstrate Convergent Regulation of Virulence Factors by Cph1 , Cph2 , and Efg1 in Candida albicans *. **276**, 48988–48996 (2001).

87. Ramage, G., VandeWalle, K., López-Ribot, J. L. & Wickes, B. L. The filamentation pathway controlled by the Efg1 regulator protein is required for normal biofilm formation and development in Candida albicans. *FEMS Microbiol. Lett.* **214**, 95–100 (2002).

88. Lane, S., Zhou, S., Pan, T., Dai, Q. & Liu, H. The Basic Helix-Loop-Helix Transcription Factor Cph2 Regulates Hyphal Development in Candida albicans Partly via Tec1. **21**, 6418–6428 (2001).

89. Panariello, B. H. D., Klein, M. I., Pavarina, A. C. & Duarte, S. Inactivation of genes TEC1 and EFG1 in Candida albicans influences extracellular matrix composition and biofilm morphology. *J. Oral Microbiol.* **9**, 1385372 (2017).

90. Gow, N. A. R., Veerdonk, F. L. Van De, Brown, A. J. P. & Netea, M. G. Candida albicans morphogenesis and host defence : discriminating invasion from colonization. *Nat. Publ. Gr.* **10**, 112–122 (2011).

91. Seider, K. *et al.* The Facultative Intracellular Pathogen Candida glabrata Subverts Macrophage Cytokine Production and Phagolysosome Maturation . *J. Immunol.* **187**, 3072–3086 (2011).

92. Ishchuk, O. P. *et al.* RNAi as a Tool to Study Virulence in the Pathogenic Yeast Candida glabrata. *Front. Microbiol.* **10**, 1–17 (2019).

93. Roetzer, A., Gratz, N., Kovarik, P. & Schüller, C. Autophagy supports Candida glabrata survival during phagocytosis. *Cell. Microbiol.* **12**, 199–216 (2010).

94. Kaur, R., Ma, B. & Cormack, B. P. A family of glycosylphosphatidylinositol-linked aspartyl proteases is required for virulence of Candida glabrata. 1–6 (2007).

95. Brown, A. J. P., Haynes, K. & Quinn, J. Nitrosative and oxidative stress responses in fungal pathogenicity. doi:10.1016/j.mib.2009.06.007

96. Duggan, S. *et al.* Neutrophil activation by Candida glabrata but not Candida albicans promotes fungal uptake by monocytes. *Cell. Microbiol.* **17**, 1259–1276 (2015).

97. Pais, P., Galocha, M. & Teixeira, M. C. Genome-Wide Response to Drugs and Stress in the Pathogenic Yeast Candida glabrata. in *Yeasts in Biotechnology and Human Health* **58**, 155–193 (Springer International Publishing, 2019).

98. Pais, P. *et al.* Microevolution of the pathogenic yeasts Candida albicans and Candida glabrata during antifungal therapy and host infection. *Microb. Cell* **6**, 142–159 (2019).

99. Ene, I. V, Cheng, S., Netea, M. G. & Brown, A. J. P. Growth of Candida albicans Cells on the Physiologically Relevant Carbon Source Lactate Affects Their Recognition and Phagocytosis by. **81**, 238–248 (2013).

100. Ene, I. V *et al.* Host carbon sources modulate cell wall architecture , drug resistance and virulence in a fungal pathogen. (2012). doi:10.1111/j.1462-5822.2012.01813.x

101. Ene, I. V *et al.* Carbon source-induced reprogramming of the cell wall proteome and secretome modulates the adherence and drug resistance of the fungal pathogen Candida albicans. 3164–3179 (2012). doi:10.1002/pmic.201200228

102. Revie, N. M., Iyer, K. R., Robbins, N. & Cowen, L. E. Antifungal drug resistance: evolution, mechanisms and impact. *Curr. Opin. Microbiol.* **45**, 70–76 (2018).

103. Campoy, S. & Adrio, J. L. Antifungals. *Biochem. Pharmacol.* **133**, 86–96 (2017).

104. Graybill, J. R., Burgess, D. S. & Hardin, T. C. Key issues concerning fungistatic versus fungicidal drugs. *Eur. J. Clin. Microbiol. Infect. Dis.* **16**, 42–50 (1997).

105. Carmona, E. M. & Limper, A. H. Overview of Treatment Approaches for Fungal Infections. *Clin. Chest Med.* **38**, 393–402 (2017).

106. Prasad, R., Shah, A. H. & Rawal, M. K. Antifungals: Mechanism of Action and Drug Resistance. in *Yeast Membrane Transporter* **892**, 327–349 (2016).

107. Perlin, D. S. Resistance to echinocandin-class antifungal drugs. *Drug Resist. Updat.* **10**, 121–130 (2007).

108. Vandeputte, P., Ferrari, S. & Coste, A. T. Antifungal resistance and new strategies to control fungal infections. *Int. J. Microbiol.* **2012**, (2012).

109. Siddhardha, B., Dyavaiah, M. & Syed, A. *Model Organisms for Microbial Pathogenesis, Biofilm Formation and Antimicrobial Drug Discovery*. *Model Organisms for Microbial Pathogenesis, Biofilm Formation and Antimicrobial Drug Discovery* (2020). doi:10.1007/978-981-15-1695-5

110. Gintjee, T. J., Donnelley, M. A. & Thompson, G. R. Aspiring Antifungals: Review of Current Antifungal Pipeline Developments. *J. Fungi* **6**, 28 (2020).

111. Roger, C., Sasso, M., Lefrant, J. Y. & Muller, L. Antifungal Dosing Considerations in Patients Undergoing Continuous Renal Replacement Therapy. *Curr. Fungal Infect. Rep.* **12**, (2018).

112. Vermes, A., Guchelaar, H. J. & Dankert, J. Flucytosine: A review of its pharmacology, clinical indications, pharmacokinetics, toxicity and drug interactions. *J. Antimicrob. Chemother.* **46**, 171–179 (2000).

113. Ryder, N. S. Terbinafine: Mode of action and properties of the squalene epoxidase inhibition. *Br. J. Dermatol.* **126**, 2–7 (1992).

114. Klobučníková, V. *et al.* Terbinafine resistance in a pleiotropic yeast mutant is caused by a single point mutation in the ERG1 gene. *Biochem. Biophys. Res. Commun.* **309**, 666–671 (2003).

115. Brenner, G. M. & Stevens, C. *Pharmacology*. (Elsevier Inc., 2012).

116. Kaur, R., Castaño, I. & Cormack, B. P. Functional Genomic Analysis of Fluconazole Susceptibility in the Pathogenic Yeast Candida glabrata: Roles of Calcium Signaling and Mitochondria. *Antimicrob. Agents Chemother.* **48**, 1600–1613 (2004).

117. Lopez-Ribot, J. L., Wiederhold, N. P. & Patterson, T. F. Fungal Drug Resistance: Azoles. *Antimicrob. Drug Resist.* 397–405 (2017). doi:10.1007/978-3-319-46718-4_27

118. François, I. E. J. A. *et al.* Azoles: Mode of antifungal action and resistance development. Effect of miconazole on endogenous reactive oxygen species production in Candida albicans. *Antiinfect. Agents Med. Chem.* **5**, 3–13 (2006).

119. Lupetti, A., Danesi, R., Campa, M., Tacca, M. Del & Kelly, S. Molecular basis of resistance to azole antifungals. *Trends Mol. Med.* **8**, 76–81 (2002).

120. Shapiro, R. S., Robbins, N. & Cowen, L. E. Regulatory Circuitry Governing Fungal Development, Drug Resistance, and Disease. *Microbiol. Mol. Biol. Rev.* **75**, 213–267 (2011).

121. Caudle, K. E. *et al.* Genomewide expression profile analysis of the Candida glabrata Pdr1 regulon. *Eukaryot. Cell* **10**, 373–383 (2010).

122. Paul, S., Schmidt, J. A. & Scott Moye-Rowley, W. Regulation of the CgPdr1 transcription factor from the pathogen candida glabrata. *Eukaryot. Cell* **10**, 187–197 (2011).

123. Costa, C. *et al.* Candida glabrata drug: H+ antiporter CgQdr2 confers imidazole drug resistance, being

activated by transcription factor CgPdr1. *Antimicrob. Agents Chemother.* **57**, 3159–3167 (2013).

124. Cavalheiro, M. *et al.* A Transcriptomics Approach To Unveiling the Mechanisms of In Vitro Evolution towards Fluconazole Resistance of a Candida glabrata clinical isolate. *Antimicrob. Agents Chemother.* **63**, 1–17 (2019).

125. Tsai, H. F., Krol, A. A., Sarti, K. E. & Bennett, J. E. Candida glabrata PDR1, a transcriptional regulator of a pleiotropic drug resistance network, mediates azole resistance in clinical isolates and petite mutants. *Antimicrob. Agents Chemother.* **50**, 1384–1392 (2006).

126. Costa, C. *et al.* The dual role of Candida glabrata drug: H+ antiporter CgAqr1 (ORF CAGL0J09944g) in antifungal drug and acetic acid resistance. *Front. Microbiol.* **4**, 1–13 (2013).

127. Costa, C. *et al.* Candida glabrata drug:H+ antiporter CgTpo3 (ORF CAGL0I10384G): Role in azole drug resistance and polyamine homeostasis. *J. Antimicrob. Chemother.* **69**, 1767–1776 (2014).

128. Costa, C. *et al.* Clotrimazole drug resistance in Candida glabrata clinical isolates correlates with increased expression of the drug: H+ antiporters CgAqr1, CgTpo1_1, CgTpo3, and CgQdr2. *Front. Microbiol.* **7**, 1–11 (2016).

129. Sanglard, D., Ischer, F. & Bille, J. Role of ATP-binding-cassette transporter genes in high-frequency acquisition of resistance to azole antifungals in Candida glabrata. *Antimicrob. Agents Chemother.* **45**, 1174–1183 (2001).

130. Healey, K. R. *et al.* Prevalent mutator genotype identified in fungal pathogen Candida glabrata promotes multi-drug resistance. *Nat. Commun.* **7**, 1–10 (2016).

131. Vale-Silva, L., Beaudoing, E., Tran, V. D. T. & Sanglard, D. Comparative genomics of two sequential Candida glabrata clinical isolates. *G3 Genes, Genomes, Genet.* **7**, 2413–2426 (2017).

132. Perlin, D. S., Shor, E. & Zhao, Y. Update on Antifungal Drug Resistance. *Curr. Clin. Microbiol. Reports* **2**, 84–95 (2015).

133. Alexander, B. D. *et al.* Increasing echinocandin resistance in candida glabrata: Clinical failure correlates with presence of FKS mutations and elevated minimum inhibitory concentrations. *Clin. Infect. Dis.* **56**, 1724–1732 (2013).

134. Goemaere, B., Lagrou, K., Spriet, I., Hendrickx, M. & Becker, P. Clonal spread of candida glabrata bloodstream isolates and fluconazole resistance affected by prolonged exposure: A 12-year single-center study in Belgium. *Antimicrob. Agents Chemother.* **62**, 1–11 (2018).

135. Karpov, D. S., Grineva, E. N., Kiseleva, S. V & Chelarskaya, E. S. Candida glabrata Rpn4-like Protein Complements the RPN4 Deletion in Saccharomyces cerevisiae. **53**, 242–248 (2019).

136. Mannhaupt, G., Schnall, R., Karpov, V., Vetter, I. & Feldmann, H. Rpn4p acts as a transcription factor by binding to PACE, a nonamer box found upstream of 26S proteasomal and other genes in yeast. *FEBS Lett.* **450**, 27–34 (1999).

137. Owsianik, G., Balzi, E. & Ghislain, M. Control of 26S proteasome expression by transcription factors regulating multidrug resistance in Saccharomyces cerevisiae. **43**, 1295–1308 (2002).

138. Spasskaya, D. S., Karpov, D. S., Mironov, A. S. & Karpov, V. L. Transcription factor Rpn4 promotes a complex antistress response in Saccharomyces cerevisiae cells exposed to methyl methanesulfonate. *Mol. Biol.* **48**, 141–149 (2014).

139. Wang, X., Xu, H., Ju, D. & Xie, Y. Disruption of Rpn4-induced proteasome expression in Saccharomyces cerevisiae reduces cell viability under stressed conditions. *Genetics* **180**, 1945–1953 (2008).

140. Teixeira, M. C. *et al.* Refining current knowledge on the yeast FLR1 regulatory network by combined experimental and computational approaches. *Mol. Biosyst.* **6**, 2471–2481 (2010).

141. Teixeira, M. C., Dias, P. J., Simões, T. & Sá-Correia, I. Yeast adaptation to mancozeb involves the up-regulation of FLR1 under the coordinate control of Yap1, Rpn4, Pdr3, and Yrr1. *Biochem. Biophys. Res. Commun.* **367**, 249–255 (2008).

142. Vermitsky, J. P. *et al.* Pdr1 regulates multidrug resistance in Candida glabrata: Gene disruption and genome-wide expression studies. *Mol. Microbiol.* **61**, 704–722 (2006).

143. Pais, P. *et al.* Candida glabrata Transcription Factor Rpn4 Mediates Fluconazole Resistance Through Regulation of Ergosterol Biosynthesis and Plasma Membrane Permeability. *Antimicrob. Agents Chemother.* (2020). doi:10.1128/AAC.00554-20

144. HAP1 | SGD. Available at: https://www.yeastgenome.org/locus/S000004246. (Accessed: 25th June 2020)

145. Klimova, N., Yeung, R., Kachurina, N. & Turcotte, B. Phenotypic analysis of a family of transcriptional regulators, the zinc cluster proteins, in the human fungal pathogen Candida glabrata. *G3 Genes, Genomes, Genet.* **4**, 931–940 (2014).

146. Kołaczkowska, A. & Dyla, M. Differential expression of the Candida glabrata CgRTA1 and CgRSB1 genes in response to various stress conditions. **432**, 169–174 (2013).

147. Johnson, S. S. *et al.* Regulation of Yeast Nutrient Permease Endocytosis by ATP-binding Cassette Transporters and a Seven-transmembrane. **285**, 35792–35802 (2010).

148. Jia, X. *et al.* RTA2, a novel gene involved in azole resistance in Candida albicans. **373**, 631–636 (2008).

149. Contribution, R. & Transporters, A. B. C. Relative Contribution of the ABC Transporters Cdr1, Pdh1, and Snq2 to Azole Resistance in Candida glabrata. *Am. Soc. Microbiol.* 1–8 (2018).

150. Tsai, H. *et al.* Microarray and Molecular Analyses of the Azole Resistance Mechanism in Candida glabrata Oropharyngeal Isolates. **54**, 3308–3317 (2010).

151. Paul, S., Bair, T. B. & Moye-rowley, W. S. Identification of Genomic Binding Sites for Candida glabrata Pdr1 Transcription Factor in Wild-Type and p0 Cells. **58**, 6904–6912 (2014).

152. History of Genetic Engineering and the Rise of Genome Editing Tools. Available at:

https://www.synthego.com/learn/genome-engineering-history. (Accessed: 31st December 2019)

153. Urnov, F. D., Rebar, E. J., Holmes, M. C., Zhang, H. S. & Gregory, P. D. Genome editing with engineered zinc finger nucleases. *Nat. Rev. Genet.* **11**, 636–646 (2010).

154. abm Inc. CRISPR vs. TALENs vs. RNAi: Which system is best for your gene silencing project? (2019). Available at: https://www.abmgood.com/marketing/knowledge_base/Gene-Silencing-CRISPR-TALEN-RNAi. (Accessed: 2nd January 2020)

155. Tijsterman, M. & Plasterk, R. H. A. Dicers at RISC: The mechanism of RNAi. *Cell* **117**, 1–3 (2004).

156. Krueger, U. *et al.* Insights into effective RNAi gained from large-scale siRNA validation screening. *Oligonucleotides* **17**, 237–250 (2007).

157. Jackson, A. L. *et al.* Expression profiling reveals off-target gene regulation by RNAi. *Nat. Biotechnol.* **21**, 635–638 (2003).

158. Kanchiswamy, C. N., Maffei, M., Malnoy, M., Velasco, R. & Kim, J. S. Fine-Tuning Next-Generation Genome Editing Tools. *Trends Biotechnol.* **34**, 562–574 (2016).

159. Gabriel, R. *et al.* An unbiased genome-wide analysis of zinc-finger nuclease specificity. *Nat. Biotechnol.* **29**, 816–823 (2011).

160. Miller, J. C. *et al.* An improved zinc-finger nuclease architecture for highly specific genome editing. *Nature Biotechnology* **25**, 778–785 (2007).

161. Urnov, F. D. Genome Editing B.C. (Before CRISPR): Lasting Lessons from the “Old Testament”. *Cris. J.* **1**, 34–46 (2018).

162. Kim, H. & Kim, J. S. A guide to genome engineering with programmable nucleases. *Nat. Rev. Genet.* **15**, 321–334 (2014).

163. Wood, A. J. *et al.* Targeted genome editing across species using ZFNs and TALENs. *Science* **333**, 307 (2011).

164. Ishino, Y., Shinagawa, H., Makino, K., Amemura, M. & Nakatura, A. Nucleotide sequence of the iap gene, responsible for alkaline phosphatase isoenzyme conversion in Escherichia coli, and identification of the gene product. *J. Bacteriol.* **169**, 5429–5433 (1987).

165. Makarova, K. S. *et al.* An updated evolutionary classification of CRISPR-Cas systems. *Nat. Rev. Microbiol.* **13**, 722–736 (2015).

166. Jansen, R., Van Embden, J. D. A., Gaastra, W. & Schouls, L. M. Identification of genes that are associated with DNA repeats in prokaryotes. *Mol. Microbiol.* **43**, 1565–1575 (2002).

167. Loureiro, A. & Da Silva, G. J. Crispr-cas: Converting a bacterial defence mechanism into a state-of-the-art genetic manipulation tool. *Antibiotics* **8**, (2019).

168. Van Der Oost, J., Westra, E. R., Jackson, R. N. & Wiedenheft, B. Unravelling the structural and

mechanistic basis of CRISPR-Cas systems. *Nat. Rev. Microbiol.* **12**, 479–492 (2014).

169. Barrangou, R. & Marraffini, L. A. CRISPR-cas systems: Prokaryotes upgrade to adaptive immunity. *Mol. Cell* **54**, 234–244 (2014).

170. Lander, E. S. The Heroes of CRISPR. *Cell* **164**, 18–28 (2016).

171. Applied Biological Materials Inc. CRISPR-Cas9: An Introductory Guide for Gene Knockout. (2018).

172. Cong, L. *et al.* Multiplex Genome Engineering Using CRISPR-Cas Systems. *Science (80-.).* **339**, 819–824 (2013).

173. Hille, F. & Charpentier, E. CRISPR-cas: Biology, mechanisms and relevance. *Philos. Trans. R. Soc. B Biol. Sci.* **371**, (2016).

174. Gasiunas, G., Sinkunas, T. & Siksnys, V. Molecular mechanisms of CRISPR-mediated microbial immunity. *Cell. Mol. Life Sci.* **71**, 449–465 (2014).

175. Pickar-Oliver, A. & Gersbach, C. A. The next generation of CRISPR–Cas technologies and applications. *Nat. Rev. Mol. Cell Biol.* (2019). doi:10.1038/s41580-019-0131-5

176. Wang, H., La Russa, M. & Qi, L. S. CRISPR/Cas9 in Genome Editing and Beyond. *Annu. Rev. Biochem.* **85**, 227–264 (2016).

177. Jiang, F. & Doudna, J. A. CRISPR – Cas9 Structures and Mechanisms. *Annu. Rev. Biophys.* 505–531 (2017).

178. Nishimasu, H. *et al.* Engineered CRISPR-Cas9 nuclease with expanded targeting space. *Science (80-.).* **361**, 1259–1262 (2018).

179. Anders, C., Niewoehner, O., Duerst, A. & Jinek, M. Structural basis of PAM-dependent target DNA recognition by the Cas9 endonuclease. *Nature* **513**, 569–573 (2014).

180. Sternberg, S. H., Redding, S., Jinek, M., Greene, E. C. & Doudna, J. A. DNA interrogation by the CRISPR RNA-guided endonuclease Cas9. *Nature* **507**, 62–67 (2014).

181. Bhaya, D., Davison, M. & Barrangou, R. CRISPR-Cas Systems in Bacteria and Archaea: Versatile Small RNAs for Adaptive Defense and Regulation. *Annu. Rev. Genet.* **45**, 273–297 (2011).

182. Westra, E. R., Swarts, D. C., Staals, R. H. J., Jore, M. M., Brouns, S. J. J., & van der Oost, J. The CRISPRs, They Are A-Changin': How Prokaryotes Generate Adaptive Immunity. *Annu. Rev. Genet.* **46**, 311–339 (2012).

183. Moon, S. Bin, Kim, D. Y., Ko, J. & Kim, Y. Recent advances in the CRISPR genome editing tool set. *Exp. Mol. Med.* (2019). doi:10.1038/s12276-019-0339-7

184. Makarova, K. S. *et al.* Evolution and classification of the CRISPR-Cas systems. *Nat. Rev. Microbiol.* **9**, 467–477 (2011).

185. Jinek, M. *et al.* A Programmable Dual-RNA – Guided DNA Endonuclease in Adaptive Bacterial

Immunity. *Science (80-.).* **337**, 816–821 (2012).

186. Krzysztof, C., Le, R. A. & Emmanuelle, C. The tracrRNA and Cas9 families of type II CRISPR-Cas immunity systems. *RNA Biol.* **10**, 726–737 (2013).

187. Lim, Y. *et al.* Structural roles of guide RNAs in the nuclease activity of Cas9 endonuclease. *Nat. Commun.* **7**, 1–8 (2016).

188. Doudna, J. A. & Charpentier, E. The new frontier of genome engineering with CRISPR-Cas9. *Science (80-.).* **346**, (2014).

189. Savić, N. & Schwank, G. Advances in therapeutic CRISPR/Cas9 genome editing. *Transl. Res.* **168**, 15–21 (2016).

190. Sander, J. D. & Joung, J. K. CRISPR-Cas systems for editing, regulating and targeting genomes. *Nat. Biotechnol.* **32**, 347–350 (2014).

191. Hsu, P. D., Lander, E. S. & Zhang, F. Development and Applications of CRISPR-Cas9 for Genome Engineering. *HHS* **157**, 1262–1278 (2014).

192. F Ann Ran, Patrick D Hsu, Jason Wright, Vineeta Agarwala, David A Scott, and F. Z. Genome engineering using the CRISPR-Cas9 system. *Nat. Protoc.* **8**, 2281–2308 (2013).

193. Komor, A. C., Kim, Y. B., Packer, M. S., Zuris, J. A. & Liu, D. R. Programmable editing of a target base in genomic DNA without double-stranded DNA cleavage. *Nature* **533**, 420–424 (2016).

194. Kolli, N., Lu, M., Maiti, P., Rossignol, J. & Dunbar, G. L. Application of the gene editing tool, CRISPR-Cas9, for treating neurodegenerative diseases. *Neurochem. Int.* **112**, 187–196 (2018).

195. Addgene. Addgene: CRISPR Plasmids and Resources. Available at: https://www.addgene.org/crispr/. (Accessed: 11th January 2020)

196. Addgene. Addgene: CRISPR Plasmids - RNA Targeting. Available at: https://www.addgene.org/crispr/rna-targeting/. (Accessed: 11th January 2020)

197. Addgene. Addgene: CRISPR Pooled gRNA Libraries. Available at: https://www.addgene.org/crispr/libraries/. (Accessed: 11th January 2020)

198. Walsh, R. M. & Hochedlinger, K. A variant CRISPR-Cas9 system adds versatility to genome engineering. *Proc. Natl. Acad. Sci. U. S. A.* **110**, 15514–15515 (2013).

199. Gurumurthy, C. B. *et al.* CRISPR: a versatile tool for both forward and reverse genetics research. *Hum. Genet.* **135**, 971–976 (2016).

200. Addgene. Addgene: CRISPR Plasmids - Single-Strand Break (Nick). Available at: https://www.addgene.org/crispr/nick/. (Accessed: 12th January 2020)

201. Addgene. Addgene: CRISPR Plasmids - Yeast. Available at: https://www.addgene.org/crispr/yeast/. (Accessed: 11th January 2020)

202. Vyas, V. K., Barrasa, M. I. & Fink, G. R. A Candida albicans CRISPR system permits genetic engineering of essential genes and gene families. *Sci. Adv.* **1**, (2015).

203. Min, K., Ichikawa, Y., Woolford, C. A. & Mitchell, A. P. Candida albicans Gene Deletion with a Transient CRISPR-Cas9 System. *mSphere* **1**, 1–9 (2016).

204. Huang, M. Y. & Mitchell, A. P. Marker Recycling in Candida albicans through CRISPR-Cas9-Induced Marker Excision. *mSphere* **2**, 1–10 (2017).

205. Namkha Nguyen, Morgan M.F Quail, A. D. H. An Efficient , Rapid , and Recyclable Editing in Candida albicans. *mSphere* **2**, 1–10 (2017).

206. Enkler, L., Richer, D., Marchand, A. L., Ferrandon, D. & Jossinet, F. Genome engineering in the yeast pathogen Candida glabrata using the CRISPR-Cas9 system. *Sci. Rep.* **6**, 1–12 (2016).

207. Lombardi, L., Turner, S. A., Zhao, F. & Butler, G. Gene editing in clinical isolates of Candida parapsilosis using CRISPR/Cas9. *Sci. Rep.* **7**, 1–11 (2017).

208. Morio, F. *et al.* Precise genome editing using a CRISPR-Cas9 method highlights the role of CoERG11 amino acid substitutions in azole resistance in Candida orthopsilosis. *J. Antimicrob. Chemother.* **74**, 2230–2238 (2019).

209. Vyas, V. K. *et al.* New CRISPR Mutagenesis Strategies Reveal Variation in Repair Mechanisms among Fungi. *mSphere* **3**, 1–14 (2018).

210. Dicarlo, J. E. *et al.* Genome engineering in Saccharomyces cerevisiae using CRISPR-Cas systems. *Nucleic Acids Res.* **41**, 4336–4343 (2013).

211. Grahl, N., Demers, E. G., Crocker, A. W. & Hogan, D. A. Use of RNA-Protein Complexes for Genome Editing in Non-albicans Candida Species. *mSphere* **2**, 1–9 (2017).

212. Cen, Y., Timmermans, B., Souffriau, B., Thevelein, J. M. & Van Dijck, P. Comparison of genome engineering using the CRISPR-Cas9 system in C. glabrata wild-type and lig4 strains. *Fungal Genet. Biol.* **107**, 44–50 (2017).

213. Cen, Y., Fiori, A. & Dijck, P. Van. Deletion of the DNA ligase iv gene in candida glabrata significantly increases gene-targeting efficiency. *Eukaryot. Cell* **14**, 783–791 (2015).

214. Doench, J. G. *et al.* Optimized sgRNA design to maximize activity and minimize offtarget effects of CRISPR-Cas9. *HHS* **34**, 184–191 (2016).

215. Köhrer, K. & Domdey, H. Preparation of high molecular weight RNA. *Methods Enzymol.* **194**, 398–405 (1991).

216. Muramoto, T., Iriki, H., Watanabe, J. & Kawata, T. Recent Advances in CRISPR/Cas9-Mediated Genome Editing in Dictyostelium. *Cells* **8**, 46 (2019).

217. Addgene. CRISPR 101: A Desktop Resource. in *Addgene* 307–313 (2017).

218. Vyas, V. K. *et al.* OSF | New CRISPR mutagenesis strategies reveal variation in repair mechanisms among fungi. Available at: https://osf.io/ARDTX/. (Accessed: 19th January 2020)

219. Addgene. Addgene: CRISPR Guide. Available at: https://www.addgene.org/guides/crispr/. (Accessed: 15th January 2020)

220. Edlind, T. D. *et al.* Promoter-dependent disruption of genes: Simple, rapid, and specific PCR-based method with application to three different yeast. *Curr. Genet.* **48**, 117–125 (2005).

221. Vyas, V. K. & Bernstein, D. A. An Introduction to CRISPR-Mediated Genome Editing in Fungi. **20**, 2–4 (2019).

222. Galocha, M. New players controlling multidrug resistance and biofilm formation in C. glabrata: the important role of Rpn4. (Instituto Superior Técnico - Universidade de Lisboa, 2017).

223. Invergo, B., Ames, R. & Usher, J. Data-driven prediction of genetic interactions in Candida glabrata. *Access Microbiol.* **1**, 8 (2019).

224. Typas, A. *et al.* A tool-kit for high-throughput, quantitative analyses of genetic interactions in E. coli HHS Public Access. *Nat Methods* **5**, 781–787 (2008).

225. Batzoglou, S., Myers, R. M. & Sidow, A. Genome-Wide Analysis of Transcription Factor Binding Sites Based on ChIP-Seq Data. *Nat. Methods* **5**, 829–834 (2010).

226. S.cerevisiae - Yeastract. Available at: http://yeastract-plus.org/yeastract/scerevisiae/view.php?existing=protein&proteinname=Hap1p. (Accessed: 6th July 2020)

227. C.albicans - PathoYeastract. Available at: http://yeastract-plus.org/pathoyeastract/calbicans/view.php?existing=locus&orfname=C2_06470W_A. (Accessed: 6th July 2020)